DEPARTMENT OF PHYSICS, UNIVERSITY OF JYVÄSKYLÄ
RESEARCH REPORT No. 1/1987

BEAM DYNAMICAL STUDIES OF CRYRING

BY
PAULI HEIKKINEN

Academic Dissertation
for the Degree of
Doctor of Philosophy

Jyväskylä, Finland
September 1987

URN:ISBN:978-951-39-9444-0
ISBN 978-951-39-9444-0 (PDF)
ISSN 0075-465X

Jyväskylän yliopisto, 2022

ISBN 951-679-578-1
ISSN 0075-465-X

DEPARTMENT OF PHYSICS, UNIVERSITY OF JYVÄSKYLÄ
RESEARCH REPORT No. 1/1987

BEAM DYNAMICAL STUDIES OF CRYRING

BY
PAULI HEIKKINEN

Academic Dissertation
for the Degree of
Doctor of Philosophy

To be presented, by permission of the
Faculty of Mathematics and Natural Sciences
of the University of Jyväskylä,
for public examination in Auditorium S-212 of
the University of Jyväskylä on October 17, 1987,
at 12 o'clock noon

Jyväskylä, Finland
September 1987

PART 1

INTRODUCTION TO ACCELERATOR PHYSICS

Preface

The work was carried out at the Research Institute of Physics (AFI), Stockholm. Without the idea of Dr. E.Liukkonen and Dr. C.J. Herrlander about this collaboration between AFI and the Department of Physics of the Jyväskylä university the work would never have been done by the author. My sincere thanks to both of my "bosses".

I am also very grateful to Dr. Anders Bárány with whom I have had many stimulating conversations about the physics that has been planned to be done in the ring, specially the merged beams experiment. He has also been of greatest value in checking the language and the contents of my texts.

The problem of intrabeam scattering was raised in the discussions with Dr. D.Möhl and Dr. H.Herr at CERN. As it turned out, intrabeam scattering is the most limiting factor as regards beam quality. Special thanks to them as well as to Dr. H.Poth from CERN who has given a lot of valuable information about electron cooling.

I also thank the Academy of Finland of the financial support that made it possible for me to take part in the CERN Accelerator School at Oxford.

At last I want to thank my wife Kaija, my daughter Heli and son Heikki of their understanding and patience because that is what they must have had when we moved from home to Sweden for one year just for my work, and when I was weeks away from home travelling in Europe, in the USA and in Canada. I wonder whether I would have had the patience.

Jyväskylä, September 1987

Pauli Heikkinen

BEAM DYNAMICAL STUDIES OF CRYRING

Abstract

This thesis consists of two parts. Part 1 (Introduction to Accelerator Physics) gives the basis of understanding the formalism and parameters that are used in accelerator physics, especially in synchrotron theory. The text is a selected collection of relevant topics in this context and it follows closely lecture notes by K. Steffen [St85]. As an appendix of part 1 there is a short introduction to electron cooling which appears in the latter part of the thesis.

Part 2 (Beam Dynamical Studies of CRYRING - Lattice Design Criteria and Operation Limits) was originally written and the work was done at the Research Institute of Physics (AFI) in Stockholm as a part of the CRYRING project. Later, after some modifications in the lattice, the text was updated and some electron cooling simulation calculations with intrabeam scattering were done at the Department of Physics, University of Jyväskylä.

CRYRING is a small acceletaror and storage ring for heavy ions and it will replace the old classical 225 cm cyclotron. CRYRING will mostly be used for atomic and molecular physics but nuclear physics will not be totally forgotten. Atomic physics, which will be done inside of the ring, requires the best beam quality. Good quality in this context means small energy spread and small beam size and divergence (transverse velocity). The beam quality will be increased by using electron cooling. Nevertheless, increasing beam quality brings along some unwanted effects. If energy spread is decreased too much the beam will get into some instabilities - the most important of them here is the microwave instability.

There are some competing processes to cooling. They attempt to increase the energy spread and the emittance (divergence) of the beam. These processes are residual gas scattering and intrabeam scattering. Due to very strict vaccuum requirements residual gas scattering will be more or less harmless as emittance growth is concerned whereas intrabeam scattering will set the limit for beam quality where one parameter is the beam intensity.

In part 2 the ion optical requirements set by the physics that will be done inside and outside of the accelerator and the operating limits as beam intensity and quality are are discussed.

PART 1

INTRODUCTION TO ACCELERATOR PHYSICS

Contents

PART 1

PART 2

Introduction

For designing an accelerator or trying to understand the behaviour of the beam in it, one needs a good set of parameters to describe the optics of the machine. In the linear approximation these parameters should not depend on the beam properties such as emittance or energy. Twiss parameters are used when dealing with circular accelerators. To be strict there are only two of them for each transverse direction: betatron wave length β and dispersion D. The other main parameters can be calculated from β and D.

To obtain beam dimensions and divergences one needs to know the Twiss parameters of the ring and only one beam parameter, the emittance E or ε. The normalized emittance $\beta\gamma\ E$ is a constant of motion and it is independent of beam energy. So, if we know the beam emittance at some energy and the machine parameters we, in principle, know what is happening in the accelerator all the time.

In the following chapters we derive the Twiss parameters from the linear motion and give some examples how these parameters are used in different situations.

During the writing of this thesis accelerator physicists at CERN decided to use the coordinate system $\{x, y, s\}$ following the beam s being parallel to beam velocity instead of the $\{z, x, s\}$ system frequently used before. This lead to changes of sign in some horizontal terms (x direction). The new convention is used in the latter part of this thesis to be consistent with computer programs obtained from CERN. However, since most of the literature used still employs the "old" coordinates, the introductory theory here uses the $\{z, x, s\}$ system in order to be more easy to be compared with other theory texts. The only place in this paper, where the change to the new coordinates appears explicitely is in the MAD-input where positive K indicates horizontal focusing while in the theory negative K gives horizontal focusing and vertical defocusing. When the reader also remembers that x is always the horizontal direction there should not be any risk of confusion.

Frequently used symbols and their meanings

Symbol	Meaning of the symbol	Unit
x	horizontal transverse coordinate	m
y	vertical transverse coordinate	m
u	general transverse coordinate, x or y	m
s	distance along beam axis	m
$u' = \theta$	$\frac{du}{ds}$	rad
u_p	transverse closed orbit shift due to a momentum deviation	m
R	average machine radius	m
β_u	transverse betatron amplitude function in plane (u, s) (betatron wave length devided by 2π)	m
α_u	$-\frac{1}{2}\frac{d\beta_u}{ds}$	
μ_u	phase advance of betatron oscillation	rad
Q_u	number of betatron oscillations per revolution in plane (u, s)	
Q'	Q-shift due to momentum deviation $\frac{\Delta p}{p}$	
D_u	transverse dispersion function	m
E_u	transverse emittance $= \pi(2\sigma_u)^2/\beta_u$	π m rad
η	$\gamma^{-2} - \gamma_t^{-2}$ revolution frequency spread per unit of momentum spread, γ_t being the value of γ at the transition energy where η changes its sign	
β	$\frac{v}{c}$, where c is the velocity of light	
γ	$(1 - \beta^2)^{-\frac{1}{2}}$	
q	charge state of the ion or charge of the ion	Coulomb
A	mass number of the ion	
T	kinetic energy	
t	kinetic energy divided by mass	

Note that the emittance is the area of the transverse phase space ellipse, but the value given is the area divided by π (π is included in the unit), and it corresponds to a beam half width of $2\sigma_u$ (2 x standard deviation). The reader should distinguish between $\beta = (v/c)$ and the focusing function β_u. The subscript is dropped to shorten the formulae in places where the significance is clear from the context. Also the meaning of q should be clear from the context whether it is the charge state or the charge of the ion.

Connections between some parameters are given below:

$$u(s) = \sqrt{\beta_u(s) E_u}\cos(\phi(s) - \phi_o) \qquad (i)$$

where ϕ_o is an arbitrary phase angle (constant for each ion)

$$\mu_u(s) = \int_o^s \frac{ds}{\beta_u(s)} \qquad (ii)$$

$$D_u(s) = \frac{u_p}{\Delta p/p} \qquad (iii)$$

where $\frac{\Delta p}{p}$ is the fractional momentum deviation

$$Q'_u = \frac{\partial Q_u}{\partial(\Delta p/p)} \qquad (iv)$$

Sometimes in the literature $Q'/Q = \xi$ is called the chromaticity whereas we define the chromaticity as Q'. Note the special meaning of the prime, which is here a derivative with respect to $\frac{\Delta p}{p}$ (usually with respect to s).

More details of synchrotron parameters can be found e.g. in [Gu77], [Bl77] and [Br84]. Note, however, that definitions of some parameters vary a bit in the literature.

1. Particle Motion in Curved Coordinate System Following a Reference Trajectory

1.1 Coordinate System

Among all particle trajectories we choose one to be a reference trajectory (center of beam). We describe particle trajectories in the vicinity of the reference trajectory using right-handed rectangular coordinate system $\{z, x, s\}$ that follows this trajectory, x and z being the horizontal and vertical coordinates respectively and $\vec{s}$ pointing in the direction of the beam.

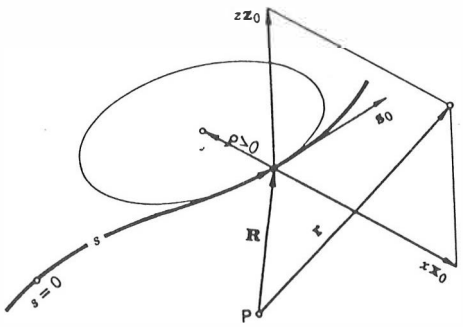

Figure 1.1
Curved coordinate system $\{z, x, s\}$

The gyration radius ρ is taken to be positive when the gyration centre is on the negative x-axis, the general gyration radius being then $(\rho + x)$. If not mentioned explicitly bending takes place only horizontally. Anyway, we could always rotate the coordinate system so that there is no bending vertically.

1.2 Motion in a Homogenous Field $B_z(x) = \text{const}$

In a homogenous magnetic field, $B = B_z(x) = \text{const}$, a particle will follow a circle with curvature

$$\frac{x''}{(1 + x'^2)^{3/2}} = -\frac{1}{\rho} = \frac{q}{p} B_z = \text{const.} \tag{1.1}$$

Here the prime denotes derivative with respect to s. Note the minus sign which comes from the choise of gyration centre to be on the negative x-axis. The gyration radius ρ becomes positive with negative B_z and positive charge q ($\vec{F} = q(\vec{v} \times \vec{B})$).

1.3 Field Expansion in the Curved Coordinate System, with $B_x = B_s = 0$ in the Symmetry Plane $z = 0$

We assume the field symmetry

$$B_z(z) = B_z(-z); \quad B_x(z) = -B_x(-z); \quad B_s(z) = -B_s(-z).$$

Then, using $\nabla \times \vec{B} = \vec{0}$ and $\nabla \cdot \vec{B} = 0$ with

$$\begin{aligned} h &= \frac{q}{p_o} B_z = -\frac{1}{\rho} && \text{dipole} \\ k &= \frac{q}{p_o} \frac{\partial B_z}{\partial x} && \text{quadrupole} \\ m &= \frac{q}{p_o} \frac{\partial^2 B_z}{\partial x^2} && \text{sextupole} \\ n &= \frac{q}{p_o} \frac{\partial^3 B_z}{\partial x^3} && \text{octupole} \end{aligned}$$

one can derive the general field expansion with symmetry plane in the curved coordinate system

$$\begin{aligned} \frac{q}{p} B_z &= h + kx + \frac{1}{2} m x^2 - \frac{1}{2} \beta z^2 + \frac{1}{6} n x^3 - \frac{1}{2} \{h(\beta - 2m) + \alpha'' + n\} x z^2 + O(4) \\ \frac{q}{p} B_x &= kz + mxz + \frac{1}{2} n x^2 z - \frac{1}{6} \{h(\beta - 2m) + \alpha'' + n\} z^3 + O(4) \\ \frac{q}{p} B_s &= h' z + \alpha' x z + (h\alpha' + \frac{1}{2} m') x^2 z - \frac{1}{6} \beta' z' + O(4) \end{aligned} \tag{1.2}$$

with $\alpha = \frac{1}{2} h^2 + k$ and $\beta = h'' - hk + m$. In the linear theory, we need only terms

$$\begin{aligned} \frac{q}{p} B_z &- h + kx \\ \frac{q}{p} B_x &= kz \\ \frac{q}{p} B_s &= h' z. \end{aligned} \tag{1.3}$$

Here, again, the prime denotes derivative with respect to s.

1.4 Betatron Oscillations

In an accelerator we need focusing in order to have the beam confined around the reference trajectory. We shall now look at the equation of motion in the $\{z, x, s\}$ frame and find the focusing condition for weak focusing.

Since the bending takes place only horizontally the time derivatives of the moving axes are

$$\dot{\vec{z}}_o = 0; \quad \dot{\vec{x}}_o = \frac{\dot{s}}{\rho}\vec{s}_o; \quad \dot{\vec{s}}_o = -\frac{\dot{s}}{\rho}\vec{x}_o, \tag{1.4}$$

where $\dot{s}$ is the velocity of the particle projection on the reference orbit.

The location of the moving frame in a fixed frame is $\vec{R}$. Then

$$\vec{r} = z\vec{z}_o + x\vec{x}_o + \vec{R}$$

and

$$\vec{v} = \dot{\vec{r}} = \dot{z}\vec{z}_o + \dot{x}\vec{x}_o + \dot{s}(1+\frac{x}{\rho})\vec{s}_o \qquad (\dot{\vec{R}} = \dot{s}\vec{s}_o) \tag{1.5}$$

$$\dot{\vec{v}} = \ddot{\vec{r}} = \ddot{z}\vec{z}_o + \{\ddot{x} - \frac{\dot{s}^2}{\rho}(1+\frac{x}{\rho})\}\vec{x}_o + \{2\dot{x}\frac{\dot{s}}{\rho} + \ddot{s}(1+\frac{x}{\rho})\}\vec{s}_o.$$

Setting

$$\dot{z} = z'\dot{s} \quad ; \quad \dot{x} = x'\dot{s}$$
$$\ddot{z} = z''\dot{s}^2 + z'\ddot{s} \quad ; \quad \ddot{x} = x''\dot{s}^2 + x'\ddot{s}$$

and using

$$\dot{\vec{v}} = \frac{q}{m}(\vec{v} \times \vec{B})$$

one can evaluate

$$\begin{aligned} z'' + \frac{\ddot{s}}{\dot{s}^2}z' &= \frac{v}{\dot{s}}\frac{q}{p}\{x'B_s - (1+\frac{x}{\rho})B_x\} \\ x'' + \frac{\ddot{s}}{\dot{s}^2}x' - \frac{1}{\rho}(1+\frac{x}{\rho}) &= -\frac{v}{\dot{s}}\frac{q}{p}\{z'B_s - (1+\frac{x}{\rho})B_z\} \end{aligned} \tag{1.6}$$

with $\frac{v}{\dot{s}} = \sqrt{(1+\frac{x}{\rho})^2 + z'^2 + x'^2}$ and, by differentiation,

$$\frac{\ddot{s}}{\dot{s}^2} = -\frac{1}{2}\frac{(v^2/\dot{s}^2)'}{v^2/\dot{s}^2}.$$

Considering only the linear part we use

$$\frac{v}{\dot{s}} \approx 1 + \frac{x}{\rho} \quad ; \quad \ddot{s} \approx 0$$
$$\frac{1}{p} \approx \frac{1}{p_o}(1 - \frac{\Delta p}{p_o})$$

and equations (1.3). Using these notations we can finally write

$$\begin{aligned} z'' + kz &= 0 \\ x'' - (k - \frac{1}{\rho^2})x &= \frac{1}{\rho}\frac{\Delta p}{p}. \end{aligned} \tag{1.7}$$

For the moment being we can forget the term $\frac{1}{\rho}\frac{\Delta p}{p}$. Then the equations (1.7) are both simply equations of motion for a harmonic oscillator if

$$\begin{aligned} k &> 0 \qquad && \text{(vertically)} \\ k - \frac{1}{\rho^2} &< 0 \qquad && \text{(horizontally).} \end{aligned} \tag{1.8}$$

For both directions to be stable simultaneously we have then the condition

$$0 < k < \frac{1}{\rho^2}.$$

Note here that the magnitude of the bending field decreases with x when $B_z < 0$ (Fig. 1.1).

The particle motion described by Eqs (1.7) is called betatron oscillation, and it was first derived and applied for weak focusing machines. The equations show that a certain kind of field can keep the beam confined in both transverse planes simultaneously. However, it is possible to get stronger overall focusing by altering focusing and defocusing fields. This will decrease the size of the beam.

1.5 General Solution of Trajectory Equations

In modern accelerators both bending strength $h(s)$ and the focusing strength $k(s)$ vary along the reference orbit (sector focused cyclotrons and alternating gradient synchrotrons / storage rings). This leads to an oscillatory motion with variable restoring force and it is described by Hill's equation

$$y'' + K(s)y = \frac{1}{\rho}\frac{\Delta p}{p}. \tag{1.9}$$

The general solution of this equation is

$$\begin{aligned} y(s) &= C(s)y_o + S(s)y'_o + D(s)\frac{\Delta p}{p} \\ y'(s) &= C'(s)y_o + S'(s)y'_o + D'(s)\frac{\Delta p}{p}, \end{aligned} \tag{1.10}$$

where C and S are two independent solutions of the homogenous equation, with initial conditions

$$\begin{pmatrix} C_o & S_o \\ C'_o & S'_o \end{pmatrix} = \begin{pmatrix} 1 & 0 \\ 0 & 1 \end{pmatrix} \tag{1.11a}$$

and $D(s)$ is a particular solution of the inhomogenous equation for $\frac{\Delta p}{p} = 1$, subject to appropriate initial conditions. For beam transfer lines one usually chooses:

$$\begin{pmatrix} D_o \\ D'_o \end{pmatrix} = \begin{pmatrix} 0 \\ 0 \end{pmatrix}. \tag{1.11b}$$

at the entrance of the channel. To satisfy more general initial conditions for $D(s)$, appropriate solutions of the homogenous part of (1.9) have to be added to this particular solution. The functions C, S and D are called principal trajectories (Cosinelike, Sinelike and Dispersion). Eqs (1.10) can be written in matrix form

$$\begin{pmatrix} y \\ y' \\ \frac{\Delta p}{p} \end{pmatrix}_s = \begin{pmatrix} C & S & D \\ C' & S' & D' \\ 0 & 0 & 1 \end{pmatrix} \begin{pmatrix} y \\ y' \\ \frac{\Delta p}{p} \end{pmatrix}_o . \tag{1.12}$$

It is worth noting that the determinant of the transformation matrix is independent of s, which can be seen by differentiation

$$(CS' - SC')' = CS'' - SC'' = -K(CS - SC) = 0.$$

From the chosen initial conditions its value is unity, and it stays unity throughout the system. Later in the text, it will be shown that the area in the phase space $\{y, y'\}$ occupied by the beam is constant, which essentially is the same as the mentioned property of the determinant to be equal to unity.

The dispersion $D(s)$ subject to the initial conditions (1.11b) can be written as [St85]

$$\begin{aligned} D(s) &= S \int_0^s \frac{1}{\rho} C \mathrm{d}\tau - C \int_0^s \frac{1}{\rho} S \mathrm{d}\tau \\ D'(s) &= S' \int_0^s \frac{1}{\rho} C \mathrm{d}\tau - C' \int_0^s \frac{1}{\rho} S \mathrm{d}\tau. \end{aligned} \tag{1.13}$$

These equations can be derived using the method of variation of constants which permits to express the solution of the inhomogenous linear equation by integrals over the homogenous solutions.

Equations (1.10) and (1.13) or transformation (1.12) together with (1.13) give us a tool to determine particle cordinates at position s when the initial coordinates are known. Next we shall give some simple examples of accelerator elements.

a) Drift space

The magnet is non-existent, and we have

$$M_x = M_z = \begin{pmatrix} 1 & l & 0 \\ 0 & 1 & 0 \\ 0 & 0 & 1 \end{pmatrix}, \tag{1.14}$$

where l is the length of the drift space.

b) Constant B along the reference trajectory; $B(s)$=const

Using a simple hard edged model where a constant field region starts and ends abrubtly we get the harmonic oscillator equation

$$y'' + Ky = 0 \quad \text{with} \quad \begin{cases} K = k = \text{const} & \text{for } z \\ K = -(k - \frac{1}{\rho^2}) = \text{const} & \text{for } x \end{cases}.$$

With $\phi = s\sqrt{|K|}$ the solution in the magnet is simply

$$\begin{pmatrix} C & S \\ C' & S' \end{pmatrix} = \begin{pmatrix} \cos\phi & \frac{s}{\phi}\sin\phi \\ -\frac{\phi}{s}\sin\phi & \cos\phi \end{pmatrix} \qquad \text{for } K > 0 \text{ focusing}$$

$$\begin{pmatrix} C & S \\ C' & S' \end{pmatrix} = \begin{pmatrix} \cosh\phi & \frac{s}{\phi}\sinh\phi \\ \frac{\phi}{s}\sinh\phi & \cosh\phi \end{pmatrix} \qquad \text{for } K < 0 \text{ defocusing.} \tag{1.15}$$

$K = 0$ gives just a drift space. Just to check one can see that the determinant is unity.

The dispersion comes easily using Eqs (1.13) with C and S given above:

$$\begin{aligned} D &= \frac{1}{\rho K}(1 - \cos\phi) \\ D' &= \frac{1}{\sqrt{K}}\sin\phi \qquad\qquad K > 0 \end{aligned} \tag{1.16a}$$

and

$$\begin{aligned} D &= -\frac{1}{\rho|K|}(1 - \cosh\phi) \\ D' &= \frac{1}{\sqrt{K}}\sinh\phi \qquad\qquad K < 0. \end{aligned} \tag{1.16b}$$

What we have done so far is not enough in determining the beam properties in an accelerator. We are only able to follow a particle when we know its initial values. We need to know what the beam looks like when it makes millions of turns around the machine. It is evident that if we can find periodic solutions for the beam envelope and the dispersion we have more adequate tools to describe the long term behaviour of the ensemble of particles.

2. Beam Motion in Accelerators

2.1 Amplitude and Phase Function

An alternative way of formulating the solution of the homogenous Hill's equation

$$y'' + K(s)y = 0$$

is to write the trajectory in quasi-harmonic form

$$y(s) = \sqrt{\varepsilon}\sqrt{\beta(s)}\cos(\phi(s) - \phi_o). \tag{2.1}$$

The function $\sqrt{\varepsilon}\sqrt{\beta(s)}$ is just another way of writing the amplitude that varies along s due to varying restoring force $K(s)$, and $\phi(s)$ is the phase of betatron oscillation that in turn advances unevenly along s depending on the focusing strength.

We use the following notations

$$\Delta\phi = \phi - \phi_o; \quad \alpha = -\frac{1}{2}\beta'; \quad \gamma = \frac{1+\alpha^2}{\beta} \tag{2.2}$$

and rewrite the equation of motion:

$$\begin{aligned}
y &= \sqrt{\varepsilon}\sqrt{\beta}\cos\Delta\phi \\
y' &= \sqrt{\varepsilon}\left\{\frac{\beta'}{2\sqrt{\beta}}\cos\Delta\phi - \sqrt{\beta}\phi'\sin\Delta\phi\right\} = -\sqrt{\varepsilon}\left\{\frac{\alpha}{\sqrt{\beta}}\cos\Delta\phi + \sqrt{\beta}\phi'\sin\Delta\phi\right\} \\
y'' &= -\sqrt{\varepsilon}\left\{\frac{\alpha'\sqrt{\beta} - \alpha\frac{\beta'}{2\sqrt{\beta}}}{\beta}\cos\Delta\phi + \frac{\beta'}{2\sqrt{\beta}}\phi'\sin\Delta\phi\right. \\
&\quad \left. + \left(\frac{\beta'}{2\sqrt{\beta}}\phi' + \sqrt{\beta}\phi''\right)\sin\Delta\phi + \sqrt{\beta}\phi'^2\cos\Delta\phi\right\} \\
y'' &= -\frac{\sqrt{\varepsilon}}{\beta}\left\{\left(\alpha' + \frac{\alpha^2}{\beta} + \beta\phi'^2\right)\cos\Delta\phi + (\beta'\phi' + \beta\phi'')\sin\Delta\phi\right\}.
\end{aligned}$$

Inserting y and y'' into Hill's equation we see that the coefficient of $\sin\Delta\phi$ must be zero

$$0 = \beta'\phi' + \beta\phi'' = (\beta\phi')'.$$

Thus $\beta\phi'$=const. We are free to choose $\beta\phi' = 1$, i.e.

$$\phi' = \frac{1}{\beta}; \qquad \Delta\phi = \phi - \phi_o = \int_0^s \frac{\mathrm{d}s}{\beta}. \tag{2.3}$$

where $\frac{\mathrm{d}s}{\beta} = \mathrm{d}\phi$ is the local phase advance of the betatron oscillation.

From y'' we have also

$$\begin{aligned} \alpha' + \frac{1+\alpha^2}{\beta} &= K\beta \quad \text{or} \\ \alpha' + \gamma - K\beta = 0 \quad \text{or} \quad \frac{1}{2}\beta'' + K\beta - \frac{1+\frac{1}{4}\beta'^2}{\beta} &= 0 \end{aligned} \tag{2.4}$$

which is a differential equation for the amplitude function $\beta(s)$.

The equation (2.4) could be used to solve $\beta(s)$ but there is a more elegant way of doing it provided that we know the transfer matrix from an entrance point ($s = 0$) to the desired position s. In a general magnet system $\beta(s)$ depends on the initial values $\beta(0)$ and $\alpha(0)$. The periodic solution can be found by choosing two orthogonal trajectories

$$\begin{pmatrix} y_1 \\ y_1' \end{pmatrix} = \begin{pmatrix} \sqrt{\varepsilon}\sqrt{\beta}\cos(\phi - \phi_o) \\ -\frac{\sqrt{\varepsilon}}{\sqrt{\beta}}(\sin\Delta\phi + \alpha\cos\Delta\phi) \end{pmatrix}$$

and

$$\begin{pmatrix} y_2 \\ y_2' \end{pmatrix} = \begin{pmatrix} \sqrt{\varepsilon}\sqrt{\beta}\sin(\phi - \phi_o) \\ -\frac{\sqrt{\varepsilon}}{\sqrt{\beta}}(\cos\Delta\phi + \alpha\sin\Delta\phi) \end{pmatrix}$$

with any value of ϕ_o and given values of β_o, α_o and transforming them throughout the system up to s by matrix multiplication. Then $\beta(s)$ can be obtained as

$$\varepsilon\beta(s) = y_1^2(s) + y_2^2(s) = W^2(s) \tag{2.5}$$

2.2 Phase Plane Ellipse

Up to this point we have been looking at the trajectories of a single particle. However, it is more useful to treat the whole beam. This is done using the concept of the phase space ellipse. The particle position in the $\{y, y'\}$ plane

$$\begin{pmatrix} y \\ y' \end{pmatrix} = \begin{pmatrix} \sqrt{\varepsilon}\sqrt{\beta}\cos(\phi - \phi_o) \\ -\frac{\sqrt{\varepsilon}}{\sqrt{\beta}}(\sin(\phi - \phi_o) + \alpha\cos(\phi - \phi_o)) \end{pmatrix} \tag{2.6}$$

is the parametric representation of an ellipse in the $\{y, y'\}$ plane with a phase parameter $\phi - \phi_o$. Varying ϕ_o from 0 to 2π, moves the point (y, y') around the ellipse which is centered about the origin (0,0) (reference trajectory). The ellipse with some special points is showh in Figure 2.1.

The area of the ellipse is

$$\pi \cdot \sqrt{\varepsilon}\sqrt{\beta} \cdot \frac{\sqrt{\varepsilon}}{\sqrt{\beta}} = \pi\varepsilon = E$$

At fixed beam energies this area stays constant on the condition that the determinant of the transfer matrix is unity. This is the message of Liouville's

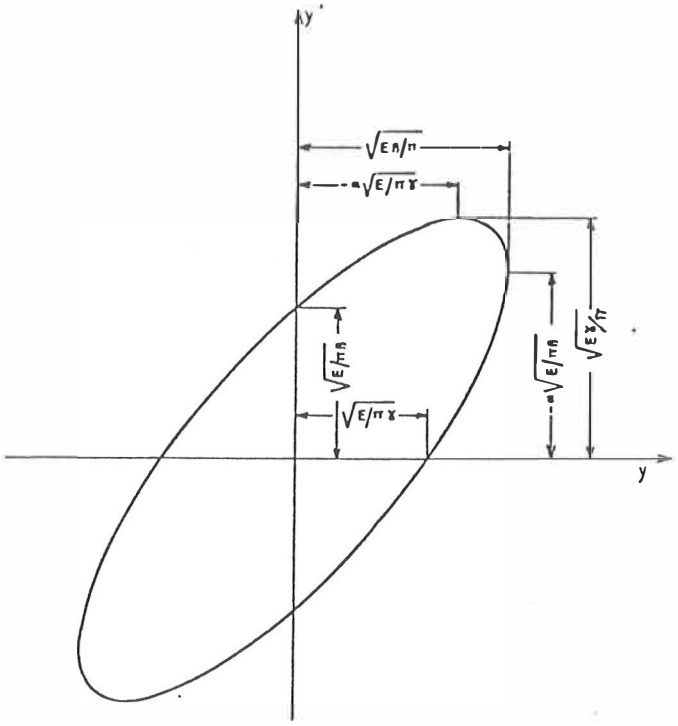

Figure 2.1
Beam ellipse in terms of amplitude function β.

theorem which means that the particle density in the phase plane and hence the area occupied by the beam in $\{y, y'\}$ space stays constant. The constant that characterizes the beam is the emittance ε (or $E = \pi\varepsilon$ in some papers). One example of a non-conservative determinant (emittance blow up) is scattering when going through a foil.

The coordinate representation of the ellipse is

$$\gamma y^2 + 2\alpha y y' + \beta y'^2 = \varepsilon \tag{2.7}$$

which can be checked by inserting (2.6) into it.

2.3 Calculation of Amplitude Function

Using the property of constant emittance (Eq. (2.7)) we are able to calculate $\beta(s)$, $\alpha(s)$ and $\gamma(s)$ when β_o, α_o and γ_o are known. By inverting the transfer matrix we

can come back from (y, y') to (y_o, y'_o)

$$\begin{pmatrix} y_o \\ y'_o \end{pmatrix} = \begin{pmatrix} S' & -S \\ -C' & C \end{pmatrix} \begin{pmatrix} y \\ y' \end{pmatrix}.$$

Using (2.7) we have at point s_o

$$\begin{aligned} &\gamma_o y_o^2 + 2\alpha_o y_o y'_o + \beta y'^2_o = \text{constant} \\ =&\gamma_o(S'y - Sy')^2 + 2\alpha_o(S'y - Sy')(-C'y + Cy') + \beta_o(-C'y + Cy')^2 \\ =&\underbrace{(C'^2\beta_o - 2C'S'\alpha_o + S'^2\gamma_o)}_{\gamma} y^2 + 2\underbrace{(-CC'\beta_o + (S'C + SC')\alpha_o - SS'\gamma_o)}_{\alpha} yy' \\ &+ \underbrace{(C^2\beta_o - 2CS\alpha_o + S^2\gamma_o)}_{\beta} y'^2 \\ =&\gamma y^2 + 2\alpha yy' + \beta y'^2. \end{aligned}$$

Then equating the coefficients, β, α and γ can be calculated from

$$\begin{pmatrix} \beta \\ \alpha \\ \gamma \end{pmatrix} = \begin{pmatrix} C^2 & -2CS & S^2 \\ -CC' & CS' + SC' & -SS' \\ C'^2 & -2C'S' & S'^2 \end{pmatrix} \begin{pmatrix} \beta_o \\ \alpha_o \\ \gamma_o \end{pmatrix}. \tag{2.8}$$

This allows us to follow the beam (the phase space ellipse) through transfer lines when the initial conditions are known.

2.4 Generalized Transfer Matrix

The generalized transfer matrix can be written in terms of amplitude and phase functions using the trajectory representation (2.6) together with the initial conditions (1.11a), and with $\Delta\phi = \phi - \phi_o$

$$\begin{pmatrix} C & S \\ C' & S' \end{pmatrix} =$$

$$\begin{pmatrix} \frac{\sqrt{\beta}}{\sqrt{\beta_o}}(\cos\Delta\phi + \alpha_o \sin\Delta\phi) & \sqrt{\beta_o}\sqrt{\beta}\sin\Delta\phi \\ -\frac{1}{\sqrt{\beta_o}\sqrt{\beta}}\{(\alpha - \alpha_o)\cos\Delta\phi + (1 + \alpha\alpha_o)\sin\Delta\phi\} & \frac{\sqrt{\beta_o}}{\sqrt{\beta}}(\cos\Delta\phi - \alpha\sin\Delta\phi) \end{pmatrix}. \tag{2.9}$$

This form is completely general and it is very useful in practical accelerator work.

In a circular accelerator the Twiss parameters (α, β and γ) repeat themselves turn after turn. So, after one revolution

$$\beta = \beta_o \qquad ; \qquad \alpha = \alpha_o.$$

In a symmetry point $\alpha = 0$ and the matrix gets a simple form

$$\begin{pmatrix} C & S \\ C' & S' \end{pmatrix} = \begin{pmatrix} \cos\mu & \beta\sin\mu \\ -\frac{1}{\beta}\sin\mu & \cos\mu \end{pmatrix},$$

where $\mu = 2\pi Q$ is the phase advance per revolution and Q the number of betatron oscillations per turn. When $\alpha \neq 0$ the matrix for one turn is

$$\begin{pmatrix} C & S \\ C' & S' \end{pmatrix} = M(L) = \begin{pmatrix} \cos\mu + \alpha \sin\mu & \beta \sin\mu \\ -\gamma \sin\mu & \cos\mu - \alpha \sin\mu \end{pmatrix} \tag{2.10}$$

where $L = 2\pi R$ is the circumference of the machine. This equation gives the periodic Twiss parameters α, β and γ when the transfer matrice for the whole accelerator has been calculated by matrix multiplication.

It can be easily seen that the generalized matrix can be split into two parts

$$M = I \cos\mu + J \sin\mu, \tag{2.11}$$

where

$$I = \begin{pmatrix} 1 & 0 \\ 0 & 1 \end{pmatrix} \quad \text{and} \quad J = \begin{pmatrix} \alpha & \beta \\ -\gamma & -\alpha \end{pmatrix}$$

and (by virtue of the third relation of (2.2))

$$J^2 = -I.$$

This property allows us to use a relation similar to De Moivre's formula for complex numbers

$$(\cos\Theta + j \sin\Theta)^m = (\cos m\Theta + j \sin m\Theta).$$

For the present case it can be shown[Co58] that the transfer matrix for m turns in the accelerator and its inverse may be written as

$$M^m = I \cos(m\mu) + J \sin(m\mu) \tag{2.12a}$$

and

$$(M^m)^{-1} = I \cos(m\mu) - J \sin(m\mu). \tag{2.12b}$$

This can also be understood by imagining what happens in the machine at a given place: β, α and γ stay constant turn after turn by definition (periodic solution) and the phase advance per turn is constant namely

$$\mu = \int_0^L \frac{\mathrm{d}s}{\beta}.$$

So, after m turns the phase advance will be $m\mu$.

A stability criterion is obtained from Eq. (2.12a). The elements of M are bounded for all m if and only if μ is real, which implies (cf. Eq. (2.10))

$$|Tr(M)| = |C + S'| = |2 \cos\mu| \leq 2. \tag{2.13}$$

Of course, this criterion must be satisfied in both transverse planes.

2.5 Periodic Dispersion

We have earlier written down the expression for dispersion with initial values $(D, D') = (0, 0)$ (Eq. (1.13)). In a circular accelerator we need the periodic solution which gives us the closed orbit shift due to $\frac{\Delta p}{p}$

$$y = \sqrt{\varepsilon\beta}\cos\Delta\phi + D\frac{\Delta p}{p}.$$

One notes from Eq. (1.9) and (1.13) that D describes the trajectory which results from the change of the orbit curvature in the bending elements on one side and the couteraction of the focusing elements on the other. Using Eq. (1.13) and the notations

$$\int_s^{s+L} \frac{1}{\rho(\tau)} C(\tau)\mathrm{d}\tau = \oint$$

$$\int_s^{s+L} \frac{1}{\rho(\tau)} S(\tau)\mathrm{d}\tau = \oint$$

and writing $C(s+L) = C$; $S(s+L) = S$ etc. we can write

$$\begin{pmatrix} C & S \\ C' & S' \end{pmatrix}\begin{pmatrix} D \\ D' \end{pmatrix} + \begin{pmatrix} S\oint - C\oint \\ S'\oint - C'\oint \end{pmatrix} = \begin{pmatrix} D \\ D' \end{pmatrix},$$

where the first term corresponds to the normal focusing and the second to sources of dispersion. The equation means that after one turn we have to come to the same point in the $\{D, D'\}$ space. Now we can write

$$(C-1)D + SD' = C\oint - S\oint$$

$$C'D + (S'-1)D' = C'\oint - S'\oint$$

yielding

$$\{(S'-1)(C-1) - SC'\}D = (S'-1)(C\oint - S\oint) - S(C'\oint - S'\oint).$$

The determinant $S'C - SC'$ is always unity and thus

$$\{2 - (C+S')\}D = \oint + S\oint - C\oint.$$

From the general transfer matrix (2.9)

$$2 - (C+S') = 2 - TrM = 2 - 2\cos\mu = 2(1-\cos 2\pi Q) = 4\sin^2\pi Q.$$

Thus

$$4\sin^2\pi Q \cdot D(s) = \int_s^{s+L} \frac{1}{\rho(\tau)} S(\tau)\mathrm{d}\tau + S(s+L)\int_s^{s+L} \frac{1}{\rho(\tau)} C(\tau)\mathrm{d}\tau - C(s+L)\int_s^{s+L} \frac{1}{\rho(\tau)} S(\tau)\mathrm{d}\tau$$

with

$$C(\tau) = \frac{\sqrt{\beta(\tau)}}{\sqrt{\beta(s)}}(\cos\Delta\phi + \alpha(s)\sin\Delta\phi)$$
$$S(\tau) = \sqrt{\beta(s)}\sqrt{\beta(\tau)}\sin\Delta\phi$$

and

$$C(s+L) = \cos 2\pi Q + \alpha(s)\sin 2\pi Q$$
$$S(s+L) = \beta(s)\sin 2\pi Q$$

according to equation (2.9).

Using the relation

$$\sin\Delta\phi + \sin(2\pi Q - \Delta\phi) = 2\sin\pi Q\cos(\Delta\phi - \pi Q)$$

we can finally write for the periodic dispersion

$$D(s) = \frac{\sqrt{\beta(s)}}{2\sin\pi Q}\int_s^{s+L} \frac{1}{\rho(\tau)}\sqrt{\beta(\tau)}\cos(\phi(\tau) - \phi(s) - \pi Q)\mathrm{d}\tau. \qquad (2.14)$$

2.6 Weak and Strong Focusing

2.6.1 Weak Focusing

Before going to strong focusing, let's take a look at weak focusing and, specifically, at constant gradient (CG) accelerators. Since the focusing strength k in the Hill's equation is constant around the machine we can calculate β_z directly from k

$$\frac{1}{\beta_z^2} = k = \frac{q}{p_o}\left(\frac{\partial B_z}{\partial x}\right). \qquad (2.15)$$

Similarily for β_x

$$\frac{1}{\beta_x^2} = \frac{1}{\rho^2} - k. \qquad (2.16)$$

If we, for example, for simplicity take $\beta_x = \beta_z$ then

$$\beta_x = \beta_z = \beta = \sqrt{2}\rho. \qquad (2.17)$$

From this we see that when going to larger accelerators (with larger energies) the beam dimensions grow as $\sqrt{\rho}$. If one increases focusing in one plane to obtain

smaller β (and $\sqrt{\varepsilon}\sqrt{\beta}$) the decreased focusing in the other plane causes larger beam size.

Another way of examining this is by considering the phase advance per turn which is

$$\mu = \oint \frac{\mathrm{d}s}{\beta} = \frac{2\pi R}{\beta} = 2\pi Q.$$

Then the number of betatron oscillations is

$$Q = \frac{R}{\beta}$$

or

$$\beta = \frac{R}{Q}. \tag{2.18}$$

From this we can see that by increasing the Q-value one can decrease the beam size. Although this derivation applies for weak focusing it is approximately true for other machines too. From (2.15) and (2.16) or (2.17) we see that for a CG machine $Q_{x,z} < 1$. Much higher Q-values can be obtained by "strong focusing", arrangement where focusing and defocusing elements alternate.

2.6.2 Strong Focusing - FODO Lattice

Most high energy accelerators consist of a number of FODO-cells (horizontally focusing element - straight section (or bending) - defocusing element - straight section (or bending)). As will be seen, this kind of structure provides stronger focusing than e.g. CG structure.

In practice the parameter $s\sqrt{|K|} = \phi$ occuring in the transfer matrices happens to be small compared to unity. This allows us to simplify the transfer matrices by concentrating the whole focusing in the centre of the element and by letting $s \to 0$. At the same time $\sin\phi \to \phi = s\sqrt{|K|}$. The focusing provided by the element will be the same as earlier, i.e. $\frac{1}{f} = |K|l$ =const where f is the focal length of the element and $\Delta s = l$ its effective geometrical length. Using these approximations the transfer matrices for (de)focusing elements get the form

$$M = \begin{pmatrix} 1 & 0 \\ \mp\frac{1}{f} & 1 \end{pmatrix}, \tag{2.19}$$

The upper sign applies to focusing, and the lower sign to defocusing. Edge focusing has been neglected here.

By using transfer matrices of type (2.19) we are able to study Twiss parameters in a FODO-lattice. For simplicity, we put $f_{\text{focusing}} = -f_{\text{defocusing}} = f = \frac{1}{\delta}$. We consider a FODO-cell of length L. Then starting at an F quadrupole, the transfer matrix for the whole cell becomes

$$\begin{aligned} M_F &= \begin{pmatrix} 1 & \frac{L}{2} \\ 0 & 1 \end{pmatrix} \begin{pmatrix} 1 & 0 \\ \delta & 1 \end{pmatrix} \begin{pmatrix} 1 & \frac{L}{2} \\ 0 & 1 \end{pmatrix} \begin{pmatrix} 1 & 0 \\ -\delta & 1 \end{pmatrix} \\ &= \begin{pmatrix} 1 - \frac{L\delta}{2} - \frac{L^2\delta^2}{4} & L + \frac{L^2\delta}{4} \\ -\frac{L\delta^2}{2} & 1 + \frac{L\delta}{2} \end{pmatrix}. \end{aligned} \tag{2.20}$$

Comparing coefficients with Eq. (2.10) yields

$$\begin{aligned} L\delta &= 4 \sin \frac{\mu}{2} \\ \beta_x &= \frac{L}{\sin \mu} \left(1 + \sin \frac{\mu}{2}\right) = \beta_{\max} \\ \beta_z &= \frac{L}{\sin \mu} \left(1 - \sin \frac{\mu}{2}\right) = \beta_{\min} \\ \alpha_x &= -\frac{1 + \sin \frac{\mu}{2}}{\cos \frac{\mu}{2}} \\ \alpha_z &= \frac{1 - \sin \frac{\mu}{2}}{\cos \frac{\mu}{2}}. \end{aligned} \tag{2.21}$$

The parameters at the D quadrupoles are obtained by exchanging the the indeces $x \leftrightarrow z$ in (2.21). The values of α are at the entrance of the quadrupole (they are zero in the middle of the quadrupoles).

The variation of $\beta_{\max}/L$ and $\beta_{\min}/L$ are shown in Figure 2.2 as a function of the phase advace per cell. In order to determine the smallest maximum we write

$$\frac{\beta}{L} = \frac{1 + \sin \frac{\mu}{2}}{2 \sin \frac{\mu}{2} \cos \frac{\mu}{2}} = \frac{1}{2} \frac{1 + \sin \tau}{\sin \tau \cos \tau}.$$

Then by differentiating with respect to τ and equating with 0 we get

$$\begin{aligned} &\frac{1}{2} \left(\cos \tau \cdot \sin \tau \cos \tau - (1 + \sin \tau) \left(\cos^2 \tau - \sin^2 \tau\right)\right) = 0 \\ &\sin^2 \tau (2 + \sin \tau) = 1 \quad ; \quad \sin \tau = \sin \frac{\mu}{2} = 0.618 \end{aligned}$$

$$\begin{aligned} \mu &= 76.34^\circ \\ \min(\beta_{\max}) &= 1.66L. \end{aligned} \tag{2.22}$$

This is the smallest $\beta_{\max}$ that can be obtained. For constant μ, in order to decrease L one must have stronger integrated gradients $\delta = Kl$ (cf. Eq. (2.21)).

As can be seen from Figure 2.2, the phase advance per cell can, in practice, be chosen between, say, 50° and 90° with almost constant $\beta_{\max}$.

2.6.3 Other Lattices

The most commonly used accelerator structure is the FODO-lattice described above. FODO-machines exist both in combined function arrangement (e.g. FNAL-booster) where the focusing and the bending are combined in gradient magnets and in the separated function version (e.g. CERN SPS) where focusing is provided by quadrupole - and bending by zero gradient dipole magnets. Another structure that is used in earlier synchrotrons (CERN PS, Brookhaven AGS) is a combined function FOFDOD-lattice. In a FOFDOD-lattice correction elements are placed between F's or D's where the two β-values differ from each other. This permits

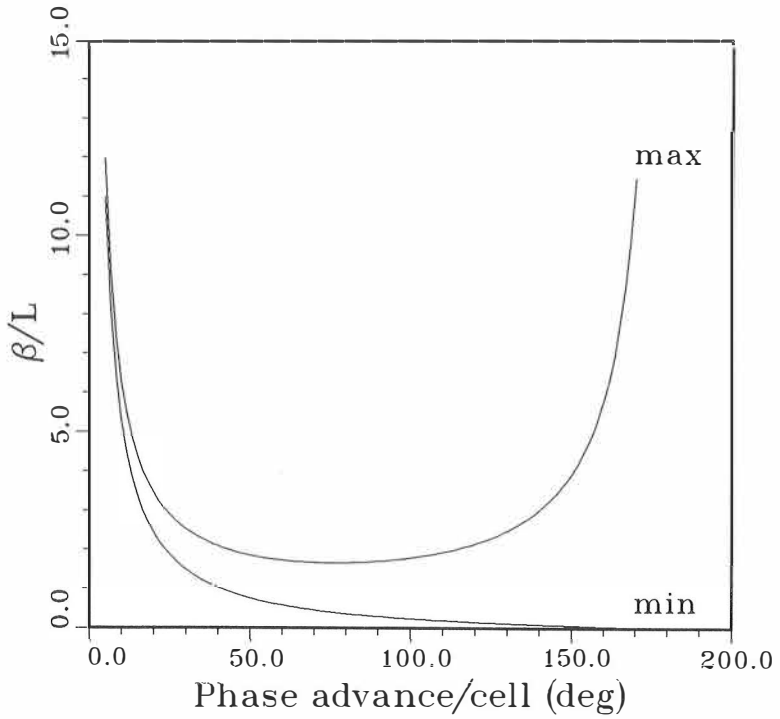

Figure 2.2
Maximum and minimum β versus phase advance μ per one FODO-cell.

one to correct both transverse planes fairly independent of each other. However, a given phase advance in a FOFDOD-lattice requires more focusing strength than in a FODO-lattice and the smallest β_{max} is usually bigger.

Small machines, like ASTRID, CRYRING [He85] and LEAR [Le80], [Le82], [Le84] cannot usually use FODO-structure due to the short circumference and many special constraints on β-values and the number and length of the straight sections. There is no general rule what kind of structure should be used in these machines. They must be designed "individually" taking into account the requirements set by the physics that will be done inside or outside of the ring together with the normal constraints coming from injection, extraction, acceleration, cooling etc.

2.6.4 Insertions

In larger accelerators it is possible to change lattice parameters locally without affecting them elsewhere in the ring by using matched insertions. The lattice functions (β, D) and their derivatives at the entrance and at the exit of these special sections are equal to those of the unperturbed lattice at the insertion points.

The most usual cases where insertions are used are *1) low β -insertions for interaction points, 2) non-dispersive straight sections, 3) long straight sections, 4) large β -insertions.*

In small machines such insertions may occupy a major part of the circumference. The structure may then be ragarded as a "series of insertions" rather that a highly periodic lattice with a few special sections.

3. A Non-ideal Beam in a Non-ideal Accelerator

3.1 The Effect of an Error in Quadrupole Strength

So far, we have considered only an ideal beam in a perfect accelerator. Next we outline the important aspects of field errors and tolerances. We shall review the effect of an error in quadrupole strength. Other field imperfections can be treated in a similar way (see e.g. [Co58, p 26–27]). The error is assumed to be so small that the change of β-values can be regarded as a small perturbation.

The true quadrupole qradient at position s can be written as

$$k(s) = k_o(s) + \delta k(s),$$

where $k_o(s)$ applies for a perfect machine. We shall calculate the effect of δk on the Q-value by looking at the change it produces in the transfer matrix for one turn. The length of the quadrupole is taken to be ds. Then the unperturbed quadrupole has a matrix

$$m_o = \begin{pmatrix} 1 & \mathrm{d}s \\ -k_o(s)\mathrm{d}s & 1 \end{pmatrix} \tag{3.1}$$

and perturbed, a matrix

$$m = \begin{pmatrix} 1 & \mathrm{d}s \\ -[k_o(s) + \delta k(s)]\mathrm{d}s & 1 \end{pmatrix}. \tag{3.2}$$

The unperturbed transfer matrix for the whole machine

$$M_o = \begin{pmatrix} \cos\mu_o + \alpha_o \sin\mu_o & \beta_o \sin\mu_o \\ -\gamma_o \sin\mu_o & \cos\mu_o - \alpha_o \sin\mu_o \end{pmatrix} \tag{2.10}$$

includes m_o.

The perturbed matrix can be calculated by first tracking through the ring (M_o) starting from the location of the quadrupole, back-tracking through the unperturbed quadrupole (m_o), and then proceeding through the perturbed quadrupole (m). By this means we have replaced the ideal quadrupole by the perturbed one. This can be written as

$$M(s) = m m_o^{-1} M_o.$$

Since

$$m m_o^{-1} = \begin{pmatrix} 1 & o \\ -\delta k(s)\mathrm{d}s & 1 \end{pmatrix}$$

the perturbed matrix becomes

$$M = \begin{pmatrix} \cos\mu_o + \alpha_o \sin\mu_o & \beta_o \sin\mu_o \\ -\delta k(s)\mathrm{d}s(\cos\mu_o + \alpha_o \sin\mu_o) - \gamma_o \sin\mu_o & -\delta k(s)\mathrm{d}s\beta_o \sin\mu_o + \cos\mu_o - \alpha_o \sin\mu_o \end{pmatrix}. \tag{3.3}$$

Remembering that $\frac{1}{2}Tr(M) = \cos\mu_o$ the change in $\cos\mu$ is

$$\begin{aligned} \Delta(\cos\mu_o) &= -\Delta\mu\sin\mu_o = -\frac{\sin\mu_o}{2}\beta_o(s)\delta k(s)\mathrm{d}s \\ 2\pi\Delta Q &= \Delta\mu = \frac{\beta(s)\delta k(s)\mathrm{d}s}{2}. \end{aligned} \tag{3.4}$$

Equation (3.4) qives the effect of an error in one short quadrupole on the Q-value. Allowing all quadrupoles to have an error $\delta k(s)$ we obtain for the whole accelerator

$$\Delta Q = \frac{1}{4\pi}\oint \beta(s)\delta k(s)\mathrm{d}s. \tag{3.5}$$

Note that Eq. (3.5) is approximate since we have kept $\beta(s)$ unchanged. For higher accuracy one should have higher order terms but these turn out to be negligible as long as $(\Delta Q/\sin 2\pi Q) \ll 1$)[Co58, p. 26–27]. The change of the tune can lead to resonant beam loss as will be discussed in section 3.3.

3.2 Chromaticity

The focusing of particles depends on their momentum (Eqs (1.1) and (1.9)). We restrict ourselves to quadrupoles here. The focusing strength of a quadrupole

$$k = \frac{q}{p}\frac{\partial B_z}{\partial x}$$

varies inversely with the momentum. Then

$$\frac{\Delta k}{k} = -\frac{\Delta p}{p}. \tag{3.6}$$

We define a quantity called the chromaticity

$$Q' = \frac{\Delta Q}{\Delta p/p} \tag{3.7}$$

or

$$\Delta Q = Q'\frac{\Delta p}{p}.$$

Combining equations (3.5) and (3.6) we get

$$\Delta Q = \frac{1}{4\pi}\oint \beta(s)\Delta k(s)\mathrm{d}s = \left[-\frac{1}{4\pi}\oint \beta(s)k(s)\mathrm{d}s\right]\frac{\Delta p}{p}$$

or

$$Q' = -\frac{1}{4\pi}\oint \beta(s)k(s)\mathrm{d}s. \tag{3.8}$$

Frequently in the litterature the quantity $Q'/Q = \xi$ is called the chromaticity. The chromaticity of the machine without sextupoles (except for those unavoidably present in the fringing field of the bending magnets) is called the natural chromaticity of the lattice.

In FODO-lattices the natural Q' is usually about $-1.3Q$ for both planes. The main source of chromaticity in large rings are the matching quadrupoles for low β -insertions. For example, in LEP [LEP79] β_{max} at the focusing quadrupoles in the low β -insertions is about $4.6\beta_{max}$(regular lattice).

In machines designed to accept large momentum spread $\frac{\Delta p}{p}$ Q' should be small in order to avoid crossing the resonances. For example, if $\frac{\Delta p}{p} = \pm 1\%$ and $Q' = 10$ one would have an "operating line" of length 0.2 in the working diagram which means that many particles in the beam (with a certain $\frac{\Delta p}{p}$) would lie on a dangerous resonance and hence be lost.

In order to correct chromaticity one needs focusing that changes with momentum. This can be obtained by combining amplitude dependent focusing and closed orbit shift due to momentum deviation, i.e. dispersion. A sextupole produces a quadrupole component Δk at a distance $D\frac{\Delta p}{p}$:

$$\Delta k = \underbrace{\frac{q}{p}\frac{\partial^2 B_z}{\partial x^2}}_{m} D\frac{\Delta p}{p} = mD\frac{\Delta p}{p}. \tag{3.9}$$

Now, combining (3.5) and (3.10) we obtain

$$\Delta Q_x = \left[\frac{1}{4\pi}\oint \beta(s) m D(s) \mathrm{d}s\right]\frac{\Delta p}{p}. \tag{3.10}$$

Replacing $m \leftarrow -m$ the same equation applies to the vertical tune shift as can be verified from (3.9) and (1.2) (replacing B_z by B_x). The quantity in the square brackets can be adjusted to compensate for the natural chromaticity. An important source of sextupole fields m are the fringing fields of dipoles and they must be carefully studied when determining the chromaticity of the accelerator[Dr82]. In order to correct both horizontal and vertical natural chromaticities independently the locations of the sextupoles have to be chosen so that in the horizontal case $\beta_x \gg \beta_z$ and in the vertical case $\beta_z \gg \beta_x$.

The natural chromaticity Q' is an average quantity. There are, however, local chromatic effects too. Due to momentum dependent focusing β-values are functions of $\frac{\Delta p}{p}$. The local change of β can be obtained from the matrix (3.3) comparing it with Eq. (2.10). There can be places in the accelerator where the user needs very small beam dimensions which means small β-values. At these places it is favourable to minimize $\frac{\partial\beta}{\partial(\Delta p/p)}$ in order to keep the interaction volume as small as possible. These local corrections are carried out with additional families of sextupoles.

3.3 Operating Point and Resonances

The Q-values, i.e. the number of betatron oscillations per turn, are often plotted in a working diagram with Q_x and Q_z as its axes. The point (Q_x, Q_z) is called the operating point. In practice there is always a certain Q-spread due to momentum

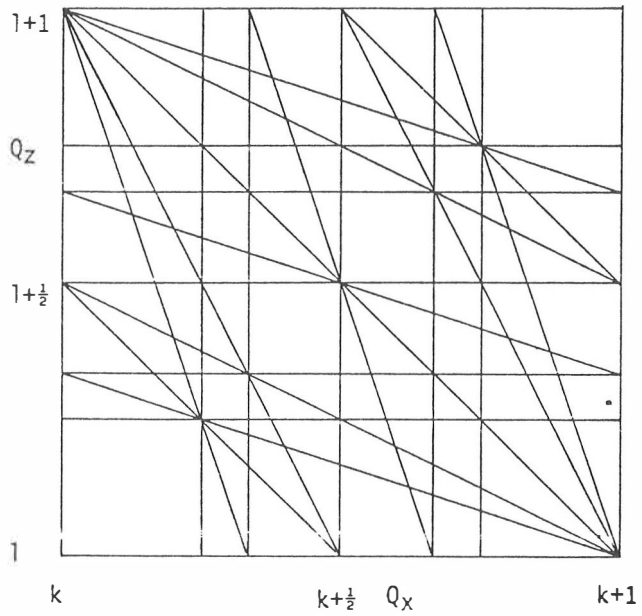

Figure 3.1
Working diagram with some resonance lines

dependent focusing and the space charge tune shift which is not the same for all particles.

There are zones in the working diagram that are dangerous for a particle circulating in the accelerator. If (Fig. 3.1)

$$nQ = p,$$

where n and p are integer, a particle got into a resonance can be lost. The same can happen when the more general resonance condition is met:

$$lQ_x + mQ_z = p, \tag{3.11}$$

Here $|l| + |m|$ is the order of the resonance and p is the azimuthal harmonic which drives it. This equation gives lines as drawn in Fig. 3.1.

The stopbands of first, second, third and fourth order and nonlinear resonance lines up to fourth order have been drawn in the diagram. The order n determines the spacing of lines: third order stopbands converge on a point which occurs at every $\frac{1}{3}$ integer Q-value including the integer itself, and so on. The order, n, is related to the order of the driving multipole so that $2n$ poles drive n^{th} order resonances. They drive also lower order resonances: a sextupole drives first and third order resonances and an octupole second and fourth order resonances, but here we are only interested in the highest order. Usually the highest "dangerous" order of resonance is four but experience has shown that when the beam is stored times for much longer than a second, higher order resonances may cause trouble.

The resonance lines are called stopbands because they have a width which depends on the field error and, in the case of non-linear resonances, on the amplitude of betatron oscillation of the particle.

We shall briefly discuss resonances of order three as this is the lowest order that is amplitude dependent and because this resonance is often used for slow extraction.

3.3.1 The Third Order Resonance

The third order resonance is driven by sextupole fields. Before going into details we introduce a normalized phase space which gives a circle when $\alpha = 0$: the usual x' is replaced by $p_x = \beta x'$ and x is kept unchanged.

We consider a short sextupole of length l, near a horizontal $\beta_{\max}$ location ($\alpha \approx 0$). Its field is

$$\Delta B = \frac{1}{2}\frac{\partial^2 B_z}{\partial x^2} x^2 = \frac{B''}{2} x^2. \tag{3.12}$$

It kicks a particle with a displacement $x = a\cos Q\Theta$

$$\Delta p_x = \frac{q}{p}\frac{\beta l B''}{2} x^2 = \frac{q}{p}\frac{\beta l B'' a^2}{2}\cos^2 Q\theta. \tag{3.12}$$

The kick changes both phase and amplitude of the betatron oscillation:

$$\frac{\Delta a}{a} = \frac{\Delta p}{a}\sin Q\theta = \frac{q}{p}\frac{\beta l B'' a}{2}\cos^2 Q\theta \sin Q\theta \tag{3.14}$$

$$\Delta\phi = \frac{\Delta p}{a}\cos Q\theta = \frac{q}{p}\frac{\beta l B'' a}{2}\cos^3 Q\theta \tag{3.15a}$$

$$= \frac{q}{p}\frac{\beta l B'' a}{8}(\cos 3Q\theta + 3\cos Q\theta). \tag{3.15b}$$

If Q is near a third integer, the kicks on three successive turns appear as in Fig. 3.2.

The second term in (3.15b) averages to zero over three turns and the phase shift is then

$$2\pi\Delta Q = \Delta\phi = \frac{q}{p}\frac{\beta l B'' a\cos 3Q\theta}{8}. \tag{3.16}$$

Close to $Q = l/3$, where l is an integer, $\cos 3Q\theta$ varies slowly, wandering within a band about the unperturbed Q_o:

$$Q_o - \frac{q}{p}\frac{\beta l B'' a}{16\pi} < Q_o < Q_o + \frac{q}{p}\frac{\beta l B'' a}{16\pi}. \tag{3.17}$$

When the perturbed Q, after a number of turns, coincides with $3p$, the argument of the cosine advances by $3Q \times 2\pi$ on each subsequent revolution (full turns) and the particle has been locked on to the resonance.

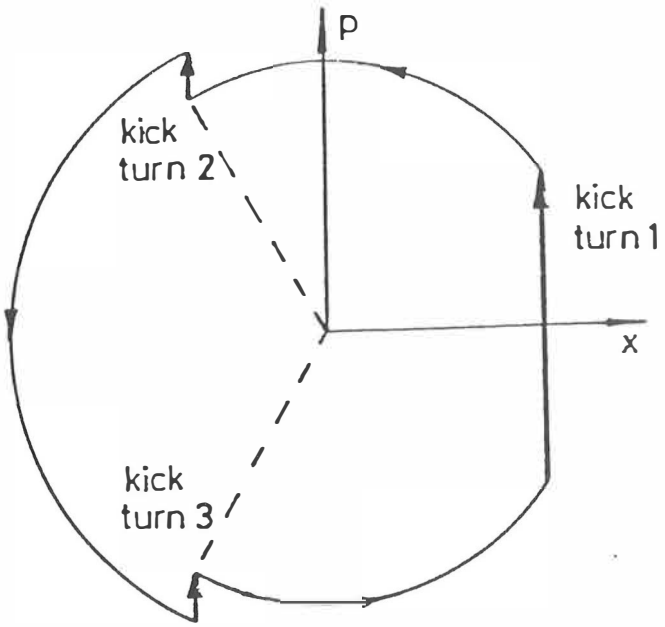

Figure 3.2

Phase space diagram following the motion of a particle at a 3rd order resonance

The amplitude perturbation (3.14) can be rewritten as

$$\frac{\Delta a}{a} = \frac{q}{p}\frac{\beta l B'' a}{8}\sin 3Q\theta. \tag{3.18}$$

This too is locked on, increasing steadily the amplitude until the particle is lost.

We see that both stopband width and growth rate are amplitude-dependent. If Q_o is a distance ΔQ from the third integer resonance line, particles with amplitudes less than

$$a < \frac{p}{q}\frac{16\pi\Delta Q}{\beta l B''} \tag{3.19}$$

will never lock on and are in a central region of stability. The limit gives the amplitude of the metastable points in the phase space where there is resonant condition but infinitely slow growth. The symmetry of Eq. (3.18) suggests that there are three fixed points at $\theta = 0, \frac{2\pi}{3}$, and $\frac{4\pi}{3}$. The fixed points are joined by a separatrix, which is the bound of stable motion. A more rigorous theory, which will be omitted here, would reveal that the separatrix is triangular in shape with three arms to which particles cling on their way out of the machine (Fig. 3.3).

Suppose now that we have an azimuthal distribution of sextupoles. Expressing this as a Fourier series

$$B''(\theta) = \sum_l B''_l \cos l\theta \tag{3.20}$$

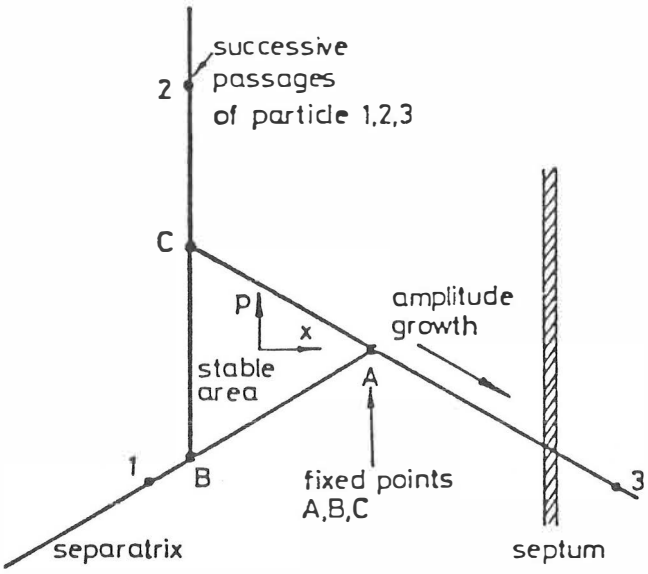

Figure 3.3

Phase space diagram at a fixed azimuthal position

we obtain

$$\Delta\phi = \sum_l \oint \frac{q}{p}\frac{\beta B''}{6} \cos 3Q\theta \cos l\theta \mathrm{d}\theta. \tag{3.21}$$

This integral is large and finite if

$$l = 3Q. \tag{3.22}$$

Here l gives the azimuthal frequency of sextupoles that act coherently when driving the stopband. Periodicities in the lattice and in the multipole pattern can thus mix to drive resonances. Eq. (3.21) qives also the "medicine" to cure unwanted resonances by using a set of sextupoles to generate a particular Fourier component which compensates the excitation due to field errors.

Third order resonance can be used in slow extraction. By choosing a proper phase and strangth of the driving sextupoles one can slowly shrink the stable area to zero, and particles will follow the arms of the separatrix until they have jumped over the septum (cf. Fig. 3.3). Note that ideally all particles will be extracted since they jump from one arm to the next every successive turns and thus come back to the same arm after three turns (with a larger amplitude).

The resonant condition for the third order resonance, $3Q$ = integer, arises because of the $\cos^3 Q\theta$ term in Eq. (3.15a), which in turn stems from the x^2 dependence of the sextupole field. The x dependence of the quadrupole fields gives a resonant condition $2Q$ = integer. These examples show how the orders of resonances and multipoles are related to each other.

The a^2 dependence in Eq (3.13) leads to a linear dependence of width upon amplitude. For the half integer resonance a^1 dependence leads to a width which is

independent of amplitude, and in the case of fourth-order resonance the a^3 term gives a parabolic dependence of width upon amplitude.

Here we have studied only cases of type $nQ = l$. We could similarily treat the case $lQ_x + mQ_z = p$. We only give a working rule [Wi85] which says that one should keep any systematic resonance

$$lQ_x + mQ_z = S(\text{number of superperiods}) \times \text{integer} \tag{3.23}$$

out of the half integer square in which Q is situated.

A1. A Short Introduction to Electron Cooling

A1.1 Background

During the last two decades two techniques of improving the quality of charged particle beams have been developed: *stochastic cooling* [Me72] and *electron cooling* [Bu66, Be81, Sø83]. Stochastic cooling has been used succesfully to accumulate antiprotons which were collided with protons in the CERN-SPS to produce the intermediate vector bosons predicted by the unifying electro-weak theory. This work lead to the Nobel Prize in 1984 (shared by Carlo Rubbia and Simon van der Meer[Me84]). Electron cooling has been tested at the Nuclear Physics Institute of the Siberian Branch of the USSR Academy of Science at Novosibirsk during the years 1966 - 1976 [De77], at CERN during the Initial Cooling Experiment (ICE), which was started at 1977, and at Fermilab.

The theory of electron cooling was initiated at Novosibirsk by G.I. Budger, A. Skrinsky, and A. Derbenev [De77, De78, Bu78] who described the basic kinetics of e^--cooling and later refined the theory.

Today, there are several electron cooling projects around the world [Be81a, Bo87, De77a, Fi84, Fr87, Ha85, Hü82, Ma85, Mö86a, No84, Ol87, Po84, Sc87] which show the need for the good quality beams that cooling processes can provide. Physics that can be done with high quality ion beams has been discussed e.g. in [Da87, Fr85, Ki84, Mi87, Po84a, Wo86]. The special problems related to heavy ions and very low velocities have been treated in [Fr84, He84, He85b].

A review of electron cooling experiments has been published by H. Poth [Po85] and the differences of electron cooling and stochastic cooling has been discussed by D. Möhl [Mö84, Mö86].

A1.2 Basic Theory of Electron Cooling

Electron cooling is used in order to decrease the longitudinal and trasverse velocity spread of an ion beam. The cooling is carried out in a storage ring where the stored beam overlaps with a "cold" electron beam in a 1 to 3 meters long section. The mean velocities of the two beams are the same and in the rest frame of the beams the motion of the particles is like a motion of two mixed gases. Both components of the mixed gas have their own temperature (average kinetic energy), and through collisions (Coulomb collisions in the case of ions) the warmer gas gives heat to the cooler one. In an electron cooler device the electrons are contineously renewed and thus the temperature of the stored beam approaches the temperature of the cold e^--beam.

The transverse and longitudinal temperature of the beams are defined as

$$\begin{aligned} T_\perp &= Mc^2\beta^2\gamma^2\langle\Theta_\perp^2\rangle \\ T_\parallel &= Mc^2\beta^2(\frac{\Delta p}{p})^2 = Mc^2\beta^2\gamma^2\langle\Theta_\parallel^2\rangle, \end{aligned} \tag{A1.1}$$

where $\langle\Theta^2\rangle$ is the square of the relative rms velocity spread, defined as

$$\Theta_\perp = \frac{v_\perp^{\rm rms}}{\gamma\beta c} \quad \text{and} \quad \Theta_\parallel = \frac{v_\parallel^{\rm rms}}{\gamma\beta c}. \tag{A1.2}$$

The velocities v are expressed in the particle frame, whereas βc is the velocity of the particle frame with respect to the laboratory frame.

According to Spitzer [Sp56] the relaxation time of the temperature for charged particles in a two-component plasma (coverned by Rutherford scattering) is

$$\tau = \frac{M_1 M_2}{4\sqrt{3\pi}nLZ_1^2Z_2^2e^4}\left(\frac{T_1}{M_1}+\frac{T_2}{M_2}\right)^{3/2}, \tag{A1.3}$$

where the relaxation time in the particle frame is defined as

$$\frac{dT_1}{dt} = \frac{-(T_1-T_2)}{\tau}. \tag{A1.4}$$

Here Z and M are the atomic number and mass, respectively, n is the particle density (number of electrons per unit volume in our present case) and T is the temperature. L is the Coulomb logarithm

$$L = \int_{\rho_{\rm min}}^{\rho_{\rm max}} \frac{d\tau}{\tau} = \ln\frac{\rho_{\rm max}}{\rho_{\rm min}}, \tag{A1.5}$$

where $\rho_{\rm min}$ and $\rho_{\rm max}$ are the minimum and maximum impact parameters of the collisions, respectively.

The factor $4\sqrt{3\pi}$ comes from averaging over the velocity distribution. It varies in different publications depending on the distribution chosen and on the definition of $1/\tau$ as temperature ($\frac{1}{T}\frac{dT}{dt} = \frac{1}{v^2}\frac{dv^2}{dt}$) or velocity spread ($\frac{1}{v}\frac{dv}{dt}$) relaxation rate. This is of no relevance here as we are only interested in the functional dependence of τ on rms velocities and on the ions itself (mass, atomic number).

Applying Eq. (A1.3) to the electron-ion interaction (electron cooling) we get[Mø82]

$$\tau_{ei} = \frac{m_e M}{4\sqrt{3\pi}n_e Z^2 e^4 L_{ei}}\left(\frac{T_e}{m_e}+\frac{T_i}{M}\right)^{3/2}. \tag{A1.6}$$

Trasforming this to the laboratory frame and using the equation of continuity $J_e = n_e e\beta c$, we obtain

$$\tau = \frac{m_e M c^4\beta^4\gamma^5 e}{4\sqrt{3\pi}J_e Z^2 e^4 L_{ei}}\left(\Theta_e^2+\Theta_i^2\right)^{3/2} \tag{A1.7}$$

or

$$\tau \propto \frac{M\beta^4\gamma^5}{J_e Z^2} \left(\Theta_e^2 + \Theta_i^2\right)^{3/2}. \qquad (A1.8)$$

This equation gives the basic parametrical dependence of the time constant:

i) The velocity spread dependence $\tau \propto (\Theta_e^2 + \Theta_i^2)^{3/2}$ leads to two velocity regions where the larger velocity spread dominates:

$$\tau \propto \max\{\Theta_e^3, \Theta_i^3\}.$$

ii) The cooling time is inversely proportional to the electron current density J_e which is quite apparent.

iii) At a constant current density τ increases strongly with energy as $\beta^4\gamma^5$.

iv) For fixed angular divergence the time constant for heavy ions goes as M/Z^2.

In addition the cooling time depends on some device characteristics. Perhaps most important is the perveance of the electron gun. The perveance gives the limiting electron current obtained for a given gun voltage:

$$I_e = PU^{3/2}. \qquad (A1.9)$$

For a constant perveance gun (and in the nonrelativistic approximation where $T = eU \propto \beta^2$):

$$I_e = PU^{3/2} \propto \beta^3 P$$

Thus for a constant perveance e^--gun and a given divergence one has

$$\tau \propto \beta.$$

However, if $\Theta_{\perp e} \gg \Theta_{\perp i}$ we have

$$\tau \propto \frac{1}{\beta^2}$$

since

$$\Theta_\perp = \frac{v_\perp^{\mathrm{rms}}}{\beta c} \propto 1/\beta$$

($v_{\perp e}^{\mathrm{rms}}$ is ideally constant and give by the cathode temperature).

There are other parameters and processes that influence the performance of a storage ring with electron cooling. To mention only some of them: the velocity spread of the electron beam due to space charge, the tune shift of the ion beam due to e^--beam, as well as effects related to the solenoidal magnetic field which guides the electrons and to the reduction of the longitudinal electron velocity spread as the e-beam is accelerated. The combination of this magnetized electron - and flattened distribution effects lead to so called fast cooling[Pa84, Di84]. To give a full account would demand a separate paper. The aim of this chapter was only to give an introduction to electron cooling so that the reader is familiar with the subject when it appears in part 2 of this thesis.

PART 2

BEAM DYNAMICAL STUDIES OF CRYRING

Lattice Design Criteria and Operation Limits

1 Introduction

A special feature of CRYRING[He85a] is that it will be a multi-purpose ring: It will be operated both in synchrotron mode and in storage mode. In storage mode various kinds of experiments are planned to be done in the ring and then one usually has to cool the beam (e^- -cooling). There are, therefore, different requirements regarding beam properties at different parts of the circumference. The size of the ring itself is limited (max circumference 50 m) to save cost and to house the machine in an existing hall. Therefore, it is not possible to have special insertions for all different functions (injection, extraction, cooling, acceleration/deceleration, merged beams, crossed beams, ...). Some functions must be combined and this calls for flexibility of optics and beam characteristics. Typical constraints for an accelerator like CRYRING are listed in table 1.1.

Table 1.1.

Typical optical constraints for CRYRING

injection	large horizontal β, small dispersion
extraction	large horizontal β Q_x near a third order resonance long enough straight section
acceleration	small dispersion
crossed beams	small β_u-values, small dispersion long enough straight section
merged beams	small divergence long enough straight section
e^-- cooling	not too large β_u-values (equilibrium emittance) not too small β_u-values (cooling time) long enough straight section
chromaticity correction	non-zero dispersion horizontal correction: $\beta_x > \beta_y$ vertical correction : $\beta_y > \beta_x$

2 Lattice Design

Before going into details of the lattice calculations we first discuss the functions of CRYRING and the beam quality that is needed.

2.1 Extraction and Injection

At this stage of study it is foreseen that multi-turn injection is used. To achieve a large duty cycle (30 %) slow extraction will be used and hence the operation point should be in the vicinity of a horizontal third order resonance. The resonance $Q_x = 2.33$ is excited with a sextupole field of appropriate harmonic content.

For injection and extraction it is good to have large horizontal β-values. It has been planned to use electrostatic deflectors as proposed for ELENA [Le84]. Because the maximum momentum of the extracted beam is $q \cdot 430$ MeV/c, we need a relatively long septum and thus it was decided to separate injection and extraction.

More rigorous studies of injection and extraction schemes has been performed and the results can be found in reference [An85].

2.2 Electron Cooling

Most experiments planned to be done in the ring need very good longitudinal and transverse energy resolution. This calls for small $\frac{\Delta p}{p}$ and small emittances. To attain such a beam quality electron cooling is used. It is the transverse cooling that depends on the lattice functions. Cooling time sets the lower limit to β_u-values and the requirement of decreasing the transverse emittance sets the upper limit[He83].

We shall discuss the upper limit first:

If space-charge effects are neglected, the equilibrium beam divergence θ_i can be written as

$$\theta_i = \sqrt{\frac{m}{M}}\theta_e \tag{2.1}$$

where m is the electron mass and M the mass of the ion. This comes from the condition that in equilibrium electrons and ions should have the same transverse temperature. Space-charge effects and intrabeam scattering increase the equilibrium divergence. The transverse electron energy is a function of the electron gun cathode temperature and a cathode temperature of 1000 °C corresponds to an average electron energy of 0.055 eV in one degree of freedom which leads to a Θ_e of typically 20 mrad for CRYRING at low beam energies. To obtain efficient cooling the divergence Θ_i of the ions corresponding to a given emittance should be large.

In any case the initial rms divergence of the beam should be larger than shown above. The rms divergence of the ion beam with an emittance E_u is

$$\theta_{\mathrm{rms}} = \sqrt{\frac{E_u}{4\beta_u}} \tag{2.2}$$

where β_u is taken at a symmetry point in the center of the cooling section where we assume $\alpha = -\frac{1}{2}\mathrm{d}\beta_u/\mathrm{d}s = 0$.

Note that the emittance corresponds to a beam half width of 2σ.

From equations (2.1) and (2.2) we see that for given emittances largest acceptable β_u to ensure cooling is proportional to the mass of the ion, so that the lightest ions give the lowest limit for the β_u. The lightest ion planned to be cooled in CRYRING is Ar. Below we determine the limits for betatron amplitude functions in the cooling section corresponding to Ar.

We start from the assumption that the electron energy is 0.1 eV in one degree of freedom and that the lowest beam energy is 200 keV/u. This energy corresponds to an electron divergence of 30 mrad which leads to an Ar-beam divergence of 0.11 mrad by virtue of Eq. (2.1). If we now require the electron temperature to be smaller than the temperature of the stored beam we get the maximum permissible β_u-values from

$$\beta_u < \frac{E_u}{4\theta_i^2} \tag{2.3}$$

where E_u is given in units [π m rad]. If one wants the final emittance to be smaller than 0.5 π mm mrad, one requires

$$\beta_u < 10 \text{ m} \tag{2.4}$$

This is not a bad assumption, since in some of the experiments planned the final emittance should of the order of 0.5 π mm mrad. If smaller emittances are required the β-values should be smaller.

Next we discuss the lower limit of β_u:

The cooling time is proportional to (see part one)

$$\tau \propto (\theta_e^2 + \theta_i^2)^{\frac{3}{2}} \tag{2.5}$$

To get the fastest possible cooling the rms divergence of the ions must be smaller than the rms divergence of the electrons. Because of the quadratic addition an ion divergence 20 % smaller than the electron divergence gives about a factor 2 longer cooling time compared to zero ion divergence. Hence we can require that the ion divergence should not be larger than 80 % of the electron divergence. The electron divergence is smallest at large beam energies. The highest energy of the cooled beam has not yet been decided for CRYRING, but it will not be larger than 10 MeV/u and most probably it will be much lower. If we, however, have such a fast beam the corresponding electron divergence is about 3 mrad (0.055 eV/degree

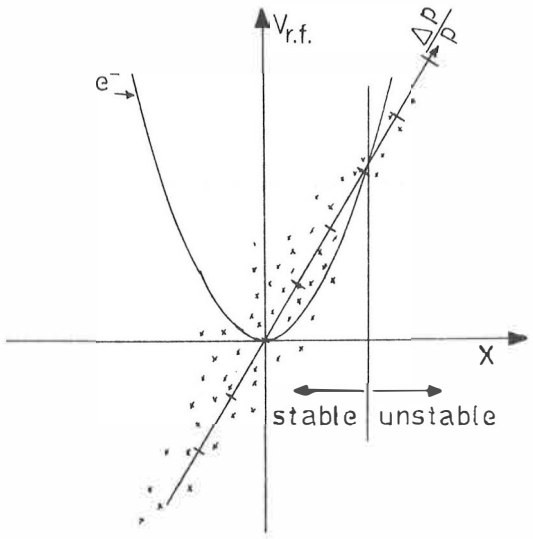

Figure 2.1
Ion and electron (rest mass) velocity distributions

of freedom). Then the maximum allowed ion divergence is about 2.4 mrad. The smallest permissible β_u-value is then (by virtue of Eq. (2.2))

$$\beta_u > \frac{E_u}{4\theta_i^2} \quad , \quad \theta_i \leq 0.8\theta_e \approx 2.4 \text{ mrad} \tag{2.6}$$

Because the injection energy will be of the order of 300 keV/u, adiabatic damping can cause the transverse emittances for a 10 MeV/u beam to be 10 π mm mrad with planned apertures. Hence the lower limit (2.6) for β_u is

$$\beta_u > 0.43 \text{ m} \tag{2.7}$$

If emittance blow up occurs β_u has to be increased accordingly. To fulfill the two requirements discussed we thus obtain for the betatron amplitude functions in the electron cooling section:

$$0.4 \text{ m} < \beta_u < 10 \text{ m} \tag{2.8}$$

The dispersion in the electron cooling section should also be determined. However, there are too many open parameters to be able to specify a unique optimum. If there is no dispersion and the transverse emittances are not too big all particles will be cooled longitudinally i.e. $\Delta p/p$ will be decreased. If the dispersion and the initial momentum spread are large enough, there is a certain portion of ions whose momentum will be increased whereas the other ions will be cooled normally (and even faster than without dispersion). The electron velocity as a function of distance from the symmetry axis is a parabola due to electron beam space charge. The ion velocity distribution follows a line whose slope is $1/D_u$. These are sketched in figure 2.1.

In longitudinal cooling the velocity of the ions tends to approach the electron velocity. Hence, the ions in the stable region move towards the crossing of the curves and the ions in the unstable region move away from the beam axis with increasing velocity. The smaller the dispersion, the steeper the $\Delta p/p$-line in figure 2.1 thus increasing the range of "stable" $\Delta p/p$-values. We must, however, remember that the cooling becomes slower when the velocity difference between electrons and ions increases, as in the case where D is too small such that the $\Delta p/p$-line matches poorly with a branch of the parabola in fiqure 2.1.

For stability reasons (Keil-Schnell limit for microwave instability[Ke69]), it may be necessary to have a "stabilizing" tail in the momentum distribution[Ho83][Ho84]. We can use dispersion in the cooling section to build up this tail but there are also other methods for making the tail (time dependent electron energy). To be able to determine the value of the dispersion we must know the momentum distribution of the ions at the beginning of the cooling, and also the properties of the cooling device. In any case, it seems safe to have a small but finite dispersion in the cooling section where the exact value is determined from a compromise between the width of the stable Δp-range and the cooling speed.

When we consider electron cooling at low beam energies, the initial momentum spread might be too large without some kind of pre-cooling (too many particles in the unstable region or just too long cooling time due to large velocity difference). One way of pre-cooling the slow beam is to first accelerate it to a higher energy to achieve smaller momentum spread, cool the beam at the higher energy and then decelerate it to lower energies, and perhaps cool the beam in several steps during the deceleration. One notes that the electron cooling itself is a challenging topic of research.

2.3 Merged Beams

One of the most interesting (and most difficult) class of experiments planned to be done in CRYRING are experiments with two merging ion beams. In such a situation it is possible to achieve very low center of mass energies, below 1 eV may be (with certain restrictions). Very low center of mass energies call for a very good energy resolution, both longitudinal and transverse. Hence one must have the smallest possible $\frac{\Delta p}{p}$ and divergence in both beams. Small divergence means a small transverse emittance and/or large β_u-values. The properties of the external beam are determined by the injection line and therefore we discuss only the focusing of the stored beam.

The center of mass energy is determined by the energy difference between the two beams and the angle between them. Even if the two beams are absolutely parallel and syncronized in energy we will get some contribution to E_{cm} from the transverse motion, since it is not possible to have zero emittance, and from the logitudinal motion since $\frac{\Delta p}{p}$ cannot be zero either. The motion of the ions in the beam increases both E_{cm} and ΔE_{cm}.

If we assume Gaussian beams we can calculate the expectation value of the center of mass energy. It doesn't actually correspond to the maximum amplitude of the

E_{cm} distribution since the transverse motion of the ions has only an increasing contribution to E_{cm} and the distribution of the square of the transverse velocity is not symmetrical. However, if $\frac{\Delta p}{p}$ for the two beams is large enough the non-symmetrical contribution from the transverse motion cannot be seen.

Below the expectation value and the standard deviation of the center of mass energy distribution in the case of merged beams are calculated. Before doing any calculations we have to make some assumptions concerning the velocity distributions of the two beams.

2.3.1 Assumptions

We assume that all the velocity components of the two beams are Gaussian (see figures 2.2 and 2.3).

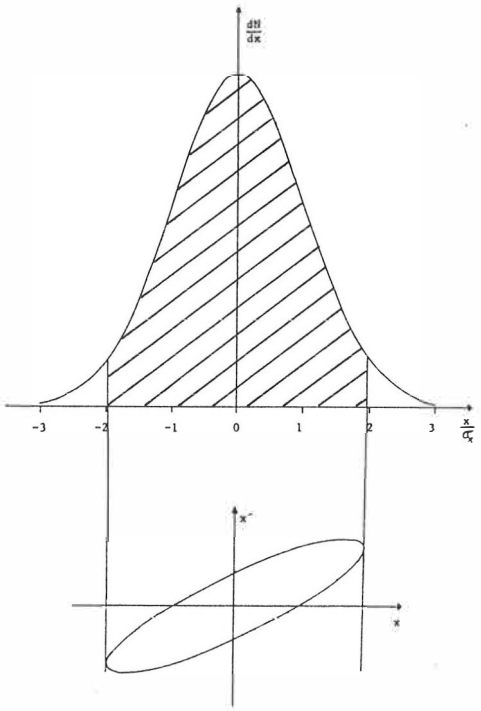

Figure 2.2
Beam distribution in the transverse phase space.

In figure 2.2 the transverse amplitude distribution is shown, but one gets a similiar distribution for the beam divergence and hence for the transverse velocity component as well. The area of the phase space ellipse, i.e. the emittance E, can be written as

$$E = \frac{u^2\pi}{\beta} = \frac{(\delta_u\sigma_u)^2\pi}{\beta}$$

or

$$E = \frac{u'^2\pi\beta}{1+\alpha^2} = u'^2\pi\beta^* = (\delta_u\sigma_u)^2\pi\beta^* \qquad (2.9)$$

where α and β are the Twiss parameters and β^* is β at a symmetry point where we have an upright phase space ellipse ($\alpha = 0$). The coefficient δ_u relates emittance to the standard deviation of the beam dimension σ_u. If the emittance E is defined to contain 95 % of particles in the phase space $\delta_u = \sqrt{6}$. Similarily (fig. 2.3) $\delta_p = 1.96$ defines the momentum range ($\Delta p/p = \pm\delta_p\sigma_p$) that contains 95 % of the ions.

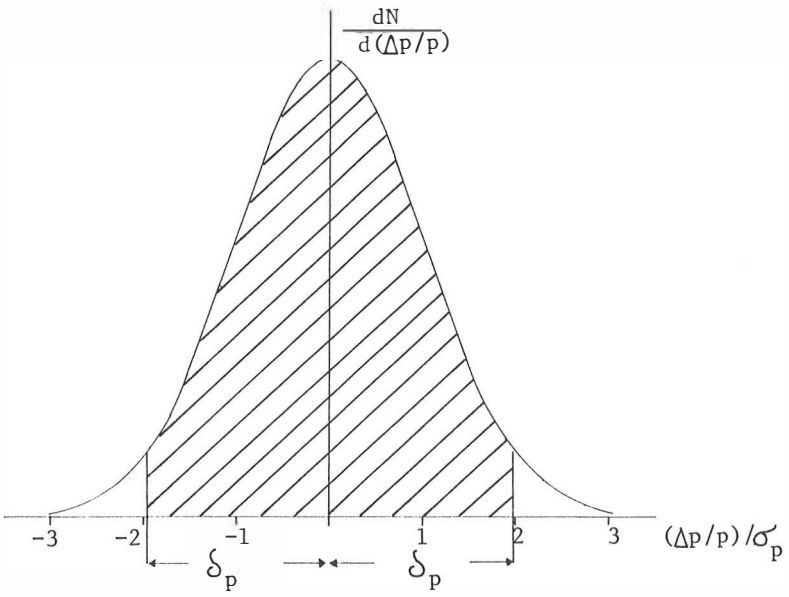

Figure 2.3
The logitudinal velocity distribution ($\frac{\Delta p}{p}$).

Finally, we assume that the velocities of the two beams do not differ too much. This is naturally always true in the practical merged beams experiments. We can allow a small angle between the two beams, but in the experiments the aim usually is to align the beams as well as possible. Furthermore, we impose no constraints on the positions of the colliding particles. The positions of two colliding particles should be equal except for a small "uncertainty" $\Delta r = \sqrt{\sigma/\pi}$ given by the cross-section of the reaction under study ($\sqrt{\sigma} \leq 10^{-7}$ cm). Non-zero dispersion together with

$\Delta p/p$ will change the position of the particle (which will also mix the longitudinal and the transverse phase space). Similarily, the divergence distribution changes with the position being broadest in the center of the beam. Since the constraint on the poisition has been left out the value for ΔE_{cm} will be somewhat larger than in the reality. Also the "transverse component" of the center of mass energy will be a little larger. In cases where the longitudinal part in the energy resolution is dominating the effect on the E_{cm} is neqligible.

2.3.2 The expectation value for the center of mass energy E_{cm}

The center of mass energy for two colliding ions is (in nonrelativistic approximation):

$$E_{cm} = \frac{1}{2}\mu u^2 \quad , \quad \mu = \frac{m_1 m_2}{m_1 + m_2} \tag{2.10}$$

where

$$u^2 = (V_1 - V_2)^2 + (V_1 x_1' - V_2 x_2')^2 + (V_1 y_1' - V_2 y_2')^2$$

The distributions of the velocity components and divergences are

$$\begin{aligned} V &\sim N(\langle V\rangle, \sigma_V^2) \\ x' &\sim N(\langle x'\rangle, \sigma_{x'}^2) \\ y' &\sim N(\langle y'\rangle, \sigma_{y'}^2) \end{aligned} \tag{2.11}$$

Since, in the case of merged beams, the divergences x' and y' are small the longitudinal velocities can be written (in the nonrelativistic case where $T = \frac{1}{2}mV^2$):

$$V_1 = \sqrt{\frac{2T_1}{m_1}} = \sqrt{2t_1} \quad , \quad V_2 = \sqrt{\frac{2T_2}{m_2}} = \sqrt{2t_2} \tag{2.12}$$

We can also substitute $V_1 \approx V_2 \approx V$ into the transverse part and hence we get for the expectation value

$$\langle E_{cm}\rangle = \frac{1}{2}\mu\left[\langle (V_1 - V_2)^2\rangle + V^2\langle (x_1' - x_2')^2\rangle + V^2\langle (y_1' - y_2')^2\rangle\right] \tag{2.13}$$

From the distributions we get

$$\begin{aligned} \langle (V_1 - V_2)^2\rangle &= (\langle V_1\rangle - \langle V_2\rangle)^2 + \sigma_{V_1}^2 + \sigma_{V_2}^2 \\ \langle (x_1' - x_2')^2\rangle &= (\langle x_1'\rangle - \langle x_2'\rangle)^2 + \sigma_{x_1'}^2 + \sigma_{x_2'}^2 \\ \langle (y_1' - y_2')^2\rangle &= (\langle y_1'\rangle - \langle y_2'\rangle)^2 + \sigma_{y_1'}^2 + \sigma_{y_2'}^2 \end{aligned} \tag{2.14}$$

If the average specific energy of the two beams is t and the specific energy difference is Δt, we can write

$$(\langle V_1\rangle - \langle V_2\rangle)^2 = V^2\left(1 - \sqrt{\frac{t + \Delta t}{t}}\right)^2 \tag{2.15}$$

where $V = \sqrt{2t}$. Writing σ_V in terms of $\frac{\Delta p}{p}$ we have (again in nonrelativistic approximation)

$$\sigma_V = V\sigma_p \tag{2.16}$$

where σ_p is the standard deviation for the $\frac{\Delta p}{p}$ distribution. Making the substitutions shown above, we can finally write

$$\langle E_{cm}\rangle = \mu t\left[\left(1-\sqrt{1+\frac{\Delta t}{t}}\right)^2 + \langle x_1' - x_2'\rangle^2 + \langle y_1' - y_2'\rangle^2 + \sigma^2\right] \tag{2.17}$$

where

$$\sigma^2 = \sigma_{p_1}^2 + \sigma_{p_2}^2 + \sigma_{x_1'}^2 + \sigma_{x_2'}^2 + \sigma_{y_1'}^2 + \sigma_{y_2'}^2$$

and

$$\sigma_p^2 = \left(\frac{\Delta p/p}{\delta_p}\right)^2$$

$$\sigma_{x'}^2 = \frac{E_x}{\delta_E^2 \pi \beta_x^*}$$

$$\sigma_{y'}^2 = \frac{E_y}{\delta_E^2 \pi \beta_y^*}$$

$$\mu = \frac{m_1 m_2}{m_1 + m_2}$$

When the two beams are perfectly parallel and sychronized in energy only the last term in the brackets remains and the c.m. energy is determined by the velocity spreads of the two beams.

2.3.3 The standard deviation of the center of mass energy

The variance of the center of mass energy is

$$\sigma^2\{E_{cm}\} = \frac{1}{4}\mu\Big\{\sigma^2\left\{(V_1 - V_2)^2\right\} + V^4\left(\sigma^2\left\{(x_1' - x_2')^2\right\} + \left(\sigma^2\left\{(y_1' - y_2')^2\right\}\right)\right\} \tag{2.18}$$

We calculate first the logitudinal part and write

$$\sigma^2\{V_\parallel^2\} = \sigma^2\{(V_1 - V_2)^2\} \tag{2.19}$$

and thus

$$V_\parallel = V_1 - V_2 \sim N\left(\langle V_1\rangle - \langle V_2\rangle, \sigma_{V_1}^2 + \sigma_{V_2}^2\right) = N(\mu, \sigma_\parallel^2) \tag{2.20}$$

The square of a variable that is normally distributed with parameters $N(0,1)$ is χ^2 distributed with one degree of freedom and its variance is 2, i.e.

$$\left(\frac{V_\parallel - \mu}{\sigma_\parallel}\right)^2 \sim \chi_1^2 \tag{2.21a}$$

and

$$\sigma^2\left\{\left(\frac{V_\parallel - \mu}{\sigma_\parallel}\right)^2\right\} = 2 \tag{2.21b}$$

So, we can write

$$\sigma^2\left\{V_\parallel^2+\mu^2-2V_\parallel\mu\right\}=2\sigma_\parallel^4$$
$$\sigma^2\{V_\parallel^2\}+4\mu^2\sigma^2\{V_\parallel\}+2\langle-2\mu V_\parallel^2V_\parallel\rangle-2\langle V_\parallel^2\rangle\langle-2\mu V_\parallel\rangle=2\sigma_\parallel^4 \qquad (2.22)$$

Knowing that

$$\langle V_\parallel\rangle=\mu \quad , \quad \langle V_\parallel^2\rangle=\sigma_\parallel^2+\mu^2 \quad \text{and} \quad \sigma^2\{V_\parallel\}=\sigma_\parallel^2$$

and combining some terms we get

$$\sigma^2\{V_\parallel^2\}+8\mu^2\sigma_\parallel^2+4\mu^4-4\mu\langle V_\parallel^3\rangle=2\sigma_\parallel^4 \qquad (2.23)$$

It is relatively easy to verify that

$$\langle V_\parallel^3\rangle=\mu^3+3\sigma_\parallel^3\mu \qquad (2.24)$$

Substituting this into the previous equation and combining terms we get

$$\sigma^2\{V_\parallel^2\}=2\sigma_\parallel^2(\sigma_\parallel^2+2\mu^2) \qquad (2.25)$$

This can be written in terms of the known parameters as

$$\sigma^2\left\{(V_1-V_2)^2\right\}=2V^4\left(\sigma_{p_1}^2+\sigma_{p_2}^2\right)\left(\sigma_{p_1}^2+\sigma_{p_2}^2+2\left(1-\sqrt{1+\frac{\Delta t}{t}}\right)^2\right) \qquad (2.26)$$

The variances of the transverse components can be written in the form of equation (2.25) and thus we can finally write down the standard deviation of center of mass energy as

$$\sigma\{E_{cm}\}=\sqrt{2}\mu t\sqrt{\begin{array}{l}\left(\sigma_{p_1}^2+\sigma_{p_2}^2\right)\left(\sigma_{p_1}^2+\sigma_{p_2}^2+2\left(1-\sqrt{1+\frac{\Delta t}{t}}\right)^2\right)\\ \ldots+\left(\sigma_{x_1'}^2+\sigma_{x_2'}^2\right)\left(\sigma_{x_1'}^2+\sigma_{x_2'}^2+2\langle x_1'-x_2'\rangle^2\right)\\ \ldots+\left(\sigma_{y_1'}^2+\sigma_{y_2'}^2\right)\left(\sigma_{y_1'}^2+\sigma_{y_2'}^2+2\langle y_1'-y_2'\rangle^2\right)\end{array}} \qquad (2.27)$$

Note, however, that in practice the distribution is not infinite but truncated by the machine acceptances. Both beams are therefore not pure Gaussian. This means that the approximations made tend to lead to a somewhat pessimistic estimate of both E_{cm} and ΔE_{cm}.

2.3.4 Merged beams in CRYRING

One of the design goals for CRYRING was to optimize the lattice functions for merged beams experiments in one straight section. This means that we have to

keep the beam divergences as small as possible in the interaction region. As the beams travel together it is evident that it is not allowed to use any quadrupoles at this straight section. The β values have to be as large as possible to have small divergence for given emittance (c.f. Eq. (2.2)).

Later in the text we shall discuss the attainable quality of the stored beam (intabeam scattering vs. cooling). Here we use approximate values of emittance and $\frac{\Delta p}{p}$ to study the possibility of merged beam experiments with very low center of mass energy and good energy resolution.

The horizontal β^* in the merged beams straight section that resulted from a lattice optimization is 2.17 m and the vertical 2.67 m. The values for the extarnal beam depend on the injection line and here we assume that the optics of this line can be adjusted so that $\beta_x^* = 5$ m and $\beta_y^* = 3$ m, for example.

As an example, we take the case of Ar^{18+} and H^-. Due to intrabeam scattering one does not want to go below the beam energy of 200 keV/u because of the strong energy dependence in the divergence and momentum growth rates ($\beta^3\gamma^4$). Even at this energy the maximum number of stored Ar ions is $\approx 10^5$ for emittances $E_x \approx 0.2\,\pi$ mm mrad, $E_y \approx 0.2\,\pi$ mm mrad and $\Delta p/p \approx 2 \cdot 10^{-4}$. The distribution of the center of mass energy in the collisions is shown in figure 2.4 for two cases. The broader distribution is perhaps more realistic and corresponds to $\frac{\Delta p}{p}(\mathrm{Ar}) = 2{\cdot}10^{-4}$, $\frac{\Delta p}{p}(\mathrm{H}) = 10^{-4}$, $E_{x,y}(\mathrm{Ar}) = 0.2\,\pi$ mm mrad and $E_{x,y}(\mathrm{H}) = 1\,\pi$ mm mrad. The expectation value for the center of mass energy $\langle E_{cm} \rangle = 1.0$ eV. The energy of the Ar beam is 200 keV/u and the energy difference of the beams is 889 eV/u. The full width of half maximum is ≈ 0.25 eV and the standard deviation of the distribution $\sigma\{E_{cm}\} = 0.105$ eV.

The narrower distribution is for the same case except that $\Delta p/p = 10^{-5}$ for both beams and that $E_{x,y}(\mathrm{Ar}) = 0.1\,\pi$ mm mrad which is the emittance that corresponds to the transverse electron temperature in the cooler device at this beam energy. The full width of half maximum of the distribution is ≈ 0.04 eV ($\sigma\{E_{cm}\} = 0.033$eV). One can see that the distribution is not symmetrical because the transverse part is dominating and it only increases E_{cm} provided that $\langle x_1' - x_2' \rangle = \langle y_1' - y_2' \rangle = 0$.

Here we have assumed that the two beams are absolutely collinear. If the beam energies stay constant a small angle between the beams shifts $\langle E_{cm} \rangle$ to higher values (see equation 2.17). At the same time the peak becomes broader (eq. 2.27) but this broadening in most cases is smaller compared to the energy shift. In practical experiments the data is collected from several injected and cooled pulses and thus it is necessary to keep the possible angle between the two beams as stable as possible.

The energy shift due to an alignement error has to be compared with the "best" width of the energy peak without errors. In this case it seems that one cannot come below FWHM $\approx 25\%$ ($\sigma\{E_{cm}\} \approx 11\%$). If the alignement errors are 1 mrad both horizontally and vertically the $\langle E_{cm} \rangle$ shift is 0.4 eV. We require that the energy shift should not exceed 0.5 FWHM and this means that the alignement errors should not be larger than 0.5 mrad. If a shift of 0.1 FWHM is allowed the

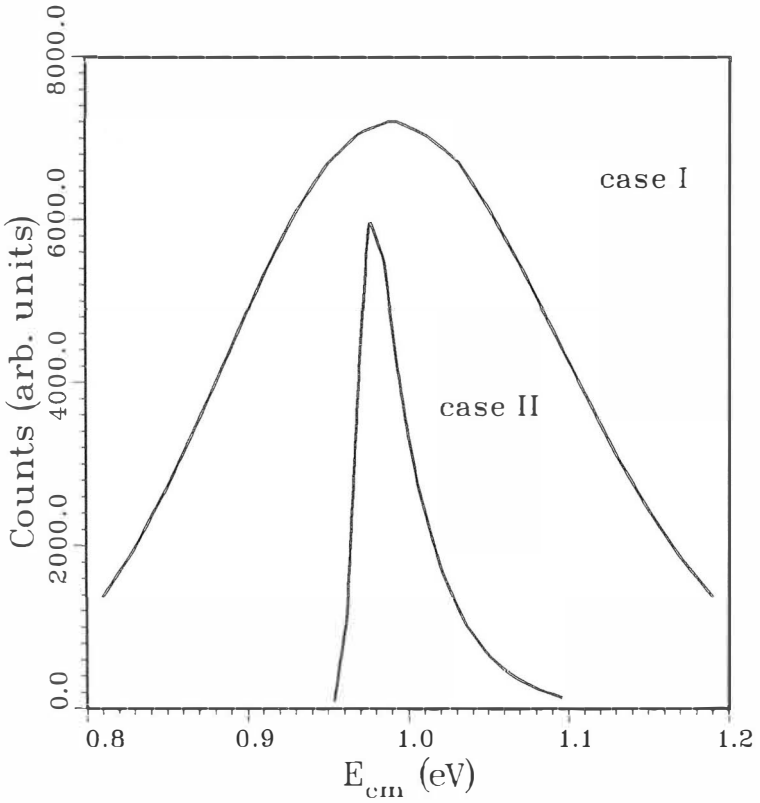

Figure 2.4

Center of mass energy distribution for merged beams with $E_{x,y}(\mathrm{Ar}) = 0.2\,\pi$ mm mrad, $E_{x,y}(\mathrm{H}) = 1\,\pi$ mm mrad, $\frac{\Delta p}{p}(\mathrm{Ar}) = 2 \cdot 10^{-4}$, $\frac{\Delta p}{p}(\mathrm{H}) = 1 \cdot 10^{-4}$ (case I), and $E_{x,y}(\mathrm{Ar}) = 0.1\,\pi$ mm mrad, $E_{x,y}(\mathrm{H}) = 1\,\pi$ mm mrad, $\frac{\Delta p}{p}(\mathrm{Ar,H}) = 1 \cdot 10^{-5}$ (case II)

alignement should be done with a precision of ≈ 0.2 mrad. Actually, the derivative of dispersion $\mathrm{d}D/\mathrm{d}s = D'$ changes the horizontal angle of the beams. D' for the stored beam is zero and for the outer beam it can be adjusted by the injection line. However, at the same time the β values are changed as well. The β values are more important for this kind of experiments since $\Delta p/p$ for the outer beam can be assumed to be small. Since $\frac{\Delta p}{p} D'$ gives the change of $\langle x' \rangle$ we require that $D' < 1$ if $\Delta p/p \approx 10^{-4}$.

Another limit for the angle between the two beams comes from the fact that the beams should overlap as much as possible to give the maximum collision rate. The diameters of the beams are of the order of 1 – 4 mm if emittances around 0.2 – 1

Table 2.1

$\langle E_{cm}\rangle$[eV] for different horizontal and vertical alignement errors $\Delta x'$, $\Delta y'$ (mrad) for Ar^{18+} ($\frac{\Delta p}{p} = 2 \cdot 10^{-4}$, $E_{x,y} = 0.2\,\pi$ mm mrad, $t = 200$ keV/u) and H^- ($\frac{\Delta p}{p} = 10^{-4}$, $E_{x,y} = 1\,\pi$ mm mrad, $t = 200.889$ keV/u)

	$\langle \Delta x' \rangle$					
$\langle \Delta y' \rangle$	0.0	0.1	0.2	0.3	0.5	1.0
0.0	1.000	1.002	1.008	1.018	1.049	1.195
0.1	1.002	1.004	1.010	1.020	1.051	1.197
0.2	1.008	1.010	1.016	1.025	1.057	1.203
0.3	1.018	1.020	1.025	1.035	1.066	1.213
0.5	1.049	1.051	1.057	1.066	1.098	1.244
1.0	1.195	1.197	1.203	1.213	1.244	1.390

Table 2.2

$\sigma\{E_{cm}\}$ [eV] for different horizontal and vertical alignement errors $\Delta x'$, $\Delta y'$ (mrad) for Ar^{18+} ($\frac{\Delta p}{p} = 2 \cdot 10^{-4}$, $E_{x,y} = 0.2\,\pi$ mm mrad, $t = 200$ keV/u) and H^- ($\frac{\Delta p}{p} = 10^{-4}$, $E_{x,y} = 1\,\pi$ mm mrad, $t = 200.889$ keV/u)

	$\langle \Delta x' \rangle$					
$\langle \Delta y' \rangle$	0.0	0.1	0.2	0.3	0.5	1.0
0.0	0.105	0.106	0.108	0.110	0.118	0.151
0.1	0.106	0.107	0.108	0.111	0.119	0.151
0.2	0.108	0.109	0.110	0.113	0.121	0.153
0.3	0.112	0.113	0.114	0.117	0.124	0.155
0.5	0.123	0.124	0.125	0.127	0.134	0.163
1.0	0.165	0.166	0.167	0.168	0.174	0.197

π mm mrad are achieved. The length of the merged beams straight section is 3.0 m which gives raise to an alignement precision of ≈ 0.3 mrad.

●verlapping of the beams requires also that the horizontal and vertical tolerances for the position of the beams are of the order of 0.2 – 1.0 mm corresponding to the rms radii of the beams. This is not an easy task. The only way to make this easier is to make the β values of the outer beam larger (the diameter of the beam goes as $\sqrt{\beta}$). This would also be favourable to the energy resolution. The emittances cannot be made larger in order to increase the beam dimensions since it would destroy the transverse energy resolution.

2.4 Crossed Beams

Among other things it has been proposed to use CRYRING for crossed beams experiments. When we have two beams with specific energies t_1 and t_2 (kinetic energy divided by mass) colliding at an angle α the center of mass energy is obtained easily from vector calculus and it is (in nonrelativistic approximation)

$$E_{cm} = \mu(t_1 + t_2 - 2\sqrt{t_1 t_2}\cos\alpha) \tag{2.28}$$

From this equation we see that the divergences of the beams directly give the transverse energy resolution, i.e. a divergence of 1 mrad gives an energy resolution of the order of 0.1 % ($\alpha \approx 90^o$). By electron cooling one should easily reach beam divergences of 1 mrad and smaller (eq. 2.1). The external beam cannot be cooled (which is also the case in the merged beams experiments) and the transverse emittances must be reduced with slits in the injection beam line.

It is not obvious how to do crossed beams experiments in order to determine absolute cross-sections, since in that case one has to know the beam profiles rather exactly and when the beam has been cooled the diameter will be of the order of mm, which makes it rather difficult to determine its profile. One way of circumventing the beam profile determination is to sweep the other beam [Br83]. So far, we have not in detail studied the capability of this method to measure absolute cross-sections with the beam sizes that CRYRING would provide.

If we then consider the luminosity of the beams we know that the diameter of each beam should be as small as possible.

The dispersion is not a severe problem here because it affects only the horizontal width of the beam and thus doesn't introduce a thick target when the detection takes place vertically. The momentum spread of the cooled beam is, anyhow, very small so that the beam width increase due to dispersion should be of the order of one mm at the most.

2.5 Lattice Calculations

In the lattice calculations the program MAD [Is85] has been used. The main goal was to find a lattice that could be used both in the storage (cooler ring) and synchrotron mode with almost the same magnet excitation, which means that the lattice functions should be suitable for experiments done in the storage mode and that the horizontal Q-value should be in the vicinity of a third order resonance to permit a slow resonant extraction. We also wanted to minimize the natural chromaticities in order to avoid too strong chromaticity correction sextupoles. Therefore the quadrupoles shouldn't be too strong either.

One possible lattice was presented at the 1985 Particle Accelerator Conference in Vancouver [He85]. However, this lattice was then modified during the extraction studies [An85]. The modified lattice is also presented in reference [He86]. However,

during the year 1986 a decision was made to place the the ion source and the RFQ[Sc85] in the former cyclotron vault which then left the whole "experimental area" for the ring. This allowed us to increase the length of the ring up to almost 50 meters. One reason for lattice modifications was that the earlier lattice had sector dipoles. Because of fast ramping the dipoles must be laminated. Since it is easier to manufacture laminated rectangular magnets than sector magnets it was decided to search for a lattice where rectangular dipoles could be used. Another natural reason was that it is always easier to find space in a longer ring for equipment such as the electron cooling device, pumps, diagnostics etc.

In Appendix 1 an input of the latest lattice[Bá87][Je87] for program MAD (version 4.02) is shown, from which at least a MAD-user can see the details of the lattice. The corresponding MAD output is also given in Appendix 1. The ring has six symmetrical superperiods as shown in figure 2.5. The lengths of the long straight sections may be somewhat varied in the final lattice.

The lattice parameters of CRYRING are shown in table 2.3

Table 2.3

The lattice parameters of CRYRING

$\beta_x^{\min}$	2.17 m
$\beta_y^{\min}$	2.67 m
$\beta_x^{\max}$	5.68 m
$\beta_y^{\max}$	7.30 m
$D_x^{\max}$	1.88 m
D_x(straight)	1.39 m
Q_x	2.30
Q_y	2.27
Q'_x	-1.36 (natural)
Q'_y	-3.30 (natural)
γ_t	2.29

The natural chromaticities can be brought near to zero with the sextupole strengts (K2) shown in the MAD-input (2.3, -3.2). The third order resonance ($3Q_x = 7$) is excited by changing the strengths of sextupoles to introduce a 7^{th} harmonic perturbation without changing the harmonic zero. In this way the chromaticity does not change.

The lattice functions are shown in figure 2.6.

In the case of merged beams the q/A ratio for positive external ions in the merged beams case (i) must be large (to get high enough velocity through acceleration from a small platform), (ii) must be smaller than that for the stored beam (larger bending radius than the stored one for approximately same velocities). This means that the variety of available positive external beams in the merged beams

experiments is relatively small. One possibility is to inject neutral beams but in that case one might meet some problems concerning divergences (transverse emittances). The case of negative external beams should be the easiest one.

Table 2.4 gives the main parameters of the ring. The lengths of elements in the MAD-input and in table 2.4 are naturally effective lengths.

Table 2.4

Main parameters of CRYRING

Circumference		48.63 m
Maximum momentum		q 430 MeV/c
Dipoles	laminated, parallel endfaces	
	no field gradient	
	number	12
	bending angle	30 degrees
	bending radius	1.2 m
	vertical gap	10.0 cm
Quadrupoles		
	horizontal focusing	
	number	12
	magnetic length	30 cm
	max gradient	5 T/m
	vertical focusing	
	number	6
	magnetic length	30 cm
	max gradient	5 T/m
Sextupoles		
	horizontal focusing	
	number	12
	magnetic length	20 cm
	max gradient	12 T/m^2
	vertical focusing	
	number	12
	magnetic length	20 cm
	max gradient	12 T/m^2

In addition to the magnetic elements listed above, we need small dipoles to introduce an orbit bump in the injection and in the extraction.

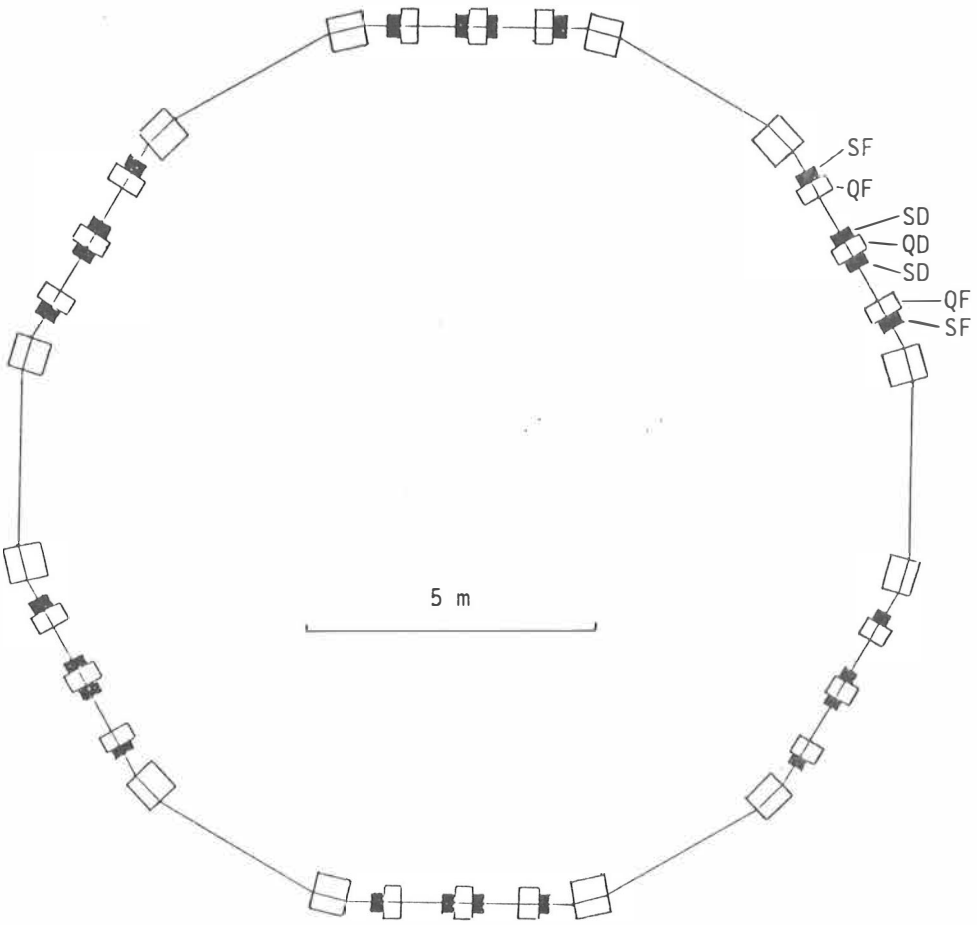

Figure 2.5
The lattice of CRYRING

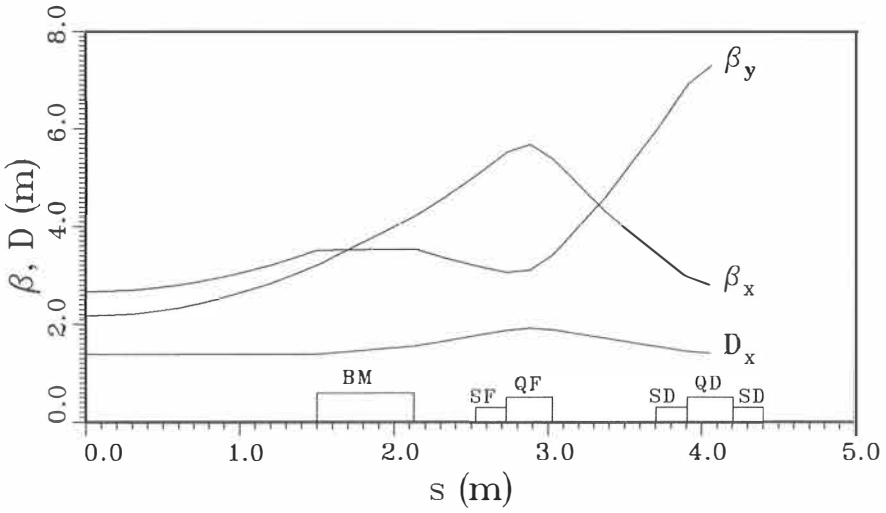

Figure 2.6
The lattice functions in one half of a superperiod of CRYRING

3 Operation Limits

In a storage ring there are always certain limits for intensity and momentum spread. In our case (low energy, small ring) the space charge tune shift sets a limit for the maximum number of ions in the ring and the microwave instability (Keil-Schnell limit) may set an upper bound for the momentum spread at a certain intensity. It seems that for highly charged ions such as Ar^{18+}, with injection energy 300 keV/u, the maximum number of ions in the ring is $10^8 - 10^9$ depending on the available aperture and whether multiturn injection is used or not. This limit goes down when the energy is decreased. However, with lower energies one usually wants very good energy precision and then the Keil-Schnell limit gives a smaller maximum intensity than the space charge tune shift. These limits are discussed below, and in particular the possibility of working above the Keil-Schnell limit is raised.

3.1 Space Charge Limit

An ion in the beam feels the electromagnetic field of the rest of the beam. This field is defocusing. Since this defocusing is not the same for all particles it cannot be totally compensated for by adjusting quadrupole fields. One can write the following expression for the maximum number of ions in the ring for a given tune shift δQ [Bo70].

$$N = \frac{\pi E_y (1 + \sqrt{E_x/E_y}) \beta^2 \gamma^3 B_f \delta Q A}{F r_o q^2} \tag{3.1}$$

where

E_x	=	horizontal emittance [π m rad]
E_y	=	vertical emittance [π m rad]
β	=	v/c
γ	=	$(1-\beta^2)^{-\frac{1}{2}}$
B_f	=	bunching factor (≤ 1)
δQ	=	tune shift
A	=	mass number
q	=	charge state
F	=	qeometrical factor (≈ 1)
r_o	=	classical proton radius ($1.5 \cdot 10^{-18}$ m)

The emittances given above are areas of phase space ellipses, and the values must be given without the factor π. The geometrical factor F depends on the beam and vacuum tube dimensions. F is 1 for a circular vacuum tube and for an elliptical tube it is a little larger. We can use $F = 1$.

Note that N for low velocities is proportional to energy if emittance is constant. However, in adiabatic acceleration/deceleration it is the normalized emittance $\beta\gamma E$

that is constant and thus in practice we have N proportional to velocity. Another important factor is that N goes down as q^{-2}. We usually want δQ to be smaller than 0.1 so that the beam doesn't get into destructive resonances. The only way to increase the intensity of the beam is then to make the emittances larger or in the case of synchrotron mode to increase the injection energy. The emittance can be increased with multiturn injection (where the horizontal phase space is filled by moving the equilibrium orbit inwards during the injection) and/or by filling the vertical phase space by using either an orbit bump or deflectors.

Below we give two tables of maximum number of ions in the ring, one for the injection energy and one for the lowest planned energy.

Table 3.1

Space charge limit for CRYRING at t = 300 keV/u
and $\delta Q = 0.1$
a) $E_x = E_y = 100\,\pi$ mm mrad (multi turn injection)
b) $E_x = E_y = 10\,\pi$ mm mrad

Ion	N (a)	N (b)
Ar^{18+}	$3 \cdot 10^9 \cdot B_f$	$3 \cdot 10^8 \cdot B_f$
Kr^{34+}	$2 \cdot 10^9 \cdot B_f$	$2 \cdot 10^8 \cdot B_f$
Xe^{44+}	$2 \cdot 10^9 \cdot B_f$	$2 \cdot 10^8 \cdot B_f$
Pb^{60+}	$1.5 \cdot 10^9 \cdot B_f$	$1.5 \cdot 10^8 \cdot B_f$

Table 3.2

Space charge limit for CRYRING at t = 200 keV/u
and $\delta Q = 0.01$
a) $E_x = E_y = 10\,\pi$ mm mrad
b) $E_x = E_y = 0.2\,\pi$ mm mrad (cooled beam)

Ion	N (a)	N (b)
Ar^{12+}	$5 \cdot 10^7 \cdot B_f$	$1 \cdot 10^6 \cdot B_f$
Ar^{18+}	$2 \cdot 10^7 \cdot B_f$	$4 \cdot 10^5 \cdot B_f$
Kr^{34+}	$1 \cdot 10^7 \cdot B_f$	$3 \cdot 10^5 \cdot B_f$
Xe^{44+}	$1 \cdot 10^7 \cdot B_f$	$3 \cdot 10^5 \cdot B_f$
Pb^{20+}	$9 \cdot 10^7 \cdot B_f$	$2 \cdot 10^6 \cdot B_f$
Pb^{60+}	$1 \cdot 10^7 \cdot B_f$	$3 \cdot 10^5 \cdot B_f$

Table 3.1 gives the maximum intensity when we are not decelerating the ions but either store them at the injection energy or accelerate them. The injection is the most critical as regards beam intensity in the synchrotron mode. When accelerating particles the bunching factor B_f is smaller than 1, and in injection

one can use a value of 0.2 - 0.3, which means that the maximum number of highly charged ions in the ring is about 10^8 (provided that emittances in injection are about 10 π mm mrad). By multi-turn injection we can fill the transverse phase space and hence the maximum number of ions may be increased up to 10^9.

In table 3.2 we can use $B_f = 1$ since usually with such a low energy we have a coasting beam. When considering merged beams experiments we should take N (b) rather than N (a) since we must have as small emittance as possible to reduce the transverse motion to its minimum. Long storage time leads to smaller acceptable δQ and hence to smaller space charge limit (which is proportional to δQ). It may be as small as 0.01 in the worst case as shown in the table. The price of good energy resolution (transverse) in this case means smaller intensity.

As can be seen in the next chapter, it turns out that for low energy experiments with good energy resolution, the intensity might be more sensitive to the microwave instability (Keil-Schnell) than to the space charge limit.

3.2 Keil-Schnell Limit

If one injects a cold beam ($\Delta p/p = 0$) in a ring the longitudinal phase space will blow up due to the microwave instability. If the momentum spread of the beam is sufficiently large this blow up will not occur. For a given momentum spread the Keil-Schnell criterion [Ke69] gives us the maximum number of ions that we can have in the ring without getting the microwave instability. For low energies the space charge component is dominating in the longitudinal coupling impedance[La85] and thus there is not much to be done to increase the K.S.-limit. In this case the limit can be written as

$$\left(\frac{\delta p}{p}\right)^2 \geq \frac{\frac{q}{A} I r_o 4\pi\epsilon_o Z_o g}{|\eta|\gamma\beta^2 e\ 2\beta\gamma^2} \tag{3.2}$$

where

$\frac{\delta p}{p}$	=	the FWHM value of the momentum distribution
Z_o	=	$\mu_o c = 377\Omega$
g	=	$1 + 2\ln(b/a)$
b	=	radius of the vacuum tube
a	=	average radius of the beam
I	=	beam current

The maximum number of ions in the ring is then

$$N \leq \frac{A}{q^2}\beta^2\gamma^3(\frac{\delta p}{p})^2 R\frac{5.3\cdot 10^{17}}{g} \tag{3.3}$$

Here we have taken $|\eta| = \gamma^{-2} - \gamma_t^{-2}$ to be equal to 0.8 since the transition γ for CRYRING is about 2.3. For $g \approx 5$ the equation above can be written as

$$N_{K.S.} \leq \frac{A}{q^2}\beta^2(\frac{\delta p}{p})^2 R\, 10^{17} \tag{3.4}$$

Above we have left γ^3 out since for energies in CRYRING it is ≈ 1. R is the average radius of the ring. Again, we have $(A/q^2)\beta^2$ dependence, which does not favour highly charged ions with low energy.

Table 3.3 gives $N_{K.S.}$ for three different beam energies corresponding to different $\frac{\delta p}{p}$.

Table 3.3

Keil-Schnell limit for ions in CRYRING ($R \approx 7.7$ m) with
a) $t = 200$ keV/u , $\delta p/p = 2 \cdot 10^{-4}$
b) $t = 300$ keV/u , $\delta p/p = 10^{-2}$ (injection)
c) $t = 5$ MeV/u , $\delta p/p = 10^{-3}$

Ion	a	b	c
Ar^{18+}	$1.6 \cdot 10^6$	$6.0 \cdot 10^9$	$1.0 \cdot 10^9$
Kr^{34+}	$9.6 \cdot 10^5$	$3.6 \cdot 10^9$	$5.9 \cdot 10^8$
Xe^{44+}	$9.0 \cdot 10^6$	$3.4 \cdot 10^9$	$5.6 \cdot 10^8$
Pb^{60+}	$7.6 \cdot 10^6$	$2.9 \cdot 10^9$	$4.7 \cdot 10^8$

From table 3.3 we can easily see that for low energies and a very small momentum spread the Keil-Schnell criterion gives a much smaller limit for the number of ions in the ring than the limit from space charge tune shift provided that the allowable tune shift is larger than 0.01. One must note that if we reduce $\delta p/p$ by a factor 10 the Keil-Schnell intensity limit goes down by a factor of $1/100$.

In merged beams experiments one needs $\Delta p/p$ of the order of 10^{-4} and hence at the first sight they don't seem very promising from the intensity point of view. There are, however, some theoretical predictions for cases where $N \gg N_{K.S.}$ that this condition could lead to a non-destructive instability with a "stabilizing tail" in the momentum distribution [Ho83]. The momentum distribution would consist of a very narrow peak and a tail which contains $N(\text{tail}) \geq 0.67 \cdot N(\text{total}) \cdot (\Re Z/\Im Z)$ particles (Z is the longitudinal coupling impedance). One could get this stabilizing tail also by electron cooling if there is enough dispersion. For the beam energies in CRYRING the imaginary part of Z is of the order of some kΩ's (space charge component) and the resistive (real) part is usually 50 Ω at the most. Therefore only a minor part of the ions has to be in the tail of the momentum distribution. Thus it seems that the Keil-Schnell limit in our case is perhaps not a severe limitation at all. However, it turns out that in most cases intrabeam scattering prevents us to come above the K.-S. limit (see the next chapter).

Note that the Keil-Schnell limit may play a role in the synchrotron mode too if one wants to have very good energy resolution. There is at least one way to improve the energy resolution of the extracted beam even if the energy resolution of the stored beam is not good enough. One can choose a fraction of the momentum distribution by having large chromaticity so that a certain part of the beam (certain momentum) gets to the third order resonance and will be extracted due

to betatron oscillation amplitude growth. Particles can be moved to the resonance by introducing a longitudinal RF-noise which changes their momentum. When the momentum of an ion becomes suitable "its operation point" is near enough to the third order resonance and the particle will be extracted with a well defined momentum.

3.3 Intrabeam Scattering

Scattering of the particles within the beam in some cases tends to decrease the phase space density[Pi74] [Pa86]. In other words, the temperature of the beam tends to increase. For machines where the focusing functions (β and D) do not vary around the ring $\gamma_t < 1$ and hence one is always above the transition energy. If the focusing functions vary along the machine in a smooth manner it may be possible to work below the transition energy. In a such case the total temperature cannot increase and heating is only possible as transfer from one direction to another. In strong focusing machines where the lattice parameters vary strongly along the ring it is possible to increase the total temperature also below the transition.

Below we discuss briefly the theory of intrabeam scattering derived by A. Piwinski [Pi74] and give the growth times for $\Delta p/p$ and betatron amplitudes presented by M. Martini [Ma84].

3.3.1 About the theory of intrabeam scattering

To the first order, the radial displacement of the particle from the closed orbit is the sum of betatron amplitude and linear closed orbit shift due to momentum deviation

$$x = x_\beta + D_x \frac{\Delta p}{p} \tag{3.5}$$

where D_x is the dispersion function. From now on we write D instead of D_x because in most rings bending takes place only in the horizontal plane and thus there is no vertical dispersion. The angle (small) between the particle trajectory and the closed orbit is then

$$x' = \frac{\mathrm{d}x}{\mathrm{d}s} = \frac{p_x}{p} = x'_\beta + D' \frac{\Delta p}{p} \tag{3.6}$$

Since the betatron oscillations satisfy the Courant and Snyder invariant[Co58]

$$\varepsilon = \gamma_x x_\beta^2 + 2\alpha_x x_\beta x'_\beta + \beta_x {x'_\beta}^2 \tag{3.7}$$

where

$$\gamma_x = \frac{1+\alpha_x^2}{\beta_x} \qquad \text{and} \qquad \alpha_x = -\frac{1}{2}\beta'_x$$

the change of the emittance can be written as

$$\begin{aligned} \beta_x \delta\varepsilon =& (1+\alpha_x^2)(2x_\beta \delta x_\beta + \delta x_\beta^2) \\ &+ 2\alpha_x\beta_x(x'_\beta \delta x_\beta + x_\beta \delta x'_\beta + \delta x_\beta \delta x'_\beta) \\ &+ \beta_x^2(2x'_\beta \delta x'_\beta + \delta {x'_\beta}^2) \end{aligned} \tag{3.8}$$

We can assume that the radial position does not change during the collision and so one can write

$$\delta x_\beta = -D\frac{\delta p}{p} \qquad \text{since} \quad \delta(\frac{\Delta p}{p}) = \frac{\delta p}{p} \tag{3.9a}$$

and

$$\delta x'_\beta = \delta x' - D'\frac{\delta p}{p} = \frac{\delta p_x}{p} - D'\frac{\delta p}{p} \tag{3.9b}$$

When knowing the dynamics of intrabeam scattering i.e. collision of particles in a repulsive Coulomb field and using the Rutherford scattering cross-section we can calculate the momentum change of the ions in the collisions. So, we can finally calculate the emittance end $\Delta p/p$ growth. The momentum change of the particles is a function of scattering angles and according to Piwinski [Pi74]

$$\begin{aligned} \frac{\delta p}{p} &= \frac{1}{2}(2\alpha\gamma \sin\bar{\psi}\sin\bar{\phi} + \gamma\xi(\cos\bar{\psi} - 1)) \\ \frac{\delta p_x}{p} &= \frac{1}{2}\left\{\left[\zeta\sqrt{1 + \frac{\xi^2}{4\alpha^2}}\cos\bar{\phi} - \frac{\xi\theta}{2\alpha}\sin\bar{\phi}\right]\sin\bar{\psi} + \theta(\cos\bar{\psi} - 1)\right\} \end{aligned} \tag{3.10}$$

where

$\bar{\psi}$ and $\bar{\phi}$	are the scattering and azimuthal angles between the particles in the center of mass frame after the collision
2α	is the angle between the incident particles in the laboratory frame

The Rutherford scattering cross-section for non-relativistic particle velocities in the C.M. system is

$$\frac{\mathrm{d}\bar{\sigma}(\bar{\psi})}{\mathrm{d}\bar{\Omega}} = (\frac{r_i}{4\bar{\beta}})^2 \frac{1}{\sin^4(\bar{\psi}/2)} \quad , \quad \mathrm{d}\bar{\Omega} = \sin\bar{\psi}\mathrm{d}\bar{\psi}\mathrm{d}\bar{\phi} \tag{3.11}$$

$\bar{\beta}c$ is the particle velocity in the C.M. system and r_i is the classical ion radius

$$r_i = \frac{q^2}{A}\,1.535 \cdot 10^{-18}\mathrm{m} \tag{3.12}$$

where q is the charge state of the ion and A the mass number. This shows how the propability of scattering increases rapidly with the charge state of the beam (q^4).

Starting from these equations one can derive (see references [Pi74] and [Ma84]) the expressions for momentum and betatron angle (or amplitude) growth rates. The growth rates for $\frac{\delta p}{p}$, x' and y' can be expressed as

$$\begin{aligned} \frac{1}{\tau_p} &= \langle\frac{nA}{2}(1 - d^2)f_1\rangle \qquad n = \begin{cases} 1 & \text{for bunched beams} \\ 2 & \text{for coasting beams} \end{cases} \\ \frac{1}{\tau_{x'}} &= \langle\frac{A}{2}[f_2 + (d^2 + \tilde{d}^2)f_1]\rangle \\ \frac{1}{\tau_{y'}} &= \langle\frac{A}{2}f_3\rangle \end{aligned} \tag{3.13}$$

Here A is a constant and it is

$$A = \frac{\delta_E \delta_p \lambda c r_i^2}{16\pi\sqrt{\pi} E_x E_y \frac{\Delta p}{p} \beta^3 \gamma^4} \qquad \lambda = \begin{cases} \frac{N}{L} & \text{coasting} \\ \frac{N_b}{2\sqrt{\pi}\sigma_s} & \text{bunched} \end{cases} \tag{3.14}$$

where

δ_E	relates emittance to the standard deviation of the beam dimension (or divergence) and
δ_p	relates $\frac{\Delta p}{p}$ to the standard deviation of $\frac{\Delta p}{p}$ distribution
N, N_b	number of particles in the beam, or per bunch
r_i	classical ion radius
L	orbit length
σ_s	standard deviation of bunch length
c	velocity of light
E_x, E_y	horizonral and vertical emittance
β	v/c
γ	E/E_o

Further, the following notations have been used

$$\begin{aligned} &\tilde{D} = \alpha_x D + \beta_x D' \qquad (D = D_x) \\ &\sigma_x^2 = \sigma_{x_\beta}^2 \beta + D^2 \sigma_p^2, \quad \sigma_z = \frac{\sigma_p \sigma_{x\beta}}{\gamma \sigma_x}, \quad d = \frac{\sigma_p}{\sigma_x} D, \quad \tilde{d} = \frac{\sigma_p}{\sigma_x} \tilde{D} \end{aligned} \tag{3.15}$$

and

$$a = \frac{\sigma_z}{\sigma_{x'}}(1 + \alpha_x^2), \quad b = \frac{\sigma_z}{\sigma_{y'}}(1 + \alpha_y^2), \quad c = q\sigma_y$$

where

$$q = 2\beta\sqrt{\frac{\sigma_y}{r_i}}$$

The scattering functions are triple integrals

$$f_i = k_i \int_0^\infty \mathrm{d}z \int_0^\pi \mathrm{d}\mu \int_0^{2\pi} \mathrm{d}\nu \sin\mu g_i(\mu\nu) \exp[-U(\mu\nu)z] \ln(1 + z^2) \tag{3.16}$$

where

$$k_1 = \frac{1}{c^2}, \quad k_2 = \frac{a^2}{c^2}, \quad k_3 = \frac{b^2}{c^2}$$

and

$$\begin{aligned} U(\mu\nu) &= [\sin^2\mu\cos\nu + \sin^2\mu(a\sin\nu - \tilde{d}\cos\nu)^2 + b^2\cos^2\mu]/c^2 \\ g_1(\mu\nu) &= 1 - 3\sin^2\mu\cos\nu \\ g_2(\mu\nu) &= 1 - 3\sin^3\mu\sin^2\nu + 6\tilde{d}\sin\mu\sin\nu\cos\nu/a \\ g_3(\mu\nu) &= 1 - \cos^2\mu \end{aligned} \tag{3.17}$$

The brackets $\langle ... \rangle$ denote the average around the machine.

The shown formulae for the growth rates take into account the variation of lattice functions around the ring and thus the fact that $\alpha \neq 0$ and $D' \neq 0$. In his paper [Pi74], Piwinski assumes constant β and D and so $\alpha = 0$ and $D' = 0$. These assumptions lead to a very interesting Piwinski invariant

$$\left(\frac{1}{\gamma^2} - \frac{D^2}{\beta_x^2}\right)\left\langle\frac{(\Delta p)^2}{p^2}\right\rangle + \langle x'^2\rangle + \langle y'^2\rangle = \text{constant} \qquad (3.18)$$

The three terms of the invariant correspond to the temperature of the beam in the two transverse and the longitudinal direction. Depending on the values of D and β_x we get two cases

1. $$\frac{D^2}{\beta_x^2} < \frac{1}{\gamma^2}$$

All three oscillation amplitudes are limited, i.e. particles can be considered to be as particles of a gas in a closed box. This means that the total temperature cannot increase, there is only transfer of oscillation energy from one direction into another. An equilibrium must exist.

2. $$\frac{D^2}{\beta_x^2} > \frac{1}{\gamma^2}$$

The total oscillation energy increases until it exceeds the acceptance limitations (walls of the vacuum chamber). There is no equilibrium.

In machines with sufficiently smooth lattice functions $D^2/\beta^2 \approx (1/\gamma_{tr})^2$ and thus the case 1 corresponds to energies below transition and 2 above transition. However, in strong focusing machines where D and β_x vary (much) along the ring and the calculation of growth speeds must be made in small steps along a superperiod. In any case, we see that it is favourable to have high transition energy to minimize the "beam heating" by intrabeam scattering.

The constant A (see eq. 3.14) shows the strong dependence on beam energy ($\beta^3\gamma^4$) and similarily the dependence on the charge state ($r_i^2 \propto q^4$).

The scattering functions f_i and hence the intrabeam growth rates may vary very rapidly with emittances and $\frac{\Delta p}{p}$ in a given lattice. Next we shall give some results of intrabeam scattering calculations applied to CRYRING.

3.3.2 Intrabeam scattering in CRYRING

As most of the experiments in CRYRING use slow highly charged heavy ions (small β, large q) intrabeam scattering is one of the most limiting factors when considering cooled beams in the ring. Therefore a computer program INTRABEAM (based on Martinis papers [Ma84] and [Ma84a]) was written to study how this fenomenon affects the beam quality. The program uses lattice parameters calculated by the program MAD. The listing of the program is in the appendix 2.

As an example 200 keV/u Ar^{18+} beam was studied. Although the scattering functions f_i are also functions of β and q^2/A this dependence is so weak compared

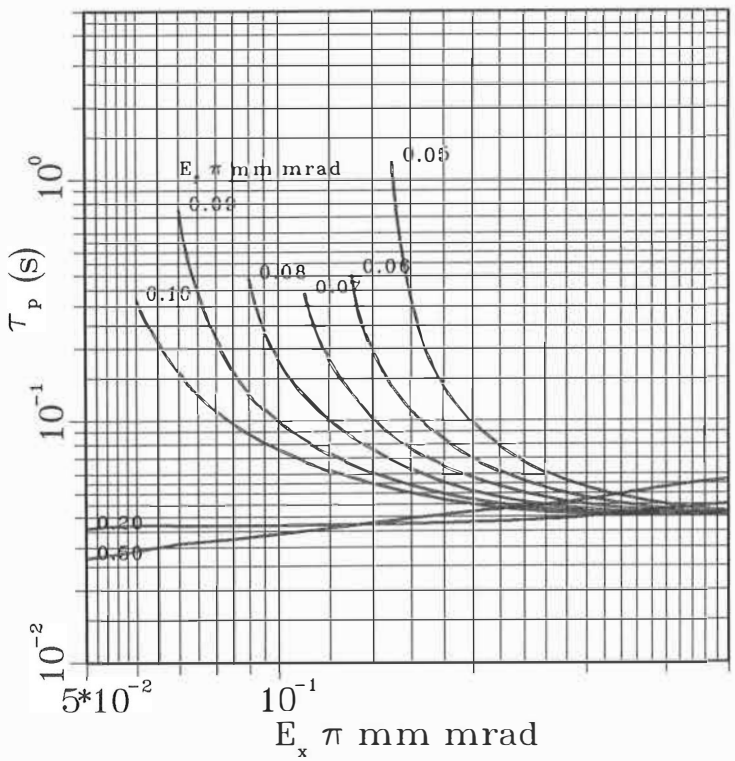

Figure 3.1
The momentum growth time (seconds) for Ar^{18+} ions with
$N = 10^5$
$\frac{\Delta p}{p} = 1.7 \cdot 10^{-4}$
at 200 keV/u

to same dependence on constant A that one can scale the $1/\tau$ values calculated for 200 keV/u Ar^{18+} to other ions and energies without any greater error using the scaling law

$$\frac{1}{\tau} \propto A \propto N \frac{q^4}{A^2} \frac{1}{\beta^3 \gamma^4} \tag{3.19}$$

The beam heating by intrabeam scattering is compensated by strong enough electron cooling. The transverse (emittance) cooling times for the studied case are of the order of some seconds when the electron rms divergence is larger than the rms ion divergence. The longitudinal cooling is usually somewhat faster (since the longitudinal rms velocity is smaller than the transverse one). Of course, the cooling times are functions of lattice functions and the cooling device parameters. The lattice functions have been optimized for cooling and so the largest uncertainty

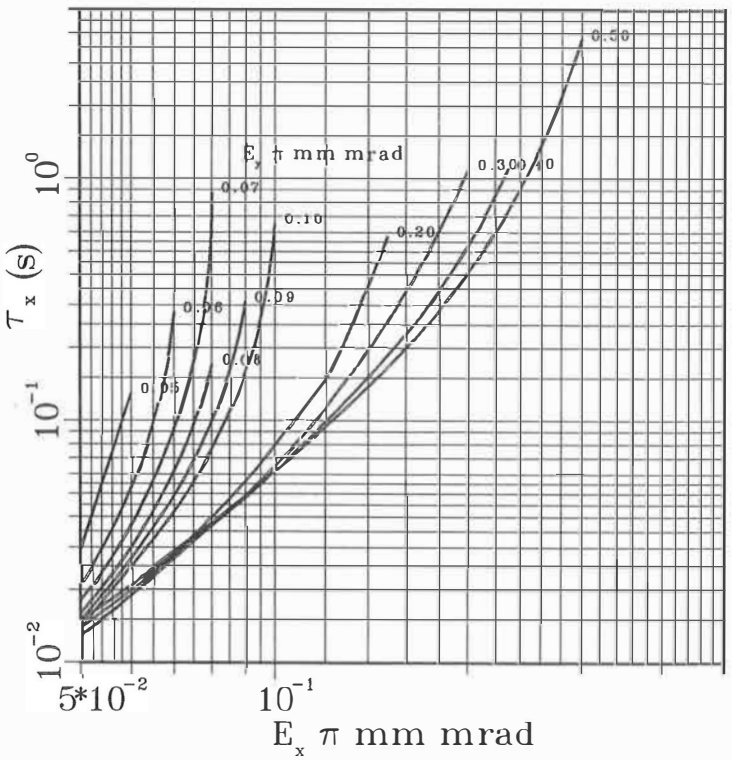

Figure 3.2
The horizontal divergence growth times (seconds)
for Ar^{18+} with $N = 10^5$ and
$\frac{\Delta p}{p} = 1.7 \cdot 10^{-4}$ at 200 keV/u

comes from the cooler device (which does not exist yet). The growth times from intrabeam scattering calculations that are presented below are for divergences and not for emittances. The relationship between the growth rates for emittance and divergence is

$$\frac{1}{\tau_{E_x}} = \frac{2}{\tau_{x'}} \tag{3.20}$$

This relation is useful if we calculate the cooling time from Spizer's formula (see Eq. (A1.3) in part one) which refers to temperature (i.e. emittance) relaxation. However, as mentioned the uncertainty in cooling times is so large that at this stage a factor of 2 is of no importance.

As an example, in figure 3.1 we show the time constant τ_p for $\Delta p/p$ with different horizontal and vertical emittances and with $\Delta p/p = 1.7 \cdot 10^{-4}$ (10^5 ions). The horizontal amplitude time constant $\tau_{x'}$ (growth time) is shown in figure 3.2 with $\Delta p/p = 1.7 \cdot 10^{-4}$. The corresponding vertical time constant is shown in figure 3.3.

When accelerating ions for nuclear physics with maximum beam intensity (limited

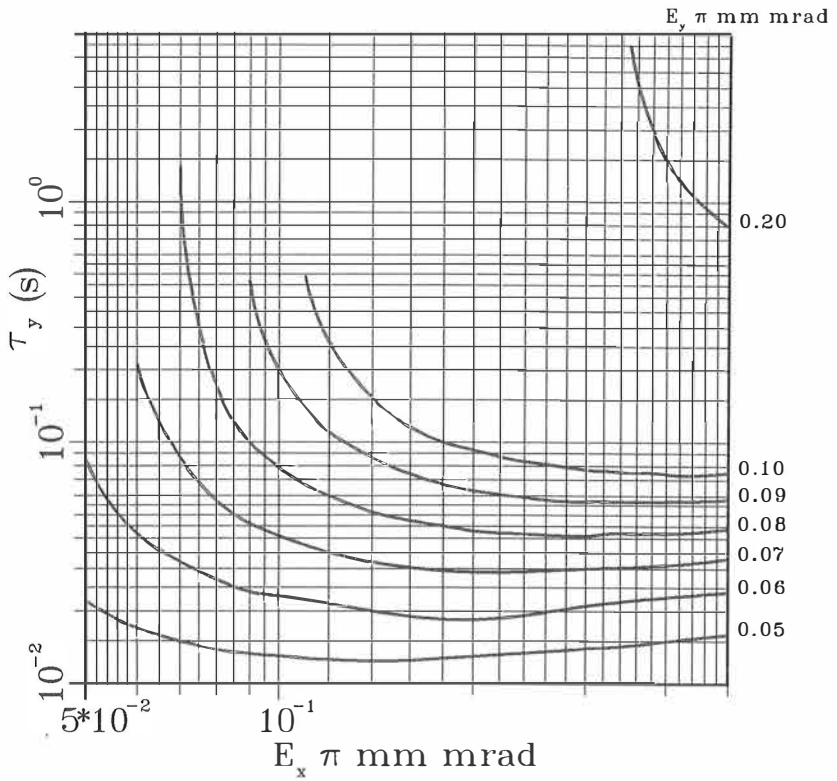

Figure 3.3

The vertical divergence growth times (seconds) for Ar^{18+} with $N = 10^5$ and $\frac{\Delta p}{p} = 1.7 \cdot 10^{-4}$

by space charge tune shift) intrabeam scattering should not be a problem. At single turn injection with injection energy of 300 keV/u the emittances are of the order of 10 π mm mrad and $\Delta p/p$ around 1 %. This gives rise to growth times

$$\tau_p = -85 \text{ s}$$
$$\tau_{x'} = 12 \text{ s}$$
$$\tau_{y'} = 8 \text{ s}$$

for 10^8 Ar^{18+} ions. As CRYRING is cycled faster than 1 acceleration/s these times do not cause any trouble. At multiturn injection the transverse emittances as well as the intensity are a factor of 10 larger and the growth times are also larger.

Comparing the equilibrium emittances and $\Delta p/p$ values with the values given by the Keil-Schnell limit it seems that in most cases intrabeam scattering prevents us to come above the K.S. limit provided that the electron cooling is not more effective than we have assumed. One may say that the quality of the cooled ion beam in CRYRING is totally dependent on the cooling device and is finally limited by heating caused by intrabeam scattering.

3.3.3 The competition of electron cooling and intrabeam scattering in CRYRING

The process of combined electron cooling and intrabeam scattering was simulated using fixed cooling time constants. When the divergence of the ion beam becomes smaller than the divergence of the electron beam the transverse cooling time does not depend anymore on the ion beam divergence and thus can be considered to be constant. When using more realistic cooling time constants the evolution of beam shrinking is different but the equilibrium values are more or less the same. The combined time constant of the process is

$$\frac{1}{\tau} = \frac{1}{\tau_c} + \frac{1}{\tau_{ibs}}$$

Positive time constant means growth and negative damping. The equilibrium is reached when

$$\tau_c = -\tau_{ibs}$$

In practice one should take also time constants for residual gas scattering, ripple in magnet currents and in electron gun voltage into account. Our simulation shows only the effect of intrabeam scattering and electron cooling assuming that the other heating mechanisms are negligible.

A typical process is seen in figure 3.4 where the initial emittances in both planes were $10\,\pi$ mm mrad and $\Delta p/p$ 1 %. The longitudinal cooling is assumed to be ten times faster than the transverse one and $\Delta p/p$ reaches a minimum rather soon. When the emittances become smaller $\Delta p/p$ starts to increase slowly since the scattering probability increases with the increasing beam density. Finally emittances reach the equilibrium and $\Delta p/p$ stops growing. In practice the difference in longitudinal and transverse cooling times is probably smaller than assumed here. Our simulations show that the equilibrium values are mainly dependent on the smallest cooling time – not on the difference between them and hence the assumption about the ratio τ_p/τ_E is not critical.

Equilibrium emittances and $\Delta p/p$ as a function of cooling times are presented in figures 3.5 and 3.6. The ion in consideration is again Ar^{18+} at the energy of 200 keV/u. The beam intensity is 10^5 ions in the ring. The transverse electron temperature was assumed to be 0.1 eV/degree of freedom which leads to corresponding Ar-beam emittance $0.1\,\pi$ mm mrad. This limit is reached only with very fast logitudinal cooling. If the longitudinal cooling time is longer than 100 ms the equilibrium $\Delta p/p$ will be around $2-3\cdot10^{-4}$. The emittances, however, seem to become rather small. The average transverse emittance is shown since the horizontal and vertical equilibrium emittances are almost equal (see figure 3.4).

The reader must note here that these numbers apply only to the case mentioned. Both electron cooling and intrabeam scattering change strongly with beam energy and the charge state of the ions. Electron cooling is more or less independent of the number of ions in the ring and so the effect of intrabeam scattering can be reduced by reducing the beam intensity. This, however, tends to reduce the interaction

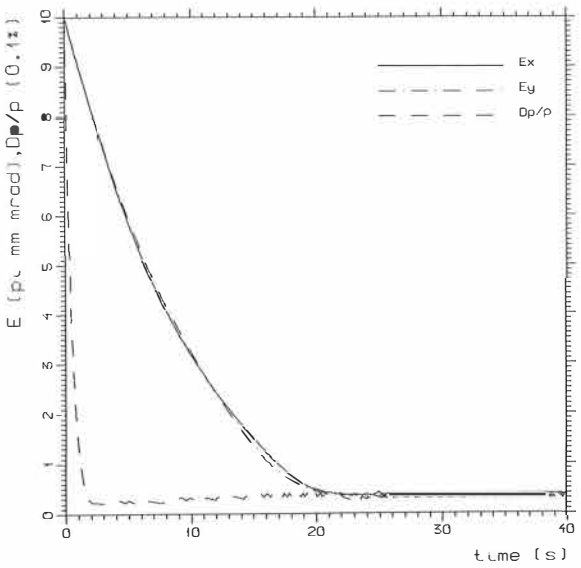

Figure 3.4

Electron cooling simulation with constant cooling times and intrabeam scattering for 10^5 Ar^{18+} ions with $\tau_{E_x,E_y} = 5$ s and $\tau_p = 0.5$ s at 200 keV/u.

rate in the experiments and the beam intensity must be determined carefully for each case to optimize the conditions.

As an example, when the number of Ar^{18+} ions is reduced from 10^5 to 10^4 at the energy of 200 keV/u and if the (final) cooling times are $\tau_E = 1.0$ s and $\tau_p = 0.3$ s the equilibrium emittance decreases from $0.17\,\pi$ mm mrad to $0.1\,\pi$ mm mrad which corresponds to the transverse electron temperature and $\Delta p/p$ decreases from $2.2 \cdot 10^{-4}$ to $1.6 \cdot 10^{-4}$. Similarily, if we increase the number of Ar^{18+} ions to 10^6 the equilibrium emittance increases to $0.47\,\pi$ mm mrad and $\Delta p/p$ increases to $3.5 \cdot 10^{-4}$. As can be seen, the equilibrium values do not change rapidly with the beam intensity. That is a good property since in practice most experiments use several injected and cooled pulses from the ion source and it is important to keep the beam quality unchanged during the whole experiment.

If the charge state of the beam is not relevant for the experiment it is more favourable to use as low charge state as possible. This comes from the fact that cooling time is proportional to A/q^2 whereas the intrabeam scattering time constant is proportional to A^2/q^4. When the charge state is reduced intrabeam scattering decreases more strongly than cooling and the equilibrium emittance and $\Delta p/p$ become smaller. If, for example, one takes Ar^{12+} instead of Ar^{18+} at 200 keV/u the equilibrium emittances decrease from $0.17\,\pi$ mm mrad to $0.12\,\pi$ mm mrad and $\Delta p/p$ decreases form $2.2 \cdot 10^{-4}$ to $1.8 \cdot 10^{-4}$ if the cooling

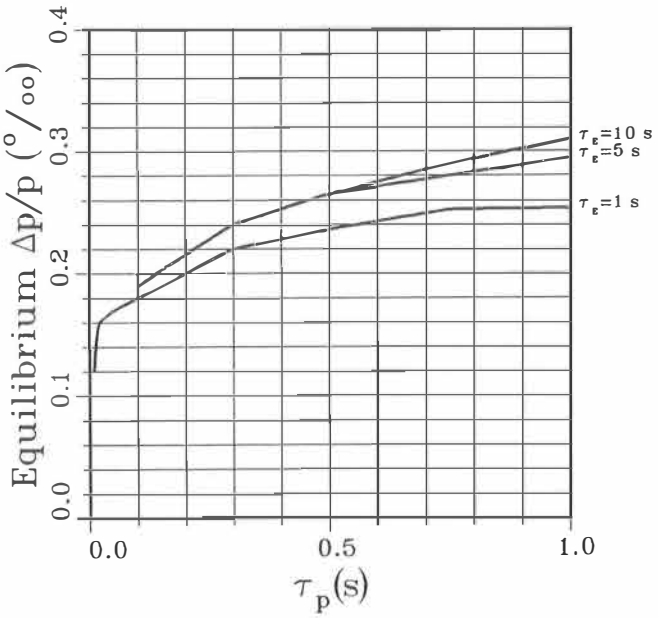

Figure 3.5

Equilibrium $\Delta p/p$ in electron cooling with constant cooling times and intrabeam scattering for 10^5 Ar^{18+} ions at 200 keV/u.

times for Ar^{18+} are $\tau_E = 1.0$ s and $\tau_p = 0.3$ s.

When comparing intrabeam scattering in the earlier version of the lattice[He86] with that in the lattice presented in this thesis one finds that the equilibrium emittance in the former lattice was much bigger. For example, with cooling times $\tau_p = 0.5$ s and $\tau_E = 5.0$ s the equilibrium emittances in the old lattice were $E_x \approx 1.5\,\pi$ mm mrad and $E_y \approx 0.9\,\pi$ mm mrad whereas in the present lattice they are $E_x \approx E_y \approx 0.25\,\pi$ mm mrad. The equilibrium $\Delta p/p$ in both lattices are almost equal ($0.3\,\pi$ mm mrad and $0.26\,\pi$ mm mrad in the former and present lattice respectively). The reason for this is mainly that the amplitude functions are "smoother" in the present lattice. The dispersion is also almost constant in the whole ring but its effect is not so apparent since the maximum dispersion in the old lattice is somewhat smaller and there were two straight sections where dispersion was almost zero which is a good condition as far as intrabeam scattering is concerned. Small equilibrium emittance gives good luminosity which is more than wellcome in the experiments where the number of ions must be reduced in order to increase the beam quality and thus the present lattice gives better counting rates than the former one.

In merged beams experiments $\Delta p/p$ seems to be the limiting factor as far as energy resolution is concerned. In order to make $\Delta p/p$ significantly smaller than 0.2 % the longitudinal cooling time should be smaller than 10 ms. Without doing any detailed electron cooling calculations $\Delta p/p$ smaller than 0.2 % seems unprobable

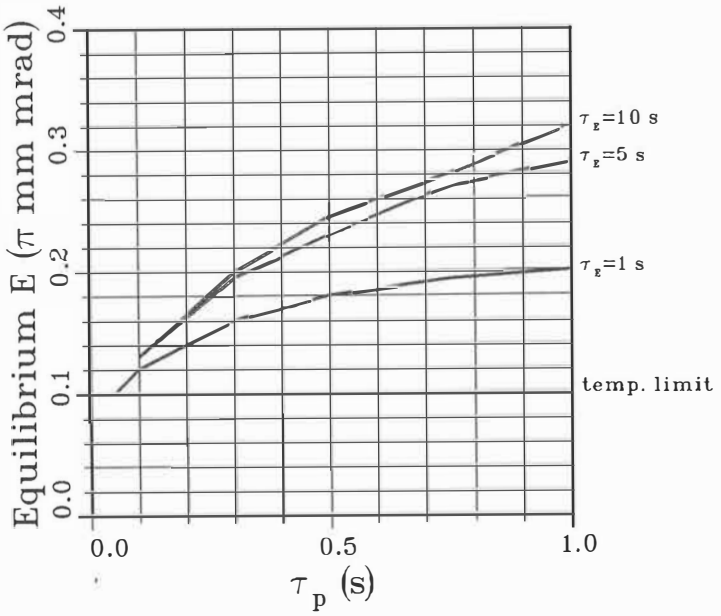

Figure 3.6

Equilibrium emittance in electron cooling with constant cooling times and intrabeam scattering for 10^5 Ar^{18+} ions at 200 keV/u.

for highly charged ions at low energies. At low energies the quality of the electron beam in the cooler becomes poorer, especially the beam intensity. This is because the corresponding electron energy and thus the gun voltage are very low. For example, if the beam energy is 200 keV/u the corresponding electron gun voltage is about 110 V. For such low voltage the normal Pierce type electron gun perveances may give too low current. Another construction for a low energy electron gun was presented by H. Herr [He84] giving reasonable electron beam properties.

Besides low voltage also the guiding magnetig field becomes critical. For the lowest beam energies the guiding field will be of the order of 5 mT which is comparable to the earth's magnetic field ($\approx$ 0.05 mT). To achieve a sufficient field homogenity ($\leq 10^{-3}$) the cooler has to be carefully shielded against the earth's magnetic field and other stray fields from the neighbouring ring magnets.

4 Discussion

4.1 Lattice Design

A solution to the lattice problem has been found[Bá87][Je87] that meets the special requirements of a storage ring to work with merged and crossed low energy ion beams and as an accelerator. The normal ion optical problems as well as those imposed by the special functions of CRYRING (optimal lattice functions) has been solved using the program MAD developed at CERN. The lattice presented earlier [An85][He86] was modified during 1986: To gain more space for the ring it was proposed to move the ion source and the RFQ from the former experimental hall to the cyclotron vault. In this way the circumference of the ring could be increased from 32.7 meters to 48.63 meters. The number of superperiods was then increased to six. Also the dipoles assumed in the lattice calculations were changed from sector to rectangular type. Moreover, the constraint of almost zero dispersion on some of the straight sections was abandoned. These modifications lead to better properties as far as intrabeam scattering is concerned. In fact, the equilibrium emittances went down by a factor of 5 approximately.

4.2 Operation Limits

There are processes that limit the beam intensity and beam quality during acceleration and storing. The fact that the ring uses mostly slow highly charged ions causes many severe problems conserning different space charge effects. In the present work these problems were put into perspective to derive criteria for the design and the application of CRYRING.

4.2.1 Space charge limit

The space charge tune shift limits the maximum number of ions to $\approx 10^9$, since in all cases the injection energy for the beam is 300 keV/u at the most. The limit of 10^9 ions corresponds to emittances after multiturn injection ($E_x = E_y = 100\,\pi$ mm mrad). For cases where the beam will be cooled the limit goes down linearily with emittance. Otherwise, the space charge effect is not the most limiting factor. For low energies the Keil-Schnell limit gives more stringent conditions for beam intensities. Moreover, intrabeam scattering usually prevents the beam emittance to reach the space charge limit.

4.2.2 Intrabeam scattering vs. electron cooling

The most important limiting factor for cooled beams in CRYRING (low emittances and small $\Delta p/p$) is intrabeam scattering. The beam heating caused by intrabeam

scattering will be counteracted by electron cooling. The equilibrium emittances for low energies depend on the beam intensity. For example, for 10^5 Ar^{18+} ions at an energy of 200 keV/u the equilibrium values are $E_{x,y} \approx 0.2\,\pi$ mm mrad and $\Delta p/p \approx 2 \cdot 10^{-4}$. These values do not reach either the space charge limit nor the Keil-Schnell limit.

For higher intensities, such as 10^8, the Keil-Schnell limit may cause problems during the cooling. If, e.g., we have 10^8 Ar^{18+} ions (300 keV/u) with $E_x = E_y = 10\,\pi$ mm mrad and if the longitudinal cooling is much faster than the transverse cooling so that $\Delta p/p = 10^{-4}$ is achieved before the emittances have been decreased significantly we have got smaller $\Delta p/p$ than the Keil-Schnell limit allows ($5 \cdot 10^{-4}$). The results from electron cooling simulations with constant cooling times show that this might happen if the longitudinal cooling time is less than 10 ms. However, the initial longitudinal cooling time is allways longer than the final time constant and this perhaps prevents the process described above. Whether this happens in practice is impossible to say without computer programs that simulate electron cooling [Wo85] in a more realistic way and that take also intrabeam scattering into account, and so we leave it to the future. **In general, intrabeam scattering seems to be so strong that it prevents the beam to reach space charge limit and the Keil-Schnell limit.**

The most critical parameter in the electron cooling seems to be the longitudinal cooling time, at least in the merged beams experiments. The transverse cooling time does not have an important effect on the equilibrium emittances and $\Delta p/p$. Its effect is seen only in the total cooling time which, of course, is an essential factor too.

The key to good beam quality and the very interesting physics accesible with cold beams in CRYRING is electron cooling and so the heaviest burden lies on the shoulders of the cooler device designers. The biggest problems in cooling are met at low beam energies. One has to be able to produce an intense, high quality, low energy electron beam that is guided in a magnetic field comparable to earth's magnetic field and stray fields from the neighbouring magnets.

As a conclusion one may say that in spite of the intensity limits CRYRING holds the promise of physics with very low beam energies and very good beam quality. As regards to merged beams, no other methods seems to exist to achieve such low center of mass energies for highly charged ions.

4.3 Merged Beams

Another exciting property of CRYRING is the possibility of doing merged beams experiments. To study collisions of highly charged ions at a very low center of mass energy with reasonable energy resolution the setup of merged beams seems to be the only practical possibility. There is no way of guiding highly charged ions at an energy of, say, 1 eV/u.

It follows from kinematics that when two particles travel in the same direction at relatively high energy in the laboratory frame the center of mass energy of

their collision is much smaller than their energy difference in the laboratory frame. Similarily, when two beams with non-zero energy spread travel together the energy spreads in the moving coordinate system are much smaller than in the laboratory frame. Using merged beams one can reach for example a center of mass energy of 1 eV for Ar^{18+} and H^- with an energy resolution of 25 % when the energy of Ar-beam is 200 keV/u and the energy difference of the beams is 889 eV/u.

It was shown above (section 2.3) that in CRYRING the lowest attainable center of mass energy in merged beams experiments is about 1 eV. We have also found that, due to beam density limitations discussed, this value can only be reached with moderate beam intensities when the FWHM of the center of mass energy distribution is clearly smaller than the expectation value of the distribution (E_{cm}). The energy resolution sets constraints on beam alignement and beam positions. The alignement was established to be about 0.5 mrad which gives rise to a magnetic field precision of about $5 \cdot 10^{-4}$. The precision of positioning the beams is found to be 0.2 – 1.0 mm depending on the width of the external beam.

The energy resolution in merged beams experiments is primarily determined by the longitudinal velocity spread of the beams. The velocity or momentum spread of the stored beam is limited by intrabeam scattering.

4.4 Beam Acceleration

In synchrotron mode CRYRING will provide beams at energies high enough to work above the Coulomb barrier with almost all the beam and target combinations. The most critical point in this mode is how fast the magnets can be cycled. One needs a repetition rate of the order of 10 Hz to provide external beam currents of 1 pnA provided that the number of ions in the ring is around 10^9. The machine presented (fig 2.5) seems well suited to house the RF-cavity and other equipment (position pick up electrodes for beam control etc.) for acceleration. The open question of the maximum repetition rate relates to magnet- and power supply technology but not (directly) to the lattice.

The injection energy will be $\approx$ 300 keV/u. The pre-acceleration is done with an RFQ, and thus the momentum spread $\Delta p/p$ of the injected beam will be 0.5 – 1 %. During acceleration $\Delta p/p$ will decrease due to adiabatic shrinking. If a better energy resolution is needed the accelerated beam can be cooled but that will decrease the repetition rate and thus the average current of the extracted beam.

The accelerated beam for nuclear and surface physics will be extracted using slow extraction. Care has been taken to adapt the lattice to the requirements of third integer resonant extraction. A suitable working point and an appropriate arrangement of sextupoles have been found, both compatible with the other modes of operation for CRYRING.

REFERENCES

[An85] H.Andersson and J.Jeansson, A Study of the CRYRING Lattice with Special Emphasis on Extraction, Diploma Work, Research Institute of Physics, Stockholm, 1985.

[Bá87] A. Bárány, C.J. Herrlander, K.-G. Rensfelt and J. Starker, Status of CRYRING, Nucl. Instr. and Meth. **B23**(1987)200-202.

[Be81] J.S. Bell and M. Bell, Electron Cooling in Storage Rings, Particle Accelerators **11**(1981)233–238.

[Be81a] M. Bell, J. Chaney, H. Herr, F. Krienen, P. Møller-Petersen and G. Petrucci, Electron Cooling in ICE at CERN, Nucl. Instr. and Meth. **190**(1981)237–255.

[Bl77] Theoretical Aspects of the Behaviour of Beams in Accelerators and Storage Rings, ed. M.H.Blewett, CERN 77–13.

[Bo70] C.Bovet et al., A Selection of Formulae and Data Useful for the Design of A.G. Synchrotrons, CERN/MPS–SI/Int. DL/70/4, 23 April, 1970.

[Bo87] F. Bosch, The Planned Heavy-Ion Storage-Cooler Ring at GSI: A Powerfull Tool for New Experiments in Atomic Physics, Nucl. Instr. and Meth. **B23**(1987)190–199.

[Br83] Physics of Ion-Ion and Electron-Ion Collisions, ed. F.Brouillard and J.W.McGowan, Nato Advanced Study Institute Series, Series B: Physics, Plenum Press 1983.

[Br84] P.J.Bryant, Introduction to Transfer Lines and Circular Machines, CERN 84–04.

[Bu66] G.I. Budger, Proc. Int. Symposium on Electron and Positron Storage Rings, Saclay, 1966, p. II–1–1.

[Co58] E.D. Courant and H.S. Snyder, Theory of the Alternating-Gradient Synchrotron, Annals of Physics **3**(1958)1–48.

[Bu78] G.I. Budger and A.N. Skrinsky, Trans. Uspekhi. Nauk. **124**(1978)561.

[Da87] S. Datz, Atomic Physics Experiments with Stored Cooled Heavy Ion Beams, Nucl. Instr. and Meth. **B24/B25**(1987)3–10.

[De77] Y.S. Derbenev and A.N. Skrinsky, Particle Accelerators **8**(1977)1.

[De77a] Y. Derbenev and I. Meshkov, Studies of Electron Cooling of Heavy Particle Beams Made by the VAPP-NAP Group at the Nuclear Physics Institute of the Siberian Branch of the USSR Academy of Science at Novosibirsk, CERN 77–08.

[De78] Y.S. Derbenev and A.N. Skrinsky, Particle Accelerators **8**(1978)235.

[Di84] N.S. Dikansky, D.V. Pestrikov, Ordering Effects in Coulomb Relaxation of a Cold Beam, Proceedings of the Workshop on Electron Cooling and Related Applications (ECOOL84), Karlsruhe, September 24–26,1984, KfK 38846, p. 275.

[Dr82] A.J. Dragt, Exact Numerical Calculation of Chromaticity in Small Rings, Particle Accelerators **12**(1982)205–218.

[Fi84] D. Fick, D. Habs, E. Jaeschke, D. Krämer, V. Metag, R. Neumann, B. Povh, R. Repnow, U. Schmidt-Rohr, R. Schuch, D. Schwalm, E. Steffens and C.A. Wiedner, The Heidelberg Heavy Ions Storage Ring (TSR), Proceedings of the Workshop on Electron Cooling and Related Applications (ECOOL84), Karlsruhe, September 24–26,1984, KfK 38846, p. 137.

[Fr84] B. Franzke, Cooling of Heavy Ion Beams, Proceedings of the Workshop on Electron Cooling and Related Applications (ECOOL84), Karlsruhe, September 24–26,1984, KfK 38846, p. 303.

[Fr85] B. Franzke, Heavy Ion Storage Rings for Atomic Physics, IEEE Trans. Nucl. Sci. **NS-32**(1985)3292.

[Fr87] B. Franzke, The Heavy Ion Storageand Cooler Ring Project ESR at GSI, Nucl. Instr. and Meth. **B24/B25**(1987)18–25.

[Gu77] G.Guinard, Selection of Formulae Concerning Proton Storage Rings, CERN 77–10.

[Ha85] C. Habfast, H. Poth, S. Seligmann, H. Haseroth, C.E. Hill, J.-L. Vallet and A. Wolf, Status and Perspectives of the Electron Cooling Device Under Construction at CERN, Contribution to the Third LEAR Workshop, Tignes, 19–26 January 1985 *also* CERN-EP/85–49.

[He83] H.Herr, A First Approach to Find Parameters for the Uppsala Storage Ring, CELSIUS - Note 83–2.

[He84] H.Herr, Electron Cooling at Very Low Velocities, Proc. of Workshop on Electron Cooling and Related Applications (ECOOL84), Sept. 24–26, 1984, KfK 3846 *also* CERN-EP/85–100.

[He85] P.Heikkinen, Lattice Studies of CRYRING, IEEE Trans. Nucl. Sci., **NS-32**(1985)2715.

[He85a] C.J.Herrlander, L.Bagge, A.Bárány, S.Borg, P.Heikkinen, S.Hultberg, L.Liljeby, Th.Lindblad, CRYRING, a Small Storage and Acceleration Ring for Heavy Ions, IEEE Trans. Nucl. Sci. **NS-32**(1985)2712.

[He85b] H. Herr, Resolution Limits with Cooled Beams, CERN–EP/85–39.

[He86] P.Heikkinen, Beam Dynamical Studies of CRYRING, Thesis for the Degree of Licentiate of Philosophy, Dept. of Phys., Univ. of Jyväskylä, Finland, Laboratory report 8/86.

[Ho83] I.Hofmann, I. Bozsik and A. Jahnke, Theoretical Study of High-Current Beams in Storage Rings, IEEE Trans. Nucl. Sci., **NS-30 No.4**(1983)2546.

[Ho84] I. Hofmann, Suppression of Microwave Instabilities, Proc. INS International Symposium on Heavy Ion Accelerators and Their Applications to Inertial Fusion, January 23–27, 1984, Tokyo, p. 238.

[Hü82] L. Hütten, H. Poth, A. Wolf, H. Haseroth and Ch. Hill, The Electron Cooling Device for LEAR, CERN/PS/LI 82–9.

[Is85] F.C.Iselin, The MAD program: reference manual, CERN 1985.

[Je87] J. Jeansson, Research Institute of Physics, Stockholm, private communication.

[Ke69] E. Keil and W. Schnell, CERN ISR–RF/69–48, 1969.

[Ke80] W. Kells et al., Studies of the Electron Beam for the Fermilab Electron Cooling Experiment, Proc. 11th Int. Conf. High Energy Accelerators, 1980 (Birkhäuser, Basel) p. 814.

[Ki84] K. Kilian, New Possibilities With Electron Cooling in Atomic, Nuclear and Particle Physics, Proceedings of the Workshop on Electron Cooling and Related Applications (ECOOL84), Karlsruhe, September 24–26,1984, KfK 38846, p. 361.

[La85] J.-L. Laclare, Introduction to Coherent Instabilities – Coasting Beam Case, Proc. of CERN Accelerator School, 1984, p. 377–, CERN 85–19.

[Le80] P. Lefévre, Design Study of a Facility for Experiments with Low Energy Antiprotons (LEAR), CERN/PS/DL 80–7.

[Le82] P. Lefévre, Construction of the LEAR Facility: Status Report, presented at the workshop on physics at LEAR with cooled low energy antiprotons, Erice (Sicily) May 9–12, 1982.

[Le84] P.Lefévre, D.Möhl, Report on Studies of Post Deceleration after LEAR, PS/LEA/PL/DM/ph 08.02.1984.

[Ma84] M.Martini, Intrabeam Scattering in the ACOL–AA Machines, CERN PS/84–9 (AA).

[Ma84a] M.Martini, A Computer Program for Intrabeam Calculations, PS/AA/Note 84–7.

[Ma85] S.A. Martin et al., COSY – a Cooler Synchrotron and Storage Ring, IEEE Trans. Nucl. Sci. **NS-32**(1985)2694.

[Me72] S. van der Meer, Stochastic Damping of Betatron Oscillations in the ISR, CERN–IST–PO/72–31(1972).

[Me84] S. van der Meer, Stochastic Cooling and Accumulation of Antiprotons (Nobel lecture in Physics 1984) preprint CERN/PS/AA 84–12.

[Mi87] F.E. Mills, Coolled Ion Beams for Physics Experiments, Nucl. Instr. and Meth. **B24/B25**(1987)38–42.

[Mø82] P. Møller Petersen, Studies of Electron Cooling in the ICE-Storage Ring at CERN, thesis for the Degree of PhD, University of Aarhus, Denmark, 1982.

[Mö84] D. Möhl, A Comparison Between Electron Cooling and Stochastic Cooling, Proceedings of the Workshop on Electron Cooling and Related Applications (ECOOL84), Karlsruhe, September 24–26,1984, KfK 38846, p. 293.

[Mö86] D. Möhl, Principle and Technology of Beam Cooling, CERN/PS 86–31 (LEA).

[Mö86a] D. Möhl, Perspectives of Ion Cooling Rings, CERN/PS 86–32 (LEA).

[No84] A. Noda, N. Takahashi, T. Tanabe, T. Katayama, Y. Hirao and M. Takanaka, Lattice Design of TARN II Cooler Ring Mode, Proceedings of the Workshop on Electron Cooling and Related Applications (ECOOL84), Karlsruhe, September 24–26,1984, KfK 38846, p. 343.

[Ol87] D.K. Olsen et al., The HISTRAP Proposal: Heavy-Ion Storage Ring for Atomic Physics, Nucl. Instr. and Meth. **B24/B25**(1987)26–37.

[Pa84] V. Parkhomchuk, Study of Fast Electron Cooling, Proceedings of the Workshop on Electron Cooling and Related Applications (ECOOL84), Karlsruhe, September 24–26,1984, KfK 38846, p. 71.

[Pa86] G. Parzen, Strong Intrabeam Scattering in Heavy Ion and Proton Beams, Nucl. Instr. and Meth. **A251** (1986)220–230.

[Pi74] A.Piwinski, Intra-Beam-Scattering, Proceedings of the IXth International Conference on High Energy Accelerators, Stanford, California, May 2–7, 1974, p. 405.

[Po84] R.E. Pollock, Some Performance Predictions for the IUCF Cooler, Proceedings of the Workshop on Electron Cooling and Related Applications (ECOOL84), Karlsruhe, September 24–26,1984, KfK 38846, p. 109.

[Po84a] B. Povh (ed): Workshop on the Physics with Heavy Ion Cooler Rings, MPI Heidelberg, report 1984.

[Po85] H. Poth, Review of Electron Cooling Experiments, CERN–EP/85–56, 29 April 1985.

[Sc85] S.O. Schriber, Present Status of RFQs, IEEE Trans. Nucl. Sci. **NS-32**(1985)3134.

[Sc87] R. Schuch, Atomic Physics at the Heidelberg Test Storage Ring (TSR), Nucl. Instr. and Meth. **B24/B25**(1987)11–17.

[Sp56] L. Spitzer, Physics of Fully Ionized Gases, Interscience Publ., New York 1956.

[St85] K. Steffen, Basic Course on Accelerator Optics, Proc. of CERN Accelerator School, 1984, p. 25–, CERN 85–19.

[Sø83] A.H. Sørensen and E. Bonderup, Electron Cooling, Nucl. Instr. and Meth. **215**(1983)27–54.

[Wi85] E.J.N. Wilson, Non-linearities and Resonances, Proc. of CERN Accelerator School, 1984, p. 96–, CERN 85–19.

[Wo85] A.Wolf, Realistic Calculations Concerning Electron Cooling in Storage Rings, CERN–EP/85–27.

[Wo86] A. Wolf, H. Haseroth, C.E. Hill, J.-L. Vallet, C. Habfast, H. Poth, B. Seligmann, P. Blatt, R. Neumann, A. Winnacker and G. zu Putlitz, Electron Cooling of Low-energy Antiprotons and Production of Fast Antihydrogen atoms,CERN–EP/86–10, 27 January 1986.

APPENDIX 1

The input data for the program MAD
The CRYRING lattice

```
TITLE!
CRYRING
PARAMETE,PI=3.141592653586
!-------------------------------------------------------
!DRIFT SPACES
D1:DRIFT,L=1.50
L1:DRIFT,L=0.4
L2:DRIFT,L=0.674
!-------------------------------------------------------
!QUADRUPOLES
QF:QUAD,L=0.3,K1=1.81008
QD:QUAD,L=0.3,K1=-2.33326
!-------------------------------------------------------
!SEXTUPOLES
SF:SEXT,L=0.2,K2=2.3
SD:SEXT,L=0.2,K2=-3.2
!-------------------------------------------------------
!BENDING
BM:SBEND,L=1.2*PI/6,ANGLE=PI/6,HGAP=0.07,FINT=0.4,E1=PI/12,E2=PI/12
!-------------------------------------------------------
LINE,A=(D1,BM,L1,SF,QF,L2,SD)
LINE,SIXTH=(A,QD,-A)
USE,SIXTH,SUPER=6
PRINT,#S/E
TWISS,TAPE
STOP
```

CRYRING "MAD" VERSION: 4.02 RUN: 25JUN-87 12:43:43

TWISS PARAMETERS FOR BEAM LINE "SIXTH" DELTA(P)/P = 0.000000 SYMM = F PAGE 1

ELEMENT SEQUENCE			I	HORIZONTAL						I	VERTICAL						
POS. NO.	ELEMENT NAME	OCC. NO.	DIST ÄMÅ	I I	BETAX ÄMÅ	ALFAX	MUX Ä2PIÅ	X(CO) ÄMMÅ	X'(CO) ÄMRADÅ	DX ÄMÅ	DX'	I I	BETAY ÄMÅ	ALFAY	MUY Ä2PIÅ	Y(CO) ÄMMÅ	Y'(CO) ÄMRADÅ	DY ÄMÅ	DY'
BEGIN	SIXTH	1	0.000		2.174	0.000	0.000	0.000	0.000	1.391	0.000		2.667	0.000	0.000	0.000	0.000	0.000	0.000
1	D1	1	1.500		3.209	-0.690	0.096	0.000	0.000	1.391	0.000		3.510	-0.563	0.082	0.000	0.000	0.000	0.000
2	BM	1	2.128		4.203	-0.966	0.122	0.000	0.000	1.552	0.536		3.546	0.513	0.110	0.000	0.000	0.000	0.000
3	L1	1	2.528		5.049	-1.150	0.136	0.000	0.000	1.766	0.536		3.193	0.370	0.129	0.000	0.000	0.000	0.000
4	SF	1	2.728		5.527	-1.242	0.142	0.000	0.000	1.873	0.536		3.059	0.299	0.139	0.000	0.000	0.000	0.000
5	QF	1	3.028		5.381	1.704	0.151	0.000	0.000	1.879	-0.497		3.419	-1.564	0.154	0.000	0.000	0.000	0.000
6	L2	1	3.702		3.414	1.215	0.176	0.000	0.000	1.544	-0.497		5.986	-2.244	0.178	0.000	0.000	0.000	0.000
7	SD	1	3.902		2.957	1.070	0.186	0.000	0.000	1.445	-0.497		6.924	-2.446	0.183	0.000	0.000	0.000	0.000
8	QD	1	4.202		2.957	-1.070	0.203	0.000	0.000	1.445	0.497		6.924	2.446	0.190	0.000	0.000	0.000	0.000
9	SD	2	4.402		3.414	-1.215	0.213	0.000	0.000	1.544	0.497		5.986	2.244	0.195	0.000	0.000	0.000	0.000
10	L2	2	5.076		5.381	-1.704	0.238	0.000	0.000	1.879	0.497		3.419	1.564	0.219	0.000	0.000	0.000	0.000
11	QF	2	5.376		5.527	1.242	0.246	0.000	0.000	1.873	-0.536		3.059	-0.299	0.234	0.000	0.000	0.000	0.000
12	SF	2	5.576		5.049	1.150	0.252	0.000	0.000	1.766	-0.536		3.193	-0.370	0.244	0.000	0.000	0.000	0.000
13	L1	2	5.976		4.203	0.966	0.266	0.000	0.000	1.552	-0.536		3.546	-0.513	0.263	0.000	0.000	0.000	0.000
14	BM	2	6.605		3.209	0.690	0.292	0.000	0.000	1.391	0.000		3.510	0.563	0.291	0.000	0.000	0.000	0.000
15	D1	2	8.105		2.174	0.000	0.388	0.000	0.000	1.391	0.000		2.667	0.000	0.373	0.000	0.000	0.000	0.000
END	SIXTH	1	8.105		2.174	0.000	0.388	0.000	0.000	1.391	0.000		2.667	0.000	0.373	0.000	0.000	0.000	0.000

TOTAL LENGTH =	48.627822	QX =	2.330004	QY =	2.237695
		QX' =	-0.040983	QY' =	0.090738
ALFA =	0.190936E+00	BETAX(MAX) =	5.527250	BETAY(MAX) =	6.923705
GAMMA(TR) =	2.288526	DX(MAX) =	1.879189	DY(MAX) =	0.000000

```
C=====================================================================
C       PROGRAM INTRABEAM
C
C       PURPOSE:
C               TO CALCULATE GROWTH TIMES FOR INTRABEAM SCATTERING
C
C       BASED ON PIWINSKI'S THEORY AND M.MARTINI'S PAPERS
C       PS/AA/Note 84-7 AND PS/84-9 (AA)
C
C       WRITTEN BY PAULI HEIKKINEN
C               AT AFI, STOCKHOLM
C               JUNE 1985
C
C       GOOD LUCK !!
C=====================================================================
C
C       PROGRAM VARIABLES:
C       ==================
C
C                       EXPLANATIONS
C                               _ REFERS TO SUBSCRIPT   (cf.Martini)
C                               + REFERS TO SUPERSCRIPT (cf.Martini)
C       INPUT:
C
C       NPOS                    NUMBER OF POSITIONS IN MAD OUTPUT (TAPE 3)
C       LEL     (500)           LENGTH OF ELEMENT
C       LSUP                    LENGTH OF SUPERPERIOD (THAT WAS READ FROM 3)
C       BETX    (500)           HORIZONTAL BETA (M)
C       BETY    (500)           VERTICAL   BETA (M)
C       ALFX    (500)           HORIZONTAL ALFA
C       ALFY    (500)           VERTICAL   ALFA
C       DX      (500)           DISPERSION      (M)
C       DXP     (500)           D(DX)/DS = DX'
C       CHARGE  INTEGER         CHARGE STATE OF THE IONS IN THE BEAM
C       MASS                    MASS NUMBER
C       CCOAST  CHAR            C OR B
C       COAST   LOGIC           .TRUE. IF COASTING BEAM - .FALSE. FOR BUNCHED
C       LEN     REAL            ORBIT LENGTH / SIGMA(LENGTH) FOR BUNCH
C       GAMMA                   ENERGY FACTOR
C       TA                      KINETIC ENERGY/A
C       BETA                    V/C
C       NPART                   NUMBER OF IONS IN THE BEAM/BUNCH
C       DPP                     DELTAP/P
C       DP                      DPP/SIGMA(P)
C       SIGP                    SIGMA(P)
C       EX                      HORIZONTAL EMITTANCE (PI M RAD)
C       EY                      VERTICAL   EMITTANCE (PI M RAD)
C       DE                      EMITTANCE/SIGMA (1.96 IF 95% OF PROFILE
C                                       SQRT(6) IF 95% OF PHASE SPACE)
C       PROGVRSN                MAD VERSION FROM UNIT 3
C       DATAVRSN                SURVEY,TWISS OR CHROM
C       DATE                    DATE OF MAD RUN
C       TIME                    TIME OF MAD RUN
C       JOBNAME                 FROM UNIT 3
C       SUPER                   NUMBER OF SUPERPERIODS
C       SYMM                    .TRUE. OR .FALSE.
C       TITLE                   TITLE OF MAD RUN
C       KEYWORD                 FROM UNIT 3
C       NAME                    ELEMENT NAME
C       TYPE                    ELEMENT TYPE
C       NSTEP                   NUMBER OF INTEGRATION STEPS
C
C       OPT                     Y/N OPTIONS OR NOT
C
C       OPTIONAL PARAMETERS:
C
C       DISPFAC                 DISPERSION MULTIPLFIER
C       CDISP                   CONSTANT DISPERSION
C       BETFAC                  BETA MULTIPLIFIER
C       CBETX                   CONSTANT BETX
C       CBETY                   CONSTANT BETY
C       NBREX                   NUMBER OF HORIZONTAL EMITTANCES
C       NBREY                   NUMBER OF VERTICAL EMITTANCES
C
C       OUTPUT SCHEME:
C
```

```
C       OFIL            A=FOR010        GOOD FOR ONE CASE
C                       B=FOR011        MAP FOR SEVERAL EMITTANCES
C                       C=FOR012        GROWTH TIMES AT ELEMENTS
C
C       DURING CALCULATION:
C
C       BTX             BETX IN THE MIDDLE OF ELEMENT
C       BTY             BETY
C       ALX             ALFX
C       ALY             ALFY
C       DISP            DX
C       DISPP           DXP
C       PI
C       R0              1.525E-18 M CLASSICAL PROTON RADIUS
C       RQ2A            = R0 * (q**2/A)
C       X               INTEGRATION VARIABLE
C       Y                       "
C       DELX            INTEGRATION STEP
C       DELY                    "
C       SII             SINE INTEGRAL
C       CII             COSINE INTEGRAL
C       FAC     (20)    FAC(N) = N!
C       N               = 1 IF BUNCHED BEAM, = 2 IF COASTING
C
C       THE FOLLOWING VECTORS (500) COULD BE SCALARS AS WELL
C       THE REASON FOR VECTOR REPRESENTATION IS A POSSIBLE
C       OUTPUT OF THESE VARIABLES AT EACH ELEMENT
C
C       SIGX    (500)   SIGMA_Hi IN MARTINI'S NOTATION
C       SIGBX   (500)   SIGMA_Hbetai
C       SIGPBX  (500)   SIGMA'_Hbetai
C       SIGY    (500)   SIGMA_Vi
C       SIGPY   (500)   SIGMA'_Vi
C       SIGZ    (500)   SIGMA_Yi
C       AI      (500)   a_i
C       BI      (500)   b_i
C       CI      (500)   c_i
C       DI      (500)   d_i
C       DDI     (500)   d+ti1de_i
C       K1      (500)   k_1i
C       K2      (500)   k_2i
C       K3      (500)   k_3i
C       F1      (500)   f_1i    SCATTERING FUNCTION
C       F2      (500)   f_2i            "
C       F3      (500)   f_3i            "
C       G1      (500)   g_1i
C       G2      (500)   g_2i
C       G3      (500)   g_3i
C
C       U               FACTOR IN SCATTERING FUNCTION f
C       LAMBDA          NPART/LEN (COASTING) cf.MARTINI
C       A               CONSTANT IN 1/TAU EQUATION
C       DTPINV          LONGITUDINAL GROWTH SPEED AT ELEMENT
C       DTXINV          HORIZONTAL      "       "
C       DTYINV          VERTICAL        "       "
C       TXINV           1/TAUX'
C       TYINV           1/TAUY'
C       TPINV           1/TAUP
C       TAUXP   (10,10) HORIZONTAL   GROWTH TIME (S)
C       TAUYP   (10,10) VERTICAL     GROWTH TIME (S)
C       TAUP    (10,10) LONGITUDINAL GROWTH TIME (S)
C
C===============================================================
C
      REAL LEL(500),BETX(500),BETY(500),ALFX(500),ALFY(500)
     1  ,DX(500),DXP(500),LEN
     2  ,SIGX(500),SIGBX(500),SIGPBX(500),SIGY(500)
     3  ,SIGPY(500),SIGZ(500),AI(500),BI(500),CI(500),DI(500)
     4  ,DDI(500),K1(500),K2(500),K3(500),F1(500),F2(500),F3(500)
     5  ,G1(500),G2(500),G3(500),FAC(20)
     6  ,GAMMA,BETA,DPP,DP,SIGP,EX(10),EY(10),DE,TA,TAUXP(10,10)
     7  ,TAUYP(10,10),TAUP(10,10),CDISP,CBETX,CBETY
     8  ,LAMBDA,X,Y,DELX,DELY,SII,CII,PI,A,R0,RQ2A,TXINV,TYINV,TPINV
     9  ,U,NPART,BTX,BTY,ALX,ALY,DISP,DISPP,LSUP,DISPFAC,BETFAC
     &  ,DTPINV,DTXINV,DTYINV
C
      INTEGER NPOS,CHARGE,MASS,SUPER,NSTEP,N,NBREX,NBREY
C
      CHARACTER*80 TITLE
      CHARACTER*8 PROGVRSN,DATAVRSN,DATE,TIME,JOBNAME,KEYWORD,NAME
      CHARACTER*4 TYPE
```

```
      CHARACTER CCOAST,OPT,OFIL
C
      LOGICAL SYMM,COAST
C*********************************************************************
C
C     FORMAT STATEMENTS:
C
900   FORMAT(A)
901   FORMAT(/'  TITLE FROM UNIT 3:'/'  ',80A,//)
1001  FORMAT(5A8,I8,L8,I8/A80)
1002  FORMAT(2A8,A4,F12.6/E16.9)
1003  FORMAT(5E16.9/3E16.9/E16.9)
1004  FORMAT(3E16.9)
1009  FORMAT(/' ',I8,' POSITIONS HAS BEEN READ FROM UNIT 3'/)
1010  FORMAT(/' TAUP  =',G12.4E2,' S'/' TAUX'' =',G12.4E2,' S'/
     &' TAUY'' =',G12.4E2,' S')
1011  FORMAT(/' ************************************************',
     1'********'/
     1'   q       A       T/A ÄMeV/uÅ          NPART         LEN ÄmÅ'/
     1' ',I3,'     ',I4,'        ',G10.4E2,'       ',G10.4E2,'    ',F8.3/)
1012  FORMAT('   EX Äpi m radÅ      EY Äpi m radÅ        DELTAP/P'/
     1'   ',G10.4E2,'         ',G10.4E2,'           ',G10.4E2)
1013  FORMAT(//' GROWTH TIMES ')
1014  FORMAT(/' OUTPUT FILE = FOR010.DAT')
1015  FORMAT('  DELTAP/P = ',G10.4E2,//)
1016  FORMAT(' ',T18,10(' ',G10.2E2))
1017  FORMAT(' ',T14,'TP',T18,10(' ',G10.2E2))
1018  FORMAT(' ',G10.4E2,T14,'TX',T18,10(' ',G10.2E2))
1019  FORMAT(' ',T14,'TY'T18,10(' ',G10.2E2))
1020  FORMAT(/' OUTPUT FILE = FOR011.DAT')
1021  FORMAT('  ')
1022  FORMAT(' ',T40,'EX   Äpi m radÅ')
1023  FORMAT(' EY Äpi m radÅ')
1024  FORMAT(/' OUTPUT FILE = FOR012.DAT')
4999  FORMAT('      BTX',T14,'BTY',T22,'DX',T30,'DX'',T37,'1/TP'
     &      ,T46,'1/TX'',T56,'1/TY'',T68,'W')
5000  FORMAT(' ',4('  ',F6.2),3('  ',G8.2E2),'  ',F6.4)
C*********************************************************************
      TYPE *,' '
      TYPE *,' ************************************************'
      TYPE *,' *                                              *'
      TYPE *,' *             PROGRAM INTRABEAM                *'
      TYPE *,' *                                              *'
      TYPE *,' ************************************************'
      TYPE *,' '
C*********************************************************************
C     INITIAL VALUES:
C
      FAC(1) = 1
      DO IND=2,20
            FAC(IND) = IND*FAC(IND-1)
      ENDDO
      COAST = .TRUE.
      PI = 4*ATAN(1.)
      R0 = 1.535E-18
      N  = 2                    !COASTING BEAM
      DISPFAC = 1.0
      BETFAC  = 1.0
      CDISP   = 0.0
      CBETX   = 0.0
      CBETY   = 0.0
      NBREX   = 1
      NBREY   = 1
C*********************************************************************
C     READ FROM UNIT 3 (MAD OUTPUT - TAPE)
C
      READ(3,1001)PROGVRSN,DATAVRSN,DATE,TIME,JOBNAME,SUPER,SYMM
     1  ,NPOS,TITLE
      IF (DATAVRSN.NE.'TWISS')THEN
            TYPE *,' TWISS WAS NOT THE FIRST DATAVRSN'
            TYPE *,' CORRECT IT AND START AGAIN'
            STOP
      ENDIF
      DO 1 I=1,NPOS
            READ(3,1002)KEYWORD,NAME,TYPE,LEL(I),EDUMMY
            READ(3,1003)ALFX(I),BETX(I),EDUMMY1,DX(I),DXP(I)
     1      ,ALFY(I),BETY(I),EDUMMY2,EDUMMY3
            LSUP = LSUP+LEL(I)
1     CONTINUE
      READ(3,1004)EDUMMY1,EDUMMY2,LEN
      CLOSE(UNIT=3)
```

```
      WRITE(6,1009)NPOS
      WRITE(6,901)TITLE
C*****************************************************************
C
C     INPUT FROM TERMINAL:
C
      TYPE *,' GIVE THE CHARGE STATE (q) AND MASS NUMBER (A)'
      READ(5,*)CHARGE,MASS
      TYPE *,' GAMMA OF THE BEAM ?'
      READ(5,*)GAMMA
      IF(GAMMA.LE.1)THEN
            TYPE *,' GAMMA.LE.1 - GIVE T/A ÄMeV/uÅ'
            READ(5,*)TA
            GAMMA = (931.48 + TA)/931.48
            BETA = SQRT(1.-1./(GAMMA**2))
      ELSE
            BETA = SQRT(1.-1./(GAMMA**2))
            TA = (GAMMA-1.0)*931.48
      ENDIF
      TYPE *,' NUMBER OF PARTICLES/COASTING BEAM - BUNCH ?'
      READ(5,*)NPART
      TYPE *,' DELTAP/P ?'
      READ(5,*)DPP
      TYPE *,' DP ? , = 1.96 FOR 95% OF GAUSSIAN BEAM'
      READ(5,*)DP
      TYPE *,' Ex AND Ey ? Äpi m radÅ'
      READ(5,*)EX(1),EY(1)
      TYPE *,' DE ?, = 1.96 IF 95% OF PROFILE, SQRT(6)=2.45 IF 95% OF'
      TYPE *,'          PHASE SPACE'
      READ(5,*)DE
      TYPE *,' COASTING OR BUNCHED BEAM'
      READ(5,900)CCOAST
      IF(CCOAST.EQ.'B')COAST=.FALSE.
      IF(.NOT.COAST)THEN
            TYPE *,' GIVE THE SIGMA OF BUNCH LENGTH'
            READ(5,*)LEN
            N = 1
            LAMBDA = NPART/(2*SQRT(PI)*LEN)
      ELSE
            LAMBDA = NPART/LEN
      ENDIF
      TYPE *,' GIVE THE NUMBER OF INTEGRATION STEPS'
      READ(5,*)NSTEP
C
C     OPTION FOR MULTIPLIED DISPERSION AND BETA-VALUES ETC.
C
      TYPE *,' EXTRA OPTIONS ? Y/N'
      READ(5,900)OPT
      IF(OPT.EQ.'Y')THEN
            TYPE *,' GIVE THE DISPERSION MULTIPLICATION FACTOR'
            READ(5,*)DISPFAC
            TYPE *,' GIVE A CONSTANT ADDED TO THE DISPERSION'
            READ(5,*)CDISP
            TYPE *,' GIVE THE BETA MULTIPLICATION FACTOR'
            READ(5,*)BETFAC
            TYPE *,' GIVE THE CONSTANTS TO BE ADDED TO BETAS X,Y'
            READ(5,*)CBETX,CBETY
            TYPE *,' GIVE NBR(EX) AND NBR(EY)'
            READ(5,*)NBREX,NBREY
            IF(NBREX.GT.1)THEN
                  TYPE *,' GIVE THE EX VALUES Äpi m radÅ'
                  READ(5,*)(EX(IEX),IEX=1,NBREX)
            ENDIF
            IF(NBREY.GT.1)THEN
                  TYPE *,' GIVE THE EY VALUES Äpi m radÅ'
                  READ(5,*)(EY(IEY),IEY=1,NBREY)
            ENDIF
            IF(DISPFAC.EQ.0.AND.BETFAC.EQ.0.)NPOS=2
      ENDIF
C
C     CHOICE OF OUTPUT SCHEME:
C
      TYPE *,' OUTPUT FILE ? A=10,B=11,C=12,<RETURN>=NO FILES'
      TYPE *,' A IS GOOD FOR ONE CASE'
      TYPE *,' B GIVES A MAP FOR SEVERAL EMITTANCES'
      TYPE *,' C GIVES THE GROWTH SPEEDS AT EACH ELEMENT'
      READ(5,900)OFIL
C*****************************************************************
C     ION RADIUS
      RQ2A = R0*(CHARGE**2)/MASS
C
```

```
C       SIGMA(DELTAP/P)
        SIGP = DPP/DP
C
C       INTEGRATION STEP IN THE SECOND INTEGRAL
        DELX = PI/NSTEP
C***********************************************************************
C       EMITTANCE LOOP:
        DO 5001 IEX=1,NBREX
        DO 5002 IEY=1,NBREY
C
C       CONSTANT A:
C
        A = (DE**4)*DP*LAMBDA*3.E8*(R0**2)*(CHARGE**4)/(16*PI*SQRT(PI)
     &      *EX(IEX)*EY(IEY)*DPP*(BETA**3)*(GAMMA**4)*(MASS**2))
C

        IF(OFIL.EQ.'C')THEN
                WRITE(12,1011)CHARGE,MASS,TA,NPART,LEN
                WRITE(12,1012)EX(IEX),EY(IEY),DPP
                WRITE(12,1021)
                WRITE(12,4999)
        ENDIF
C       INITIALIZE SPEEDS
        TPINV = 0.0
        TXINV = 0.0
        TYINV = 0.0
C***************************************************************
C
C       POSITION LOOP
        DO 100 I=2,NPOS          !1<->BEGIN
C
C       LATTICE FUNCTIONS IN THE MIDDLE OF THE ELEMENT I
C       LINEAR APPROXIMATION
C
                BTX      = 0.5*(BETX(I)+BETX(I-1))*BETFAC+CBETX
                BTY      = 0.5*(BETY(I)+BETY(I-1))*BETFAC+CBETY
                ALX      = 0.5*(ALFX(I)+ALFX(I-1))*BETFAC
                ALY      = 0.5*(ALFY(I)+ALFY(I-1))*BETFAC
                DISP     = 0.5*(DX(I)+DX(I-1))*DISPFAC+CDISP
                DISPP    = 0.5*(DXP(I)+DXP(I-1))*DISPFAC
C
                SIGBX(I) = SQRT(EX(IEX)*BTX)/DE
                SIGY(I)  = SQRT(EY(IEY)*BTY)/DE
                SIGPBX(I)= SQRT(EX(IEX)*(1+(ALX**2))/BTX)/DE
                SIGPY(I) = SQRT(EY(IEY)*(1+(ALY**2))/BTY)/DE
                SIGX(I)  = SQRT((SIGBX(I))**2+((DISP*SIGP)**2))
                SIGZ(I)  = SIGP*SIGBX(I)/(GAMMA*SIGX(I))
                AI(I)    = SIGZ(I)/SIGPBX(I)*SQRT(1+(ALX**2))
                BI(I)    = SIGZ(I)/SIGPY(I)*SQRT(1+(ALY**2))
                CI(I)    = 2*SIGZ(I)*BETA*GAMMA*SQRT(SIGY(I)/RQ2A)
                K1(I)    = 1./(CI(I)**2)
                K2(I)    = (AI(I)/CI(I))**2
                K3(I)    = (BI(I)/CI(I))**2
                DI(I)    = SIGP*DISP/SIGX(I)
                DDI(I)   = SIGP*(ALX*DISP+BTX*DISPP)/SIGX(I)
C
                F1(I) = 0.0
                F2(I) = 0.0
                F3(I) = 0.0
C***********************************************************************
C       SCATTERING FUNCTION INTEGRATION BEGINS
C
                DO 3 J=1,NSTEP
                X = (J-0.5)*PI/NSTEP
                DELY = 2*PI*X/NSTEP
                DO 4 L=1,NSTEP
                Y = (L-0.5)*2*PI*X/NSTEP
                U = ((SIN(X)*COS(Y/X))**2+(SIN(X)*(AI(I)*SIN(Y/X)-DDI(I)*
     &              COS(Y/X)))**2+(BI(I)*COS(X))**2)/(CI(I)**2)
C
C       SINE AND COSINE INTEGRALS - 10 TERMS
                SII = 0.0
                CII = 0.577216 + LOG(U)
                DO 5 K=1,10
                SII = SII+((-1)**(K-1))*(U**(2*K-1))/((2*K-1)*FAC(2*K-1))
                CII = CII+((-1)**K)*(U**(2*K))/(2*K*FAC(2*K))
5               CONTINUE
                G1(I) = 1.-3*(SIN(X)*COS(Y/X))**2
                G2(I) = 1.-3*(SIN(X)*SIN(Y/X))**2+6*DDI(I)*SIN(X)*
     &                  SIN(Y/X)*COS(Y/X)/AI(I)
                G3(I) = 1.-3*(COS(X)**2)
```

```
C
C       SCATTERING FUNCTIONS
C
                F1(I) = F1(I)+DELX*DELY*(SIN(X)/X)*(G1(I)/U)*(SIN(U)*
     &                  (PI/2-SII)-COS(U)*CII)
                F2(I) = F2(I)+DELX*DELY*(SIN(X)/X)*(G2(I)/U)*(SIN(U)*
     &                  (PI/2-SII)-COS(U)*CII)
                F3(I) = F3(I)+DELX*DELY*(SIN(X)/X)*(G3(I)/U)*(SIN(U)*
     &                  (PI/2-SII)-COS(U)*CII)
4               CONTINUE
3               CONTINUE
C
C       SCATTERING FUNCTION INTEGRATION STOPS
C*************************************************************************
                F1(I) = F1(I)*2*K1(I)
                F2(I) = F2(I)*2*K2(I)
                F3(I) = F3(I)*2*K3(I)
                DTPINV = A*N*(1-DI(I)**2)*F1(I)/2
                DTXINV = A*(F2(I)+(DI(I)**2+DDI(I)**2)
     &                   * F1(I))/2
                DTYINV = A*F3(I)/2
                TPINV = TPINV+ LEL(I)*DTPINV
                TXINV = TXINV+ LEL(I)*DTXINV
                TYINV = TYINV+ LEL(I)*DTYINV
                IF(OFIL.EQ.'C')WRITE(12,5000)BTX,BTY,DISP,DISPP,DTPINV
     &          ,DTXINV,DTYINV,LEL(I)/LSUP
100     CONTINUE
C
C       POSITION LOOP STOPS
C*************************************************************************
C       AVERAGE GROWTH SPEEDS IN THE WHOLE RING
        TPINV = TPINV/LSUP
        TXINV = TXINV/LSUP
        TYINV = TYINV/LSUP
        IF(TPINV.NE.0)THEN
                TAUP(IEX,IEY) = 1./TPINV
        ELSE
                TYPE *,' TAUP INFINITE'
        ENDIF
        IF(TXINV.NE.0)THEN
                TAUXP(IEX,IEY) = 1./TXINV
        ELSE
                TYPE *,' TAUX'' INFINITE'
        ENDIF
        IF(TYINV.NE.0)THEN
                TAUYP(IEX,IEY) = 1./TYINV
        ELSE
                TYPE *,' TAUY'' INFINITE'
        ENDIF
C*************************************************************************
C
        IF(NBREX*NBREY.EQ.1)THEN
                WRITE(6,1011)CHARGE,MASS,TA,NPART,LEN
                WRITE(6,1012)EX(IEX),EY(IEY),DPP
                WRITE(6,1013)
                WRITE(6,1010)TAUP(IEX,IEY),TAUXP(IEX,IEY),TAUYP(IEX,IEY)
        ENDIF
        IF(OFIL.EQ.'A')THEN
                WRITE(10,1011)CHARGE,MASS,TA,NPART,LEN
                WRITE(10,1012)EX(IEX),EY(IEY),DPP
                WRITE(10,1013)
                WRITE(10,1010)TAUP(IEX,IEY),TAUXP(IEX,IEY),TAUYP(IEX,IEY)
        ENDIF
        IF(OFIL.EQ.'C')THEN
                WRITE(12,1013)
                WRITE(12,1010)TAUP(IEX,IEY),TAUXP(IEX,IEY),TAUYP(IEX,IEY)
        ENDIF
C*************************************************************************
5002    CONTINUE
5001    CONTINUE
C
C       EMITTANCE LOOP STOPS
C*************************************************************************
        IF(OFIL.EQ.'A')WRITE(6,1014)
        IF(OFIL.EQ.'C') WRITE(6,1024)
        IF(OFIL.EQ.'B')THEN
                WRITE(11,1011)CHARGE,MASS,TA,NPART,LEN
                WRITE(11,1015)DPP
                WRITE(11,1022)
                WRITE(11,1016)(EX(I),I=1,NBREX)
                WRITE(11,1021)
```

```
        WRITE(11,1023)
        DO J=1,NBREY
          WRITE(11,1017)(TAUP(I,J),I=1,NBREX)
          WRITE(11,1018)EY(J),(TAUXP(I,J),I=1,NBREX)
          WRITE(11,1019)(TAUYP(I,J),I=1,NBREX)
          WRITE(11,1021)
        ENDDO
        WRITE(6,1020)
ENDIF
END
```